

The Nature of Weak Adsorption on Transition Metals

Adsorption of Nitrogen and Xenon
as Studied by Field Emission Probe-Hole Microscopy
and Photoelectric Emission

B. E. NIEUWENHUYS

BIBLIOTHEEK
GORLAEUS LABORATORIA DER R.U.
Wassenaarseweg 76
Postbus 75 - LEIDEN

STELLINGEN

I

Rivière maakt een principiële fout door "ESCA" op grond van het relatief grote penetratievermogen van de primaire straling in de vaste stof minder geschikt te achten voor oppervlakte-analyse.

J.C. Rivière, *Physics Bulletin* 20 (1969) 85

II

De argumenten van Lewis en Gomer voor het moleculaire karakter van de electropositieve component van geadsorbeerd waterstof op platina zijn niet steekhoudend.

R. Lewis en R. Gomer, *Surface Sci.* 17 (1969) 333

III

Eckstrom en zijn medewerkers menen ten onrechte dat het oppervlak van hun door opdampen in een argon atmosfeer bereide nikkel- en rhodiumfilms grotendeels uit (110) vlakken bestaat.

H.C. Eckstrom, G.G. Possley, S.E. Hannum en W.H. Smith,
J. Chem. Phys. 52 (1970) 5435

IV

De kritiek die Williams en Boudart hebben op de studies van diverse auteurs die met behulp van "Auger Electron Spectroscopy" de oppervlaktesamenstelling van legeringen onderzocht hebben, geldt, indien de kritiek terecht zou zijn, ook voor hun eigen werk.

F.L. Williams en M. Boudart, *J. Catalysis* 30 (1973) 438

V

Bij de toekenning van de 50 rekvibraties in de infraroodspectra van lanthanideperchloraat complexen van thioxaanoxyde houden Vicentini en Perrier ten onrechte geen rekening met de aanwezigheid van ligand absorpties in hetzelfde frequentiegebied.

G. Vicentini en M. Perrier, *J. inorg. nucl. Chem.* 36 (1974) 77

VI

De bewering van Misra dat de isostere adsorptiewarmte van stikstof op de door hem gebruikte nikkeelfilms niet met de Clausius-Clapeyron vergelijking bepaald kan worden, is onjuist.

D.N. Misra, Ind. J. Pure Appl. Phys. 10 (1972) 663

VII

Perdereau schrijft het verdwijnen van de koolstofpiek in het Auger electrospectrum van gecontamineerd nikkel als gevolg van verhitting boven 400°C ten onrechte toe aan desorptie van koolstof.

M. Perdereau, Surface Sci. 24 (1971) 239

VIII

Procop, Völter en medewerkers maken een principiële fout door te stellen dat uit de helling van een adsorptie-isochoor de activeringsenergie van desorptie volgt en niet direct de isostere adsorptiewarmte.

Z. Shai, A.V. Sklyarov, M. Procop en I. Völter, Kin. Kat. 13 (1972) 1105

M. Procop en J. Völter, Surface Sci. 33 (1972) 69

IX

Zolang het systeem van de bij promoties vereiste stellingen gehandhaafd blijft, dienen de universitaire bibliotheken bij de keuze van abonnementen op wetenschappelijke tijdschriften niet uitsluitend van het wetenschappelijk gehalte van de betrokken tijdschriften uit te gaan.

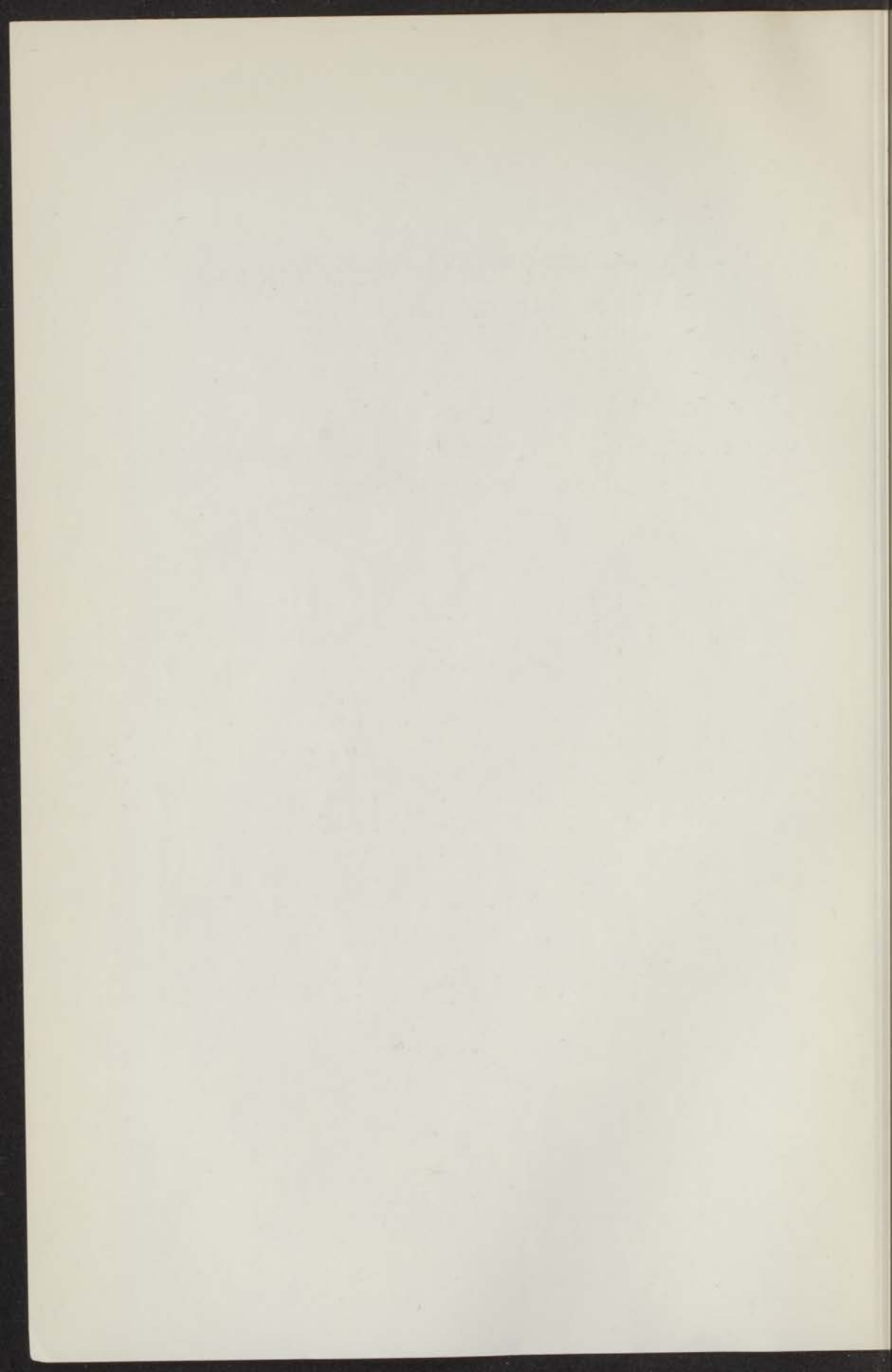
The Nature of Weak Adsorption on Transition Metals

Adsorption of Nitrogen and Xenon
as Studied by Field Emission Probe-Hole Microscopy
and Photoelectric Emission

Broekschrift

Bernard Eibert Nieuwenhays

1974



The Nature of Weak Adsorption on Transition Metals

Adsorption of Nitrogen and Xenon
as Studied by Field Emission Probe-Hole Microscopy
and Photoelectric Emission

Proefschrift

ter verkrijging van de graad van Doctor in de Wiskunde
en Natuurwetenschappen aan de Rijksuniversiteit te
Leiden, op gezag van de Rector Magnificus Dr. A. E.
Cohen, Hoogleraar in de Faculteit der Letteren, volgens
besluit van het college van dekanen te verdedigen op
woensdag 1 mei 1974 te klokke 15.15 uur

door

Bernard Egbert Nieuwenhuys

geboren te Haarlem in 1944

PROMOTOR: PROF. DR. W. M. H. SACHTLER

on Transition Metals

Adsorption of Nitrogen and Xenon
as Studied by Field Emission Probe Hole Microscopy
and Photoelectric Emission

Photoelectric

The authors are indebted to the Deutsche Forschungsgemeinschaft for the financial support of this work. The authors are also indebted to the Deutsche Forschungsgemeinschaft for the financial support of this work. The authors are also indebted to the Deutsche Forschungsgemeinschaft for the financial support of this work.

Deutscher Fachschriften-Verlag

Heidelberg, 1972

Aan mijn ouders

C O N T E N T S

	page
SUMMARY	11
Chapter I GENERAL INTRODUCTION	15
1. Adsorption of gases on metals	15
2. Field electron emission microscopy	18
3. Outline of the present study	23
References	24
Chapter II CRYSTAL FACE SPECIFICITY OF NITROGEN ADSORPTION ON A PLATINUM FIELD EMISSION TIP	25
Summary	25
1. Introduction	25
2. Experimental	27
1. Apparatus	27
2. Sample preparation and cleaning	29
3. Results and discussion	30
1. Work functions of single crystal planes of platinum	30
2. Adsorption of nitrogen on platinum	33
1. Changes in work function by adsorption	33
2. Desorption experiments	36
3. General discussion	39
Acknowledgements	42
References	43
Chapter III ADSORPTION OF NITROGEN ON SINGLE CRYSTAL FACES OF IRIIDIUM, STUDIED BY FIELD EMISSION MICROSCOPY	45

	page
Summary	45
1. Introduction	45
2. Experimental	45
3. Determination of the work functions	46
4. Results	49
5. Identification of adsorption states of nitrogen on iridium and their face-specificity	54
1. Tip region of the (210), (531), (320) and (731) faces	54
2. (110) region	55
3. (100) area	55
4. Region around (510) - (310)	55
5. Region around (711) - (511)	55
6. (111) region	56
6. General discussion	56
Acknowledgements	59
References	59
 Chapter IV	
PHOTOELECTRIC DETERMINATION OF THE CHANGES IN WORK FUNCTION OF NICKEL, RHODIUM AND PLATINUM FILMS BY NITROGEN ADSORPTION	61
Introduction	61
Experimental	61
Results and discussion	61
References	64
 Chapter V	
THE CHANGES IN WORK FUNCTION OF GROUP Ib AND VIII METALS BY XENON ADSORPTION, DETERMINED BY FIELD ELECTRON AND PHOTOELECTRON EMISSION	67
Abstract	67
1. Introduction	68
2. Experimental	68
3. Results	69
A. The surface potential of Xe on various	

	page
metal films as a function of the temperature of previous annealing	69
B. The surface potential of individual regions of an Ir and a Pt field emitter	72
4. Discussion	75
Acknowledgements	76
References	77
 Chapter VI CRYSTAL FACE SPECIFICITY OF XENON ADSORPTION ON IRIDIUM FIELD EMITTERS	 78
Abstract	78
1. Introduction	79
2. Experimental	80
3. Determination of the surface potential of Xe on the different tip regions	81
4. Determination of the heat of adsorption	82
5. Results	83
6. Discussion	92
a. Adsorption at low coverage	92
b. Adsorption at high coverage	95
References	99
 Chapter VII ADSORPTION OF XENON ON PLATINUM, STUDIED BY FIELD EMISSION MICROSCOPY	 100
Summary	100
Zusammenfassung	101
1. Introduction	102
2. Experimental	103
3. Results and discussion	103
References	112
 Chapter VIII ADSORPTION OF XENON ON GROUP VIII AND Ib METALS, STUDIED BY PHOTOELECTRON EMISSION	 113
Summary	113

	page
1. Introduction	114
2. Experimental	115
3. Measuring procedure	115
4. Results	117
5. Discussion	122
A. Bonding models for Xe on transition metals	122
I. The polarization model	122
II. The charge transfer-no bond (CTNB) model	123
B. Dispersion forces	126
C. Evaluation of the results	127
I. The relation between Q and the s.p.	127
II. Calculation of Q_a from the measured s.p.	128
6. Conclusions	131
References	132
 Chapter IX	
SOME GENERAL REMARKS ON THE BOND OF ADSORBED NITROGEN AND XENON	134
 APPENDIX	
Surfaces modeled in the f.c.c. structure	137
 SAMENVATTING	142

100
 101
 102
 103
 104
 105
 106
 107
 108
 109
 110
 111
 112
 113
 114
 115
 116
 117
 118
 119
 120
 121
 122
 123
 124
 125
 126
 127
 128
 129
 130
 131
 132
 133
 134
 135
 136
 137
 138
 139
 140
 141
 142
 143
 144
 145
 146
 147
 148
 149
 150
 151
 152
 153
 154
 155
 156
 157
 158
 159
 160
 161
 162
 163
 164
 165
 166
 167
 168
 169
 170
 171
 172
 173
 174
 175
 176
 177
 178
 179
 180
 181
 182
 183
 184
 185
 186
 187
 188
 189
 190
 191
 192
 193
 194
 195
 196
 197
 198
 199
 200

S U M M A R Y

This work consists of three parts. The first part (chapter I) is a general introduction where some principles of adsorption of gases on solid surfaces are reviewed. Reasons are given why the solution of some fundamental problems requires adsorption measurements on single crystal planes. Several experimental techniques for studying adsorption of gases on metal surfaces are outlined and the principles of those techniques are described which are used in this study viz. field emission microscopy and photoelectron emission. In particular the unique possibilities of the field emission probe-hole technique are emphasized for studying separately all faces of a metal single crystal under identical experimental conditions. The reasons are explained for the choice of the adsorption systems described in this thesis.

The second part (chapters II - IV) deals with the adsorption of N_2 on a number of transition metals.

The probe-hole tube designed by us is described in chapter II where further the adsorption of N_2 on different crystal faces of Pt is presented as studied by field emission microscopy. In chapter III results are given of a similar field emission study of N_2 adsorption on Ir. Chapter IV describes work on the change in the photoelectric work function of Ni, Rh and Pt films by N_2 adsorption as a function of the temperature of previous annealing of the films.

On all these metals N_2 is only weakly adsorbed. The initial heat of adsorption appears to be 9 kcal/mole on all the exposed crystal faces of Pt, both on the smooth regions (111) and (100) and on rough regions around (320) and (331). N_2 adsorption on Ir is markedly crystal face specific. Temperature programmed desorption reveals three binding states: γ_1 on the (100) face with a maximum heat of adsorption of 7-8 kcal/mole, γ_2 on the

regions around (110) with a maximum heat of adsorption of 10 - 11 kcal/mole and γ_3 on the roughest tip regions (210), (320), (531) and (731) with an initial heat of adsorption of 13 - 14 kcal/mole.

The change in work function by N_2 adsorption is crystal face specific for both metals. On Pt N_2 adsorption results in a large decrease in work function. This decrease is much larger on rough crystal faces than on the smooth faces (111) and (100). On Ir, on the other hand, N_2 adsorption causes a large decrease in work function on the smooth (100) plane but only a very small decrease on the rough tip areas (731) and (210). The emission currents from these rough faces recorded at constant voltage decrease strongly during N_2 adsorption in spite of the small decrease in work function. The work function change on Pt films brought about by N_2 adsorption decreases with increasing temperature of previous annealing. On Ni and Rh films, contrary to Pt films, the change in work function increases with annealing temperature.

These results are discussed in relation with literature data of N_2 adsorption on Ni, Pd, Pt, Rh and Ir. Our results confirm the hypothesis of Van Hardeveld et al. that N_2 adsorption is crystal face specific. However, the crystal face dependence is much more complicated than suggested by these authors. Moreover, these metals markedly differ in the nature of the nitrogen complexes. Arguments are given that the adsorption cannot be described as physical adsorption but that the interaction is of a chemical nature.

The third part of this thesis (chapters V - VIII) reports on investigations of the adsorption of Xe on transition metals.

Chapter V deals with a study where the surface potential of Xe on films of various metals was determined as a function of the temperature of previous annealing of the films.

In chapters VI and VII results are presented of field emission studies of Xe adsorption on different crystal faces of Ir and Pt, respectively. The initial heat of adsorption decreases both on Pt and on Ir in the order (321) > (111) \sim (100) > (210) > (110). The surface potential of Xe on Ir is larger on the close-packed regions (111) and (100) than on the rough regions around (210) and (110). The heat of adsorption decreases with coverage, in particular on the smooth tip regions.

In chapter VIII determinations of the surface potential and the

heat of adsorption of Xe on various transition metals are given. The results show that the surface potential of Xe is directly related to the heat of adsorption, within the experimental accuracy both quantities being linearly proportional.

Fundamental problems of the adsorption of inert gas atoms are discussed on the basis of these results.

First the controversy in the literature is analyzed concerning the nature of the adsorption sites and the way of packing of Xe adatoms on the metal surface at high coverage (chapters VI and VII). From the variation in the initial heat of adsorption with the tip region it is concluded that at low coverage Xe is adsorbed in specific surface sites which provide a maximum coordination of the adatom with metal atoms. The extremely small decrease in heat of adsorption with coverage proves that on the rough faces site adsorption remains preferred to the formation of a close-packed layer up to the highest Xe pressure used in our experiments ($\sim 10^{-7}$ Torr). On the smooth regions (111) and (100), however, the heat of adsorption decreases strongly with coverage. It is argued that on these faces a close-packed Xe layer is formed at high coverage. These results are of relevance for surface area determinations by means of "physical" adsorption.

The nature of the bonding between Xe and transition metals is discussed in chapter VIII. It is shown that the bonding can certainly not be described in terms of mere dispersion forces.

A model frequently used for explaining the large surface potential of Xe, assuming a classical polarization of Xe in a hypothetical surface field combined with dispersion force interaction is also rejected. In this respect the following facts are relevant:

- 1) The model is unable to explain the high heats of adsorption on Group VIII metals as measured in this work.
- 2) It fails to explain the observed interdependence of the heat of adsorption and the surface potential.
- 3) It predicts the wrong sign for the adsorption dipole.

Our results

- (a) the linear proportionality of surface potential and heat of adsorption,
- (b) the relatively strong bonding of Xe on crystal faces with a high work function and
- (c) the measured values for the heats of adsorption of Xe on various transition metals are in excellent agreement with a model which describes the

bonding between Xe and the metal as a charge transfer-no bond interaction.

It appears thus that the adsorption of inert gases on a transition metal surface is apparently a weak chemical adsorption according to the definition given in the introduction since electron transfer takes place.

Chapter I

GENERAL INTRODUCTION

The work described in this thesis deals with the adsorption of nitrogen and xenon on surfaces of metals of the Groups VIII and Ib of the periodic system of the elements. The main objective is to identify the nature of the adsorption bond between gas atoms and the surfaces of transition metals. Since it is clear that this interaction may depend on both electronic (chemical) and geometrical effects, the present work is based on the strategy to separate these two variables. This is achieved by (1) studying the adsorption of a given gas on different crystal faces of a given metal single crystal, i.e. to vary the geometry in a known manner and (2) comparing the adsorption of the same gas on different metals, in particular on the corresponding crystal faces or on films of comparable face distribution in their surface. The techniques used are field electron emission microscopy and photoelectron emission. In this introductory chapter some principles of gas adsorption on metals are given and the potentialities of field electron emission microscopy for the investigation of adsorption on metals are discussed.

1. Adsorption of gases on metals

A chemical reaction between a solid and a gas is generally preceded by adsorption of the gas on the surface of the solid. It is, therefore, evident that adsorption studies will contribute to a better understanding of all the elementary processes taking place at the solid-gas interface. This kind of studies is thus of fundamental importance for all branches of science and technology dealing with surfaces, such as surface science in general, ultra-high vacuum technology, space research, electron emission by metals, thin film technology, heterogeneous catalysis, corrosion phenomena and problems in lubrication, purification of gases and air pollution.

During the last 15 years an important progress was achieved in the study of the adsorption of gases on metals. This is partly due to the improvement in ultra-high vacuum technology. Nowadays the production of vacua with a residual gas pressure $< 10^{-11}$ Torr has become a standard procedure. This enables us to keep an originally clean metal surface free from contaminants during a time period large enough for studying specific surface properties of the bare surfaces and for investigating the adsorption of a chosen gas on the surface without contamination from background gases.

Numerous techniques have been developed for the investigation of gas adsorption by a metal surface. We mention here:

- 1) Methods based on monitoring the change in a physical property of the metal brought about by the adsorption. Examples are measurements of the work function, the magnetic moment and the electrical conductivity of thin metal layers.
- 2) Methods based on the direct recording of the change in the number and the nature of molecules in the gas phase or on the metal by adsorption and/or desorption. This category comprises methods as the determination of the heat of adsorption by calorimetry or indirectly by determination of isosteres; thermal desorption spectroscopy; measurements of the sticking coefficients and isotope-exchange methods.
- 3) Other useful techniques for adsorption studies on metals are Auger electron spectroscopy; infrared spectroscopy and low-energy electron diffraction.

Each of these experimental techniques has its specific advantages and limitations.

While due to the present ultra-high vacuum technique a clean metal surface can be maintained in an uncontaminated state for a reasonable time, the production of a clean metal surface is still encountered by severe difficulties. The most commonly used cleaning methods are

- 1) heating to a temperature where the impurities are evaporated, or where they diffuse from the surface into the bulk.
- 2) the deposition of films by sublimation from thoroughly degassed samples.
- 3) cleaning by chemical means, such as oxidation and subsequent reduction.
- 4) bombardment with chemical non-reactive ions or electrons with high kinetic energy.
- 5) field desorption and field evaporation. With the former technique surface impurities are removed from the metal surface under the action of a

high electric field. By means of field evaporation several surface layers can be "peeled off" in a controlled way so that a clean surface is obtained which is ideally ordered on an atomic scale. However, the field strength required for this process is so high, in the order of 5 V/\AA , that this method is in practice limited to needle shaped specimens with a tip radius of not more than about 1000 \AA .

The most commonly used technique for cleaning bulk metal samples, such as filaments, ribbons and single crystal planes, is method (1). This technique is, however, only satisfactory with a small number of metals, as can be concluded from the results obtained with methods of surface analysis such as Auger electron spectroscopy. Mostly a combination of different cleaning methods is required for producing a truly uncontaminated surface, e.g. a combination of 1) with 3), 4) or 5).

Numerous experimental results prove that a gas may be bonded in widely different ways on a given metal surface, so that at a high coverage several adsorption complexes can be distinguished. These are often discerned by different heats of adsorption, infrared absorption bands, or work function changes; sometimes even the sign of the dipole moment is reversed. One obvious reason for the coexistence of several adsorption states on a given surface is the presence of various crystal planes on the surface. The environment of the surface metal atoms differs considerably for different crystal planes of a metal lattice. It may, therefore, be expected that adsorption depends strongly on the crystal plane, as is manifested by a pronounced face specificity in heat of adsorption, dipole moment, infrared absorption band etc. Single crystal planes are, therefore, of essential importance for adsorption studies.

This holds also for studies on heterogeneous catalysis. Metal catalysts are mostly prepared by deposition of the metal on a high-area carrier. The influence of the carrier and the metal dispersion on the specific activity of supported metals is a controversial subject in catalysis. The catalyst preparation can influence the size of the active particles and consequently their surface structure as pointed out by Van Hardeveld et al.¹. In this way the catalytic activity per unit surface area and even the selectivity for a reaction might be varied. Similar particle size effects were also reported for adsorption of simple gases on supported metals. A fundamental study of the adsorption of simple gases on well defined crystal planes is, therefore, also of essential importance for the interpretation of part-

ticle size effects in catalysis.

Up to now most adsorption studies have been carried out on polycrystalline samples exposing various crystal faces each with an unknown contribution. In the study described in this thesis a technique is used which provides the unique opportunity to study separately all faces of a metal single crystal under identical experimental conditions: the field emission probe-hole technique. For this reason it is an ideal technique for studying the crystal face specificity of gas adsorption on metals.

Conventionally adsorption is divided into two different classes, viz. physical adsorption, the bonding being due to the weak Van der Waals' dispersion forces and chemisorption in which a chemical bond between the adsorbent and adsorbate is formed. Physical adsorption is similar in nature to the condensation of an inert gas on the surface of its own crystal or liquid. Ideally, the best criterion to distinguish these two types of adsorption is that in chemisorption electron share or electron transfer takes place between adsorbent and adsorbate while these effects are absent in physical adsorption. Experimentally it is sometimes difficult to decide which kind of adsorption is operating. Criteria based on the heat of adsorption e.g. have no general validity since heats of chemisorption are sometimes comparable in magnitude to heats of physical adsorption. The adsorption systems described in this thesis are characterized by a rather low heat of adsorption and are thus examples of systems where the nature of adsorption cannot be identified from the heat of adsorption only.

2. Field electron emission microscopy

Field electron emission is based on the quantum mechanical phenomenon of tunneling of electrons through a narrow potential barrier. A high external electric field of $0.2 - 0.5 \text{ V/\AA}$ with its negative pole at the metal is applied in order to reduce the width of the potential barrier at the surface to such an extent that electrons near the Fermi level of the metal can tunnel through this barrier. The high electric field required for this type of electron emission is easily attained with a relatively low voltage when the emitting material has the form of a tip with small radius of curvature. In the field emission microscope, invented in 1937 by E.W. Müller, a sharp metal tip with a radius of curvature of the order of 1000 \AA is placed opposite to an electrically conductive fluorescent screen. A field emission microscope used in this study for preliminary measurements is shown in Fig. 1.

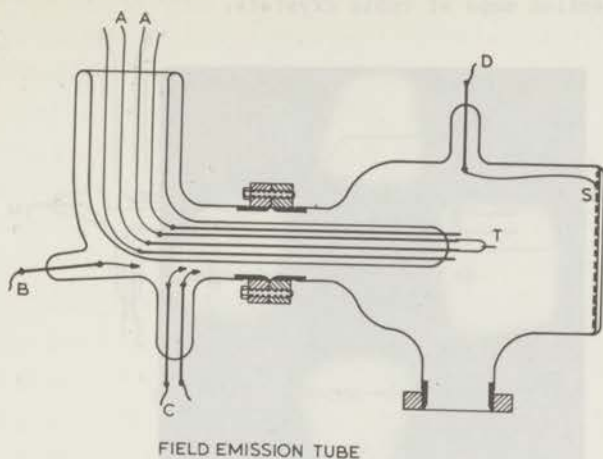


Fig. 1

A tip with such a small radius is nearly always part of a single crystal since its dimensions are smaller than those of the crystallites usually constituting the metal wire. The surface of a cleaned tip approximates a hemispherical shape. This implies that the tip surface will exhibit various crystal faces, differing in surface structure and consequently in electron work function. Stable, smooth faces characterized by a high electron work function appear beside unstable, atomically rough faces with a lower work function. The electrons leaving the tip under the action of the high negative potential follow the lines of force which are orthogonal to the surface. Consequently, the emitted electrons diverge radially outwards from the tip to the anode, i.e. the screen. Upon striking the fluorescent screen the electrons produce a highly magnified image of the emitting tip surface, approximately according to a stereographic projection. A magnification factor in the order of 10^6 and a resolution of about 20 \AA can be achieved when using metal tips with radii in the order of 1000 \AA . The work function of a tip area strongly influences the number of electrons emitted by that area. The electron image on the screen shows, therefore, a symmetrical pattern of bright and dark areas corresponding to the crystal face distribution on the tip surface. Figure 2 shows a field electron image of a clean tip of Ir, having the face centered cubic (f.c.c.) lattice structure. The important crystal faces can easily be identified to certain areas on the image from

the symmetry of the pattern. All other areas can be indexed with the aid of stereographic projection maps of cubic crystals.

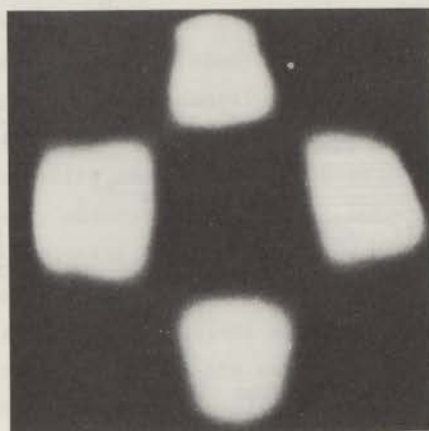


Fig. 2

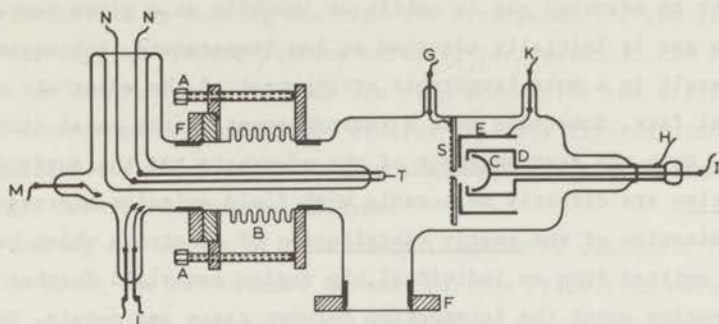
Field emission pattern of iridium

An important improvement of the technique was achieved by the development of the so-called probe-hole technique, where the emission current from a small segment of a selected crystal face on the surface is selectively diaphragmated out of the total electron beam and is measured. This method was already proposed in 1943 by Müller but was only applied to adsorption studies in the last ten years. Basically a field emission probe-hole tube may be considered as a conventional field emission microscope with two important alterations:

- 1) The introduction of a minute hole in the centre of the fluorescent screen behind which an electron collector is mounted.
- 2) The electron current from the desired tip region can be directed into the hole either by means of deflection of the electron beam by an adjustable magnetic or electric field or by mechanical shifting of the tip with the aid of a manipulator as in the present work.

The tube constructed by us for this study is shown schematically in Fig. 3. An extensive description of the tube is given in chapter II. The main advantage of the probe-hole technique is that each individual tip region is accessible for studies by means of the electrons emitted by that tip area. It provides us, therefore, with the unique opportunity to study separately all

crystal faces of a metal under identical experimental conditions.



FIELD EMISSION PROBE-HOLE TUBE

Fig. 3

It is beyond the scope of this thesis to describe here all potentialities of field electron emission. Only those applications which are based on the changes in the electron emission properties of a metal brought about by gas adsorption will be mentioned:

- a. When the emission currents of the individual faces are measured at different values of the field strength, both before and after gas adsorption, the change in work function ($\Delta\phi$) due to adsorption can be determined for each crystal face with the aid of the Fowler-Nordheim equation, given in chapter II. $\Delta\phi$ provides direct information on the sign of the dipole moment associated with the surface bond.
- b. Determination of the heat of adsorption (Q) of a gas on each crystal face of the metal. Two different kinds of measurements are possible.
 - (1) Determination of the activation energies for adsorption and desorption from the temperature dependence of the rate of adsorption and desorption of the gas.
 - (2) Determination of the heat of adsorption from a set of adsorption isosteres.
- c. Diffusion of adsorbed gases over metal surfaces. Initially one side of a field emission tip, cooled to a very low temperature, is covered with the adsorbate. By gradually warming the tip it is possible to measure the temperature where migration of the adsorbate sets in. Diffusion rates can be measured on different crystal faces and different temperatures

thus allowing the determination of the activation energy for diffusion on several tip regions. In this way it is also very easy to examine whether an adsorbed gas is mobile or immobile at a given temperature.

- d. When a gas is initially adsorbed at low temperature, subsequent heating may result in a more favourable arrangement of the adsorbate over the crystal face. Sometimes even a rearrangement of the metal atoms takes place. Both the rearrangement of the adsorbate and the surface reconstruction are directly measurable with field emission microscopy.
- e. Determination of the energy distribution of electrons which have been field emitted from an individual tip region can yield further valuable information about the interaction between gases and metals. Up to recently most work in this field was devoted to clean surfaces, we mention the determination of absolute work functions using both the total energy distribution and the Fowler-Nordheim plot; the information obtained about the electron band structure and about specific surface states on solids. Recently an increasing interest is noticed in the application of this technique for adsorption studies. Especially the phenomenon of field emission resonance tunneling is interesting since it can provide information about the atomic states of adsorbed molecules and can therefore stimulate theoretical studies of the adsorbed state.

In conclusion it can be said that field emission microscopy is a very powerful tool for adsorption studies. Especially the possibility of studying adsorption on various well defined crystal faces under exactly identical conditions allows in a very direct way the determination of the crystal face specificity in adsorption processes. It is an advantage that the cleanliness of the surface prior to an adsorption experiment can simply be checked by visual observation of the emission image. By utilizing field desorption and field evaporation as a cleaning method for the metal tip well ordered crystal faces are prepared with the same perfection as in the bulk. Field emission microscopy is also in this respect superior to other methods. The surface perfection can, moreover, be checked by employing the field emission tube as a field ion microscope². This is achieved by surrounding the specimen tip with an inert gas, usually helium, and reversing the polarity of the high field between tip and screen. If this field is high enough - roughly a factor 10 higher than in the usual field electron emission tube - the inert gas atoms are ionized at the protruding surface atoms. Ions thus formed are radially accelerated towards the fluorescent

screen where they produce a very faint but highly enlarged image of the protruding surface atoms of the tip. A resolution of 2 \AA can easily be attained with this technique by cooling the tip. The arrangement of the surface atoms can thus directly be viewed; lattice defects, for instance, can be made visible on an atomic scale. Despite its high resolution the utility of the field ion microscope for adsorption studies is still limited since the very high electric field necessary to ionize the image gas (for helium 4 V/\AA) can strongly interfere with the adlayer.

During the course of this study it appeared desirable to obtain information about the differences between various transition metals in their adsorption of nitrogen and xenon. Although these data can be obtained by field emission microscopy, the measurements would take a great deal of time. Since for these measurements it was not considered essential to work with single crystals, another experimental technique was chosen for these studies, viz. photoelectron emission from thin metal films. This technique has been extensively described in recent dissertations of our laboratory^{3,4}, we, therefore, refrain from repeating this here.

3. Outline of the present study

In this work a number of adsorption studies are described: adsorption of xenon and nitrogen on several transition metals. The thesis consists of a number of chapters, being reprints of publications or manuscripts of publications submitted to scientific journals. The different subjects in this thesis are, therefore, introduced and discussed separately in the relevant chapters.

Chapters II, III and IV deal with the adsorption of nitrogen on metals where this adsorption is non-dissociative, viz. platinum, iridium, rhodium and nickel. This study was done in view of recent results by Van Hardeveld c.s.^{1,5}, who had studied the adsorption of nitrogen on supported metals and concluded that this adsorption displays an extraordinary crystal face specificity.

Chapter II reports on the adsorption of nitrogen on different crystal faces of platinum as studied by field emission microscopy.

In chapter III results are given of a similar field emission study of nitrogen adsorption on iridium.

Chapter IV describes work on the change in the photoelectric work function

of nickel, rhodium and platinum films by nitrogen adsorption as a function of the temperature of previous annealing of the films.

Chapters V - VIII report on investigations of the adsorption of xenon on transition metals.

Chapter V deals with the change in work function of metal films upon xenon adsorption as a function of the temperature of presintering.

In chapter VI results are presented of a field emission study of xenon adsorption on different crystal faces of iridium.

In chapter VII results are given of a similar field emission study of xenon adsorption on platinum.

In chapter VIII a study is described in which the change in work function and the heat of adsorption of xenon were determined on various transition metals.

It has long been recognized^{6,7} that the inert gas - metal bond cannot be understood by assuming the adsorption as due entirely to dispersion forces. A satisfactory description of the interaction not being available, this study was undertaken in order to obtain data relevant to the problem. With this objective in mind a systematic investigation has been carried out of xenon adsorption on a number of metals and, in particular, on some well defined crystal faces of these metals.

Chapter IX contains a general discussion on the nature of the adsorption of nitrogen and xenon on transition metals.

References

- 1) R. van Hardeveld and A. van Montfoort, *Surface Sci.* 4 (1966) 396.
- 2) E.W. Müller and T.T. Tsong, "Field Ion Microscopy", Elsevier, New York, 1969.
- 3) Th.G.J. van Oirschot, Thesis (1970), Leiden.
- 4) R. Bouwman, Thesis (1970), Leiden.
- 5) R. van Hardeveld and F. Hartog, *Advan. Catalysis* 22 (1972) 75.
- 6) J.C.P. Mignolet, *Disc. Faraday Soc.* 8 (1950) 105.
- 7) J.C.P. Mignolet, in "Chemisorption" (W.E. Garner, ed.) p. 118, Butterworths, London, 1957.

Chapter II

CRYSTAL FACE SPECIFICITY OF NITROGEN ADSORPTION ON A PLATINUM FIELD EMISSION TIP

B. E. NIEUWENHUYS and W. M. H. SACHTLER

Gorlaeus Laboratoria, Rijksuniversiteit, Leiden, The Netherlands

Received 5 June 1972; revised manuscript received 16 August 1972

The adsorption of nitrogen on platinum is studied with a field emission microscope equipped with a probe-hole assembly to enable quantitative emission measurements on individual crystal faces. The results are implemented by photoelectric measurements on platinum films. Adsorption at 80 K is found to result in a large and face-specific decrease in the work function. On crystal planes containing B_5 and B_6 sites this decrease is larger than on those exposing B_3 and B_4 sites only. No significant crystal face specificity is found, however, for the rate of temperature programmed desorption of nitrogen. It follows that the heat of nitrogen adsorption is essentially equal for faces with B_3 , B_4 , B_5 and B_6 sites. This result is at variance with certain postulates in the literature.

1. Introduction

Numerous results obtained with LEED^{1,2)} and field electron and ion microscopy^{3,4)} established a distinct face-specificity for adsorption of gases by metal single crystals. It is therefore not surprising that face-specificity of adsorption has been invoked by many authors studying adsorption by supported metals or evaporated metal films in order to rationalize observations which are otherwise difficult to understand. The present paper examines such a case: adsorption of nitrogen by platinum. For nitrogen adsorption on nickel, palladium and platinum face-specificity had been postulated^{5,6)}, although it had never been ascertained by direct measurements on well-defined single crystals.

Several authors studied the adsorption of nitrogen on nickel. Before 1964 it was generally accepted that nitrogen is not adsorbed at room temperature at pressures below 10^{-2} Torr but adsorption has been observed at lower temperatures⁷⁻²¹⁾. The reported heat of adsorption is 10 kcal/mole decreasing to 3-5 kcal/mole at high coverages^{13,15)}.

New research was stimulated by results of Eischens and Jacknow²²⁾ in 1964. These authors found a strong infrared absorption band at 2202 cm^{-1} at room temperature and a nitrogen pressure of at least 10^{-2} Torr. This

band was attributed to the N-N stretching vibration of nitrogen chemisorbed in the structure $\text{Ni-N}\equiv\text{N}^+$. Van Hardeveld and Van Montfoort⁵⁾ found that the 2202 cm^{-1} band on supported nickel and similar infrared bands on palladium and platinum are only observable if the diameter of the metal crystallites is within the range of 15–70 Å. According to these authors particles with diameters in this range possess a considerable concentration of special sites, "B₅-sites", in their surface which are negligible in larger particles. The infrared active species was assigned to adsorption on these sites. These B₅-sites for which an adatom with the same diameter as the metal atom is contacting five metal atoms are present on rough planes as (110) and (113). Also for nitrogen on silica supported iridium an infrared absorption band in the 2200 cm^{-1} range has been reported²³⁾.

King²⁴⁾ investigated the nitrogen desorption spectra from nickel and palladium films deposited in ultra high vacua. For nickel he observed three states, γ_1 , γ_2 and γ_3 with binding energies <7 kcal/mole, 6–10 kcal/mole and 9–14 kcal/mole respectively. The γ_1 state was ascribed to adsorption on (111) planes, the γ_2 to the (100) plane and the γ_3 state to the (110) and higher index planes. On palladium only the γ_1 and γ_2 states were characterized.

In two recent publications by Bradshaw et al.^{25, 26)} a study of the adsorption of nitrogen on thin nickel films using the infrared transmission technique is described. Only in the case of films deposited onto a cooled rocksalt substrate in a nitrogen atmosphere a sharp band was obtained at about 2202 cm^{-1} . This band was absent, however, for nitrogen adsorbed on films deposited in ultra-high vacuum which showed a band at 2255 cm^{-1} with shoulders at 2230 cm^{-1} and 2180 cm^{-1} . As these films were about 50 Å thick this experimental result appears contradictory to the concept of Van Hardeveld and Van Montfoort. The question arises whether the simple correlation of infrared bands of adsorbed nitrogen with the relative concentration of B₅-sites resulting from a certain particle size is correct. The conflicting experimental evidence shows that a more direct study of the adsorption of nitrogen on fcc metals with well-defined surface structure is highly desirable.

AIM OF PRESENT WORK

Briefly speaking, we want to get an answer to the question: is there really a structure sensitive nitrogen adsorption on nickel, palladium and platinum? More in particular: is nitrogen adsorbed on B₅-sites more strongly than on sites present on the (111) and (100) planes?

For this purpose a field electron microscope provided with a probehole was used to study the adsorption of nitrogen on different crystal faces of a metal tip. For the present purpose it is not so important which of the metals nickel, palladium and platinum is used as adsorbent as Van Hardeveld c.s.⁵⁾

showed that adsorption of the infrared active species on these metals is very similar. We selected platinum as the adsorbing metal because literature data suggest that a platinum tip is less difficult to clean than a nickel tip.

Beside the main objective stated, this study comprises measurements of the relative work function of some crystal planes of platinum which to our knowledge has never been measured before.

Some nitrogen experiments were carried out on unsintered and sintered thin platinum films using the photoelectric method in order to get a more complete picture of the nature of nitrogen adsorption on different platinum samples.

2. Experimental

2.1. APPARATUS

The tube used for measuring field emission from individual crystal faces is schematically shown in fig. 1. A platinum tip is spot-welded on a platinum heating loop of 0.2 mm in diameter. The tip assembly is mounted on tungsten

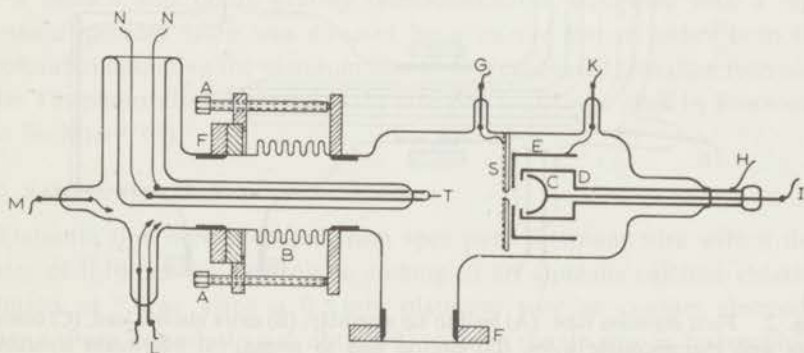


Fig. 1. Field emission probe-hole tube: (A) adjusting screws, (B) bellows, (C) collector, (D) shield, (E) lens electrode, (F) flange, (G) electric lead to screen, (H) electric lead to shield, (I) Kovar rod connected with collector, (K) electric lead to lens electrode, (L) connection with thermocouple wires, (M) extra electric lead, (N) lead to tip assembly, (S) fluorescent conductive screen, (T) tip assembly.

rods which are led through a dewar, normally filled with liquid nitrogen and welded to gold wires. A pair of $1\frac{1}{2}$ in. \times $2\frac{3}{4}$ in. conflat flanges permits an easy replacement of the emitter.

The glass screen is coated with stannous oxide and willemite rendering it conducting and fluorescent. A hole in the centre of the screen (diameter 1.5 mm) serves as a diaphragm to the electrons emitted from the tip. The emitter can be positioned in the desired direction by means of stainless steel bellows and three adjusting screws, thus allowing the image of the

selected crystal face to be centred on the probe-hole. The electrons emitted by this area pass through the hole and arrive at a hemispherical collector, connected with a Kovar rod which is in direct contact with the electrometer. An auxiliary electrode, the "suppressor" prevents that scattered electrons and secondary electrons released from the screen can reach the collector and that secondary electrons which may originate inside the collector can escape. A Faraday cage cylinder surrounding the collector is directly connected with a Kovar tube around the Kovar rod and is in contact with the screen of a rigid coaxial line to the electrometer preamplifier. In this way an almost perfect shielding of the collector and other electrometer connections from stray fields is obtained. Collector, suppressor and the shielding cylinder were

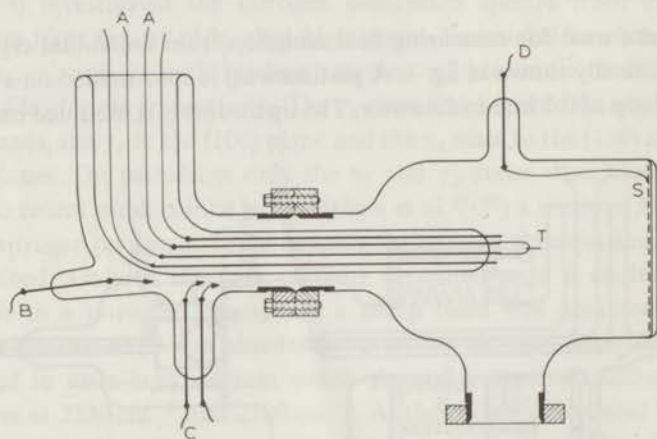


Fig. 2. Field emission tube: (A) lead to tip assembly, (B) extra electric lead, (C) connection with thermocouple wires, (D) electric lead to screen, (S) fluorescent conductive screen, (T) tip assembly.

made from stainless steel coated with a gold layer. The electrode assembly of the tube is also suitable for electron energy distribution measurements.

The tip can be brought to any desired temperature above 78 K by heating the loop electrically. The temperature of the loop, as a function of the heating current was calibrated using chromel-alumel thermocouple wires (not completely drawn in fig. 1). These are connected with fused tungsten rods which can be cooled with melting ice to form a cold reference junction. For our purpose this temperature measuring method appeared to be more convenient than the usually applied calibration of the resistance of a small section of the emitter supporting filament versus the temperature.

For some measurements a simpler field electron microscope without

probe-hole device was used (fig. 2). Most pictures shown below were made with this tube.

The field electron microscope was connected to an ultra-high vacuum system. After baking the whole system at a temperature of about 700 K pressures below 10^{-10} Torr are easily obtained with the aid of a Varian 50 l sec^{-1} Vac-Ion pump.

Nitrogen with an impurity level below 10^{-5} is further purified before entering the field emission tube by the use of freshly deposited nickel films in the supply system.

Total emission and collector currents were measured with Cary 401 vibrating reed electrometers. A Hewlett-Packard digital voltmeter was used for the output readout of the electrometer. High voltage for field desorption and field evaporation was supplied by a Brandenburg 2–30 kV dc stabilized power supply. An ultra-high stable 0–6 kV power supply (Power Designs model 1556) was used in the electron emission experiments.

For the photoelectric measurements a narrow light beam monochromatized by a Bausch and Lomb grating monochromator, equipped with a high pressure mercury lamp was directed by a mirror system either onto the phototube containing the platinum film or to a calibrated tantalum reference tube. The phototube is identical to the tube previously described by Bouwman and Sachtler^{27,28}).

2.2. SAMPLE PREPARATION AND CLEANING

Platinum tips were prepared from spec pure platinum wire with a diameter of 0.10 mm by electrolytic etching in an aqueous calcium chloride solution at 5 V ac using a 0.5 mm platinum wire as counter electrode. After a sharp smooth tip was obtained, washing the tip wire in hydrochloric acid, sometimes even electropolishing the whole assembly in hydrochloric acid, was necessary to prevent spurious emission from solid etching products stuck on the tip wire.

Data in the literature show that it is very difficult to obtain thermally cleaned platinum tips^{29–33}). We, therefore, utilized field desorption and field evaporation at room temperature to clean the tip after heating to 900 K. This method was very convenient because our adsorption experiments do not require temperatures above room temperature where diffusion of contaminants to the emitter surface might occur. Field evaporation at liquid nitrogen temperature will produce more ideal ordered surfaces but for our purpose field evaporation at room temperature was sufficient and preferred because chances of tip rupture were found larger with low temperature field evaporation.

The platinum films were evaporated from beads on specially shaped

tungsten filaments. After pre-evaporation of some platinum and volatile contaminants with the cathode being shielded by a magnetically movable shutter, a platinum film was deposited on the cathode at 80 K.

3. Results and discussion

3.1. WORK FUNCTIONS OF SINGLE CRYSTAL PLANES OF PLATINUM

Fig. 3 shows two field emission patterns of platinum tips cleaned by field desorption and field evaporation at room temperature. The principal crystal faces are indicated in the pictures. The patterns are different from other field emission pictures in the literature, made from thermally cleaned

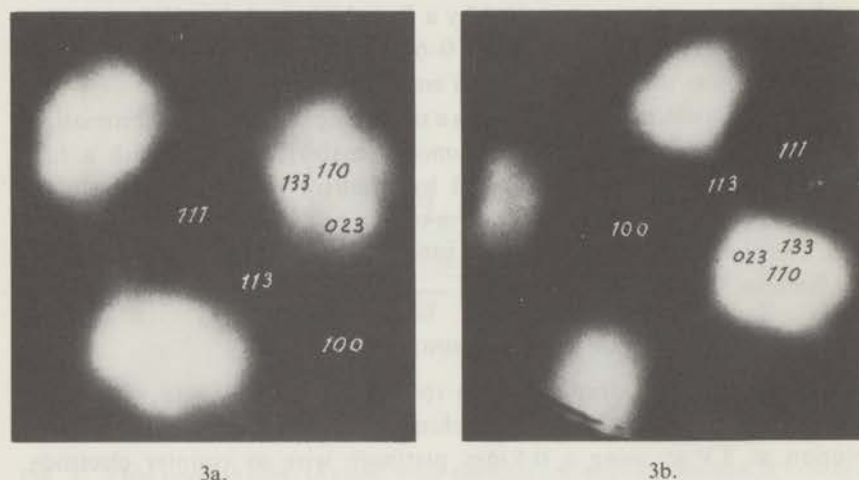


Fig. 3. Field emission from (a) {111} and (b) {100} oriented platinum tips formed by field evaporation at 300 K.

platinum emitters. In our tips the (110) faces are hardly visible as dark areas. Separate experiments showed that the (110) faces are better developed when field evaporation is carried out at 80 K. A similar relationship between temperature of field evaporation and development of certain faces was observed by us for tungsten and molybdenum. This observation will not be further discussed in the present paper.

Work functions were determined from the Fowler-Nordheim equation written as:

$$\ln i/V^2 = \ln A - B\Phi^3/V, \quad (1)$$

where i is the emission current at an applied voltage V between tip and screen, $\ln A$ is the pre-exponential term which is field independent, Φ is the work

function and B is usually a constant containing besides some universal constants the field voltage proportionality C :

$$F = CV; \quad (2)$$

C is inversely proportional to the radius of curvature r of the emitting area:

$$C = 1/Dr, \quad (3)$$

where D depends on the tip shape and slightly on the polar angle. The slope of the Fowler-Nordheim plot obtained by plotting $\ln i/V^2$ versus $1/V$ may be calculated for various tip faces and for the total emission. Fig. 4 shows an example of F-N plots for the total emission from a platinum tip, for the (100) face of this tip and for the total emission and (100) face after adsorption of nitrogen at 78 K.

The values of B must be known for the determination of the work function of different tip areas. In first approximation B is constant for all

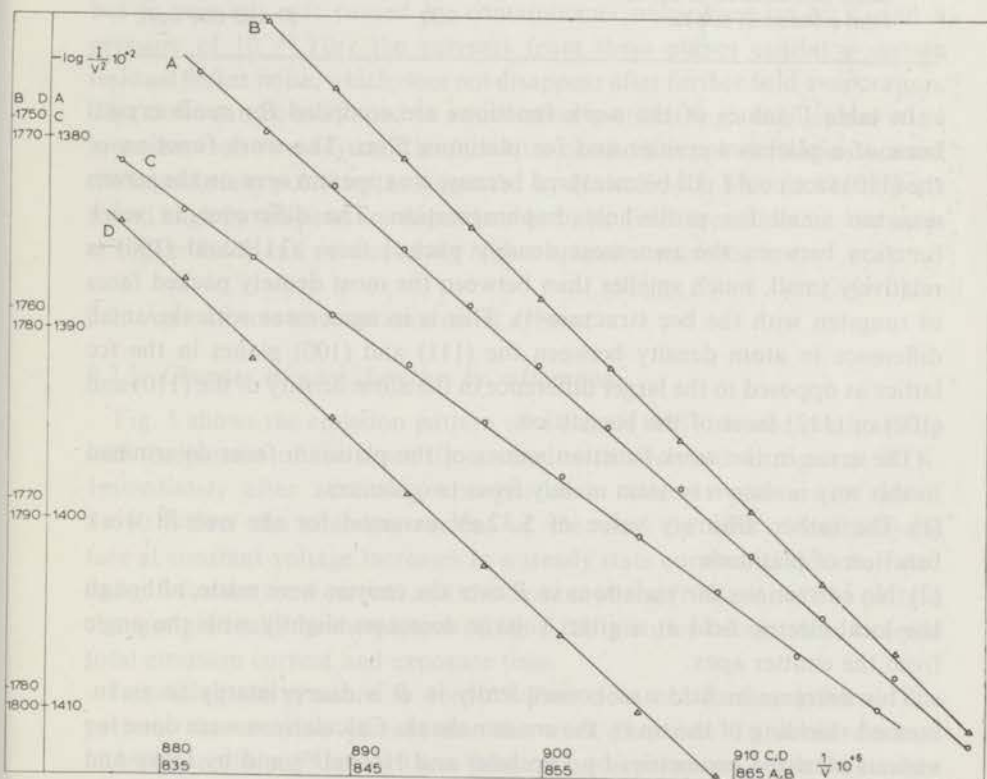


Fig. 4. Fowler-Nordheim plots for the total surface (A, C) and (100) face (B, D) clean and nitrogen covered.

tip faces. B may then be determined from the slope of the F - N plot for a plane with known work function or from the slope of the F - N plot for the total tip and an average work function. No work functions for any of the crystal faces of platinum being known, we followed Lewis and Gomer³³) by assuming an average work function of 5.32 eV for the total emitting area.

TABLE I

Work functions of some crystal faces of a platinum field emitter and of platinum films

Substrate	Work function (eV)	Reference
Total field emitter	5.32	This work
field emitter (111) face	5.93	This work
field emitter (100) face	5.84	This work
field emitter (331) face	5.12	This work
field emitter (320) face	5.22	This work
Film freshly evaporated at 80 K	5.45	27 and this work
Same film sintered at 300 K	5.63	27 and this work
Film sintered at 600 K	5.72	27 and this work

In table I values of the work functions are compiled for some crystal faces of a platinum emitter and for platinum films. The work function of the (110) face could not be measured because its apparent area on the screen was too small for probe-hole diaphragmation. The difference in work function between the two most densely packed faces (111) and (100) is relatively small, much smaller than between the most densely packed faces of tungsten with the bcc structure³⁴). This is in agreement with the small difference in atom density between the (111) and (100) planes in the fcc lattice as opposed to the larger difference in the atom density of the (110) and (100) or (112) faces of the bcc lattice.

The error in the work function values of the platinum faces determined in this way is shown to stem mainly from two sources:

- (1) The rather arbitrary value of 5.32 eV assumed for the overall work function of platinum.
- (2) No corrections for variations in B over the emitter were made, although the local electric field at a given voltage decreases slightly with the angle from the emitter apex.

This decrease in field and consequently in B is due primarily to an increased shielding of the tip by the emitter shank. Calculations were done for various idealized geometries by Drechsler and Henkel³⁵) and by Dyke and Dolan³⁶). It is possible to estimate the variation in B with apex angle as our measurements were carried out with both (111) and (100) oriented platinum

tips. So it appears that the differences in the uncorrected values of the work functions obtained with different oriented tips are mostly within the measuring accuracy. The estimated error in the values of table I is 0.05 eV disregarding a possible error in the assumed value of 5.32 eV of the overall work function.

In the immediate vicinity of the actual (111) and (100) faces lower values for the work function were measured, for instance, 5.6 eV for the tip areas near (111). It appears thus that the local radius of these densely packed planes is relatively small in the field evaporated tips, much smaller than in thermally cleaned tips. This is in agreement with field ion micrographs: thermally annealed tips exhibit large low index planes and low temperature field evaporated tips show small flat low index planes surrounded by terraces with the same atom arrangement.

The probe-hole currents from the (111) and (100) planes are very stable but high index planes exhibit a flicker noise in the probe current. This is strongly increased by the presence of very small amounts of contaminants, but is certainly not caused by contaminants only. Even at 80 K and a pressure of 10^{-11} Torr the currents from these planes exhibit a certain residual flicker noise, which does not disappear after further field evaporation. This noise can be attributed to minor atom motions, e.g., oscillations of an atom between two adjacent surface sites or short range oscillation around the equilibrium positions as suggested by Holscher³⁷). This flicker noise is found slightly temperature dependent but also field dependent: it increases at higher fields and consequently higher emission currents.

3.2. ADSORPTION OF NITROGEN ON PLATINUM

3.2.1. *Changes in work function by adsorption*

Fig. 5 shows the emission pattern of a clean {111} oriented platinum tip and the pattern of the same tip covered with adsorbed nitrogen at 80 K. Immediately after admitting nitrogen at a constant pressure of about 1×10^{-8} Torr the emission current of the total tip and of each crystal face at constant voltage increases to a steady state current, as demonstrated in fig. 6 for the total current and the current of the (100) plane. The pattern changes gradually to the picture of fig. 5, all pictures being taken at equal total emission current and exposure time.

Increasing the pressure to 1×10^{-6} Torr does not further influence the pattern, the emission current nor the work function. To avoid electron molecule collisions during these adsorption experiments, care was taken that the total emission current never exceeded 5×10^{-9} A. This precaution is important because nitrogen molecules will form N_2^+ ions which can

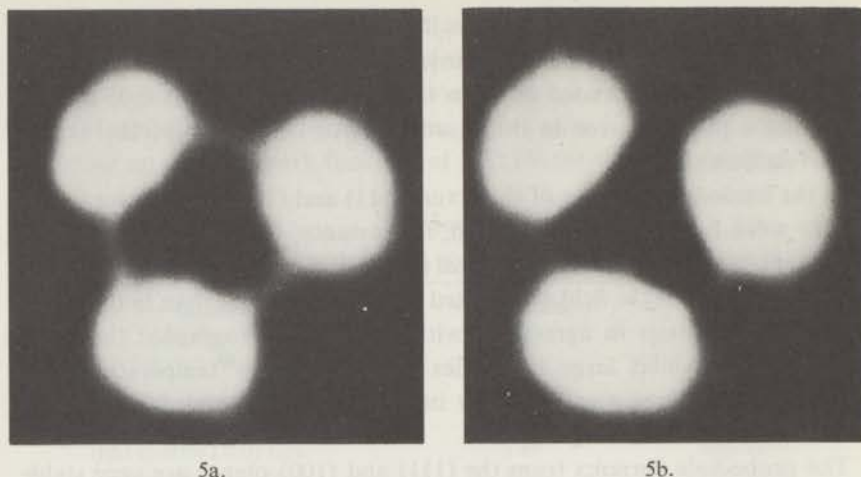


Fig. 5. Field emission from platinum (a) before and (b) after nitrogen adsorption at 80 K.

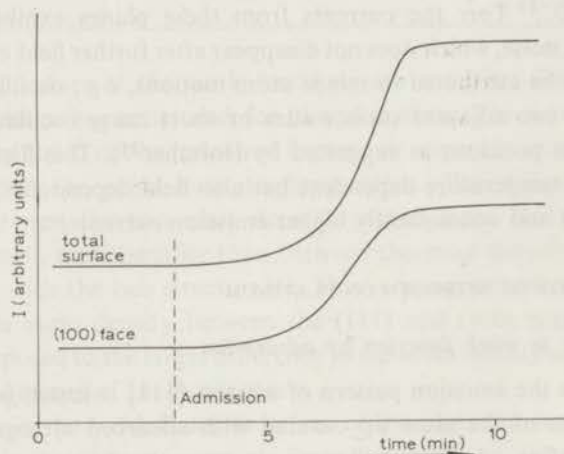


Fig. 6. Change in field emission current, at constant voltage by nitrogen adsorption at 80 K.

markedly influence the adsorption of nitrogen on metals as shown by Winters^{38,39}).

Many of our adsorption experiments were carried out in the absence of an external electric field. Admission of nitrogen up to an equilibrium pressure of 10^{-3} Torr followed by pumping to pressures in the low 10^{-9} Torr range results in values for the surface potential identical to those obtained at 10^{-8} Torr in the presence of the electric field necessary for a field emission

current of about 5×10^{-9} A. Also the desorption characteristics did not differ for tips previously exposed to a nitrogen pressure of 10^{-8} or 10^{-3} Torr.

In table 2 some values are given for the change in work function caused by nitrogen adsorption at 80 K obtained with the F-N equation as described in the previous section and corresponding changes in the pre-exponential factor. Included are values for the changes in the work function of platinum films caused by nitrogen adsorption at 80 K determined by photoelectron emission and the corresponding changes in the emission constants.

TABLE 2

Changes in work functions, Fowler-Nordheim pre-exponential factors and Fowler emission constants by nitrogen adsorption on platinum at 80 K

Substrate	$\Delta\Phi$ (eV)	$\Delta \log A$	$\Delta \log M$
Total field emitter	-0.65	-1.2	
field emitter (111) face	-0.34	-0.5	
field emitter (100) face	-0.31	-0.6	
field emitter (331) face	-0.76	-1.6	
field emitter (320) face	-0.77	-1.7	
Film freshly evaporated at 80 K	-0.51		-0.26
Same film sintered at 300 K	-0.30		+0.09

These changes in work function are much larger than those reported for nickel films^{14, 16, 18}) and nickel tips¹⁹). They depend on the surface structure as nitrogen adsorption on (100) and (111) causes a smaller decrease in work function than on the strongly emitting faces of the platinum tip. This is in agreement with the change of the field emission pattern due to nitrogen adsorption. The area of the brightly emitting faces increases and the areas of the dark regions around (111) and (100) planes shrink slightly. The poorly developed (110) faces hardly visible in the clean pattern are almost unobservable after nitrogen adsorption.

As shown in table 2 the decrease in work function by nitrogen adsorption is smaller for films annealed at room temperature than for unsintered films. During sintering closely packed stable crystal planes grow at the expense of less stable planes. The work function of platinum films increases in this equilibration process. The variation of the decrease in work function with the sintering temperature is, thus, completely in line with the field emission results.

Nitrogen admission at room temperature up to about 10^{-6} Torr in field emission experiments and 10^{-3} Torr on films does not influence the emission constant nor the work functions. The field emission pattern does

not change either. Also nitrogen admission to 10^{-2} Torr in the field electron microscope and subsequent pumping to about 5×10^{-7} Torr fails to cause any changes in emission characteristics or patterns within experimental accuracy. All these data demonstrate that no adsorption of nitrogen occurs on platinum in these circumstances. Lowering the temperature to 80 K at these pressures does not cause any changes in emission characteristics and field emission pattern in addition to those described before. It appears, hence, that there is no adsorption hysteresis, characteristic for activated adsorption processes.

3.2.2. Desorption experiments

Thermal desorption of nitrogen adsorbed at 80 K from a field emitter leads to the complete reappearance of the pattern and the emission characteristics of the clean emitter. In order to get information about differences in binding energies of nitrogen on different crystal faces a temperature programmed desorption method was used. A nitrogen covered platinum tip was rapidly heated to a prefixed temperature and the change in emission current at constant voltage was followed as a function of time. After readsorption of nitrogen by decreasing the temperature to 80 K the above procedure was repeated several times with different desorption temperature programs and for different crystal faces. This principle had been used before by several authors who followed the change in field emission image upon desorption visually. In this way Rootsart et al.⁴⁰⁾ and Ehrlich⁴¹⁾ found distinct differences in desorption rate of xenon from the (111) and the (411) faces of

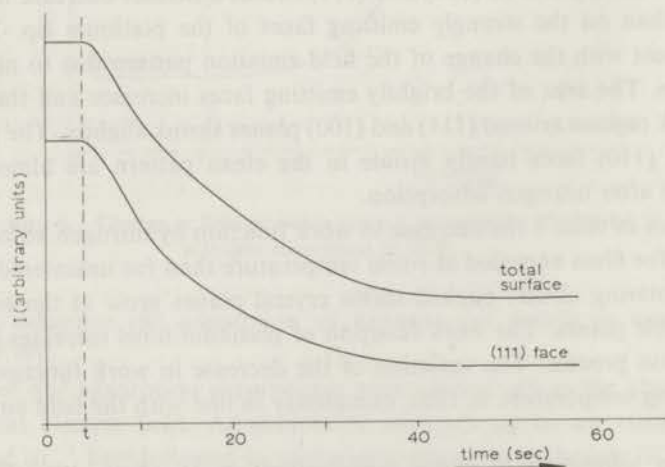


Fig. 7. Change in field emission currents at constant voltage of a nitrogen covered platinum tip after a rapid temperature rise from 80 K to 140 K.

tungsten. Introduction of the probe-hole is decisive to apply this method also for the investigation of the closely packed and, hence, low emitting crystal faces from which desorption cannot be studied by visual observation.

It was found that with a given crystal face the desorption time depends markedly on the heating current, as expected. When, however, different crystal faces are compared with identical heating programs, the desorption plots are equal. For illustration fig. 7 shows as an example two such desorption plots of nitrogen, one of the total emission and one of the (111) face, obtained after heating the tip to 140 K. Clearly, we must conclude that the rates of depletion are virtually equal for different crystal faces.

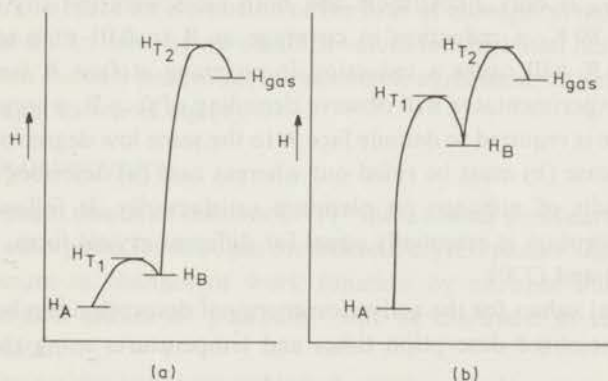


Fig. 8. Enthalpy diagram illustrating the relative enthalpies of the adsorbed states on two different crystal faces A and B, the transition states T₁ and T₂ and of the gaseous state.

For the evaluation of these results two alternative cases might be considered. Either (a) the heats of adsorption are almost equal on the faces considered or (b) there are large differences in heat of adsorption but as the adsorbate on different faces is in diffusional equilibrium desorption to the gas phase takes place from the faces of lowest heat of adsorption. The following considerations show, however, that the second alternative fails to explain the experimental results.

Case (a). The difference in heat of adsorption ($Q_{\text{ads}} = -\Delta H_{\text{ads}} = H_{\text{gas}} - H_{\text{ads}}$) on two faces A and B is small, $H_A \sim H_B$ (fig. 8a). In this case both faces become denuded at essentially the same temperature, the measured depletion plots will be essentially equal for A and B.

Case (b). The difference in heat of adsorption between two faces A and B is large: $-\Delta H_A > -\Delta H_B$. As in first approximation the standard entropies of adsorption may be assumed to be essentially non-face specific, this case implies also a large difference in the Gibbs free energies of adsorption on

the two faces considered, i.e. $G_A < G_B$ (see fig. 8b). Accepting diffusional equilibrium of the adsorbate on different crystal planes, the degrees of coverage θ_A and θ_B are related by the general relation

$$\frac{\theta_A}{1 - \theta_A} = \frac{\theta_B}{1 - \theta_B} \exp\left(-\frac{G_A - G_B}{RT}\right). \quad (4)$$

It follows from eq. (4) that in this case the coverage at face A remains high at the temperature where the coverage at face B is visibly reduced.

It is, perhaps, not superfluous to show with a simple numerical example that even for a relatively small difference in adsorption energy case (b) is strongly at variance with our experimental observation. Assuming e.g. that $G_B - G_A$ is only 2 kcal/mole and both faces were initially completely covered at 80 K, a reduction in coverage at B to 0.01 at a temperature rise to 120 K will cause a reduction in coverage at face A from 0.99 to 0.98. The experimenter will observe denuding of face B, whereas a higher temperature is required to denude face A to the same low degree of coverage.

Clearly, case (b) must be ruled out whereas case (a) describes the experimental results of nitrogen on platinum satisfactorily. It follows that the heat of adsorption is essentially equal for different crystal faces, e.g., (111), (100), (331) and (320).

Numerical values for the activation energy of desorption can be estimated from the measured desorption times and temperatures using the equation

$$r_{des} = \frac{kT}{h} \theta \exp \frac{\Delta S^*}{R} \exp \frac{-E_{des}}{RT}, \quad (5)$$

where r_{des} is the rate of desorption, k and h are Boltzmann's and Planck's constants, respectively and θ the degree of coverage. Making the usual Frenkel assumption $\Delta S^* = 0$, eq. (5) can be approximated by

$$E_{des} = RT \ln \left(\frac{kT}{h} \right) \tau_{des}, \quad (6)$$

where τ_{des} is the half-life value of the desorption process starting at full coverage. As the activation energy for adsorption is approximately zero, the calculated activation energy for desorption is nearly equal to the heat of adsorption.

The highest heat of adsorption estimated by application of equation (6) was 9 kcal/mole for all observed crystal faces: (111), (100), (331), (320) and for the total emission area. Further our desorption experiments indicate that the heat of adsorption at high coverages is not larger than 3 kcal/mole. So it appears that the heat of adsorption decreases markedly with the degree of coverage. The error in the value of 9 kcal/mole for the initial heat of

adsorption is mainly caused by the uncertainty in the validity of eqs. (5) and (6). In Frenkel's original equation⁴²⁾

$$\tau' = \tau_0 \exp \frac{-E_{des}}{RT}, \quad (7)$$

τ_0 was taken equal to 10^{-13} sec. De Boer^{43,44)} and Kruyer⁴⁵⁾ pointed out that the application of transition state theory can lead to values for τ_0 varying from 10^{-12} to 10^{-16} sec. This would mean an error in the estimated value of heat of adsorption of about 1–2 kcal/mole. Some authors reported values for τ_0 higher than 10^{-12} sec⁴⁶⁾. Although we did not perform accurate isochoric measurements it was possible by varying the pressure and the temperature to make an estimation of the heat of adsorption independent of eqs. (5) and (6). In this way we obtained values for the initial heat of adsorption between 7 and 9 kcal/mole, in reasonable agreement with the value obtained by application of eq. (6).

3.3. GENERAL DISCUSSION

The pertinent results of this work: (1) "there are no significant differences in heat of adsorption for nitrogen on different crystal planes" and (2) "there are differences in changes of work function by nitrogen adsorption on different crystal planes of platinum" will be discussed in relation with literature data.

Only a few articles have been published on nitrogen adsorption on platinum in comparison to the more extensively studied system nitrogen on nickel. For platinum Trapnell¹²⁾, Wiesendanger⁴⁷⁾ and Morgan and Somorjai⁴⁸⁾ found that no adsorption of nitrogen occurs on platinum films, filament and on a (100) plane, respectively, at 300 K and low pressures. These observations are, clearly, in agreement with our results. Rendulic and Knor⁴⁹⁾ found a considerable "nitrogen etch" on platinum at 80 K on a field ion microscope tip imaged with neon. Especially the (100) and (111) areas are attacked. These results were interpreted by assuming chemisorption of nitrogen atoms originating from molecules dissociated in the presence of the high electric field. Van Oostrom⁵⁰⁾ and Lewis and Gomer⁵¹⁾ showed that adsorption of gases on tungsten can be strongly influenced by the high electric field necessary for field ionization. These results do therefore not apply to the observations at much lower field described in the present paper. Coleman and Inkley⁵²⁾ found an appreciable adsorption of nitrogen on silica and alumina supported platinum at 300 K. This adsorption depended strongly on the nature of the platinum surface in agreement with the infrared studies by Van Hardeveld and Van Montfoort⁵⁾.

It is interesting to note that results on clean surfaces – films and FEM-

tips – show a pronounced difference between nitrogen adsorption on nickel, palladium and platinum. Ehrlich¹⁹) reports for nitrogen adsorption on a nickel tip a small decrease in work function, less than 0.1 eV whereas the present work reveals a decrease in work function by 0.65 eV for nitrogen on platinum. King²⁴) showed that nitrogen adsorption on films is different for nickel and palladium. On the other hand, Van Hardeveld and Van Montfoort⁵) concluded that the presence of the earlier mentioned infrared active nitrogen on the metals nickel, palladium and platinum dispersed on a support, depends more on the crystallite size than on the chemical nature of the metal. A comparison of the infrared data with the present work is therefore of interest.

The observations by Van Hardeveld and Van Montfoort⁵):

- (a) The infrared band on nickel, palladium and platinum is only observable on metal crystallites within the range $\sim 15 < d < 70 \text{ \AA}$.
- (b) Only a limited number of the adsorbed nitrogen molecules is infrared active.
- (c) The heat of adsorption on supported nickel with a mean particle size of 19 \AA is 12 kcal/mole falling to 2 kcal/mole at high coverage whereas the initial heat of adsorption on nickel with a mean particle size of 110 \AA is 5 kcal/mole were rationalized by these authors by assuming that nitrogen is adsorbed more strongly on B_5 -sites than on smooth faces such as (111) and (100) containing B_3 - and B_4 -sites.

The present results are, clearly, at variance with this postulate. The heat of adsorption is found roughly equal on all faces. Some of them, viz. (100) and (111), are bare of B_5 -sites, all other faces imaged in the field emission pattern do possess B_5 -sites or even B_6 -sites (see fig. 9).

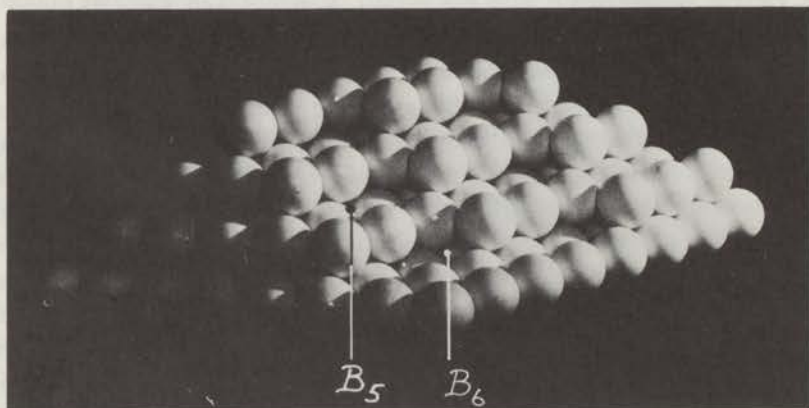


Fig. 9. Marble ball model of the (320) face with B_5 - and B_6 -sites.

First, the question arises whether the infrared active species observed by Eischens *c.s.*²²) and Van Hardeveld *c.s.*⁵) at high pressures and room temperature can be the same as those studied on single crystal tips at much lower pressures and temperatures. All observers consistently agree that adsorption is non-activated and reversible. In equilibrium the same degree of coverage of a given adsorption complex is present at two sets of conditions, p_1, T_1 and p_2, T_2 respectively, which are defined in fair approximation by the integrated isochore equation:

$$\ln \frac{p_1}{p_2} = - \frac{\Delta H_{\text{ads}}}{R} \left(\frac{1}{T_2} - \frac{1}{T_1} \right). \quad (8)$$

Upon inserting for $-\Delta H_{\text{ads}}$ our value of 9 kcal/mole which appears also to be in reasonable agreement with literature data on nickel (Van Hardeveld *c.s.* report: "below 12 kcal/mole"), eq. (8) shows that the same coverage would be expected for $p_1=25$ Torr, $T_1=293$ K and $p_2=10^{-7}$ Torr, $T_2=130$ K. We therefore conclude that the complexes studied at room temperature by their infrared bands on supported metals are directly comparable to those observed by FEM at 80 K but much lower pressures.

It seems to us that confrontation of the infrared data with the present results opens, in principle, three possibilities:

(1) The heat of adsorption of nitrogen on B_5 -sites is, indeed, equal for supported and unsupported platinum, but the heat of nitrogen adsorption on the smooth faces (111) and (100) is lower for the supported than for the unsupported ones. The question then arises: which physical phenomenon can explain the lowering of the adsorption energy on these crystal faces by supporting the metal? Possible causes to be discussed include metal/support interaction and contaminant effects.

(2) The heat of nitrogen adsorption (at low coverage) is fairly equal on all crystal faces for both supported and for unsupported samples, but only on certain crystal faces is the adcomplex able to absorb infrared light in the 2200–2300 cm^{-1} range.

If this hypothesis is correct the pertinent question arises which phenomena can explain this striking difference in optical properties of complexes of comparable stability.

(3) The differences observed by infrared for different Ni/SiO₂ or Pt/SiO₂ should not be discussed at all in terms of particle size effects or, more in particular, different concentrations of certain sites in the adsorbing surface as derived from marble models.

Hypotheses (1) and (3) assume or suggest that for the supported samples a metal/support interaction or contaminant effects are important. Upon further pursuing these ideas the possibility could be discussed that the

observed differences are to be ascribed to nickel or platinum ions incorporated in the support matrix. One could further speculate about oxide patches present on the supported metals since results of Eley et al.⁵³) suggested that most supported catalysts used in infrared studies contain oxide patches and Müller⁵⁴) reported that nitrogen is more strongly adsorbed on a nickel surface partially covered with oxygen than on clean nickel. While we see no reason to exclude a priori hypotheses (1) and (3) their thorough discussion would only be possible after studying the supported systems in a more elaborated way which is evidently beyond the scope of the present paper. We shall, therefore, only make a few remarks with respect to possibility (2).

The observed relative large differences in the changes in work function $\Delta\Phi$ by nitrogen adsorption on different crystal faces are striking. In terms of hypothesis (2) this face specificity would be connected with differences in optical properties of adsorbed nitrogen. The differences in $\Delta\Phi$ indicate that the dipole moment μ_1 between an adsorbed nitrogen molecule and the metal is different on different crystal faces, μ_1 being larger on rough planes than on the smooth planes (111) and (100).

The intensity of the infrared absorption band, on the other hand, depends besides on the concentration on the term $(d\mu_2/dx)^2$, i.e. on the change with elongation of the dipole moment μ_2 between the two N atoms of an adsorbed nitrogen molecule. While there is no doubt that μ_1 and μ_2 must be interrelated the hypothesis (2) thus leads to the explicit postulate that $(d\mu_2/dx)^2$ should be largest on those rough faces where μ_1 is largest. This interesting consequence appears physically sound.

In conclusion we repeat that Van Hardeveld's suggestive model stimulated our measurements on well defined surfaces. This goal now being achieved, the relevant information most urgently needed in the present state of the problem might be provided by an infrared study on well defined surfaces cleaned in ultra-high vacuum in order to decide between the possibilities described above.

Acknowledgements

The investigations were supported by the Netherlands Foundation for Chemical Research (S.O.N.) with financial aid from the Netherlands Organization for the Advancement of Pure Research (Z.W.O.).

The authors are indebted to Messrs F. C. Kauffeld and W. C. Bauer for skilfully constructing the field emission microscope tubes and to Mr. D. Th. Meijer for his assistance during part of the measurements.

References

- 1) J. W. May, *Advan. Catalysis* **21** (1970) 151.
- 2) H. E. Farnsworth, *Advan. Catalysis* **15** (1964) 31.
- 3) R. Gomer, *Field Emission and Field Ionization* (Harvard Univ. Press, Cambridge, Mass., 1961).
- 4) W. M. H. Sachtler, *Angew. Chem.* **7** (1968) 668.
- 5) R. van Hardeveld and A. van Montfoort, *Surface Sci.* **4** (1966) 396.
- 6) R. van Hardeveld and F. Hartog, *IV Intern. Congr. Catalysis*, preprint no. 70, Moscow (1968).
- 7) G. C. A. Schuit and N. H. de Boer, *J. Chim. Phys.* **51** (1954) 482.
- 8) R. J. Kokes and P. H. Emmett, *J. Am. Chem. Soc.* **80** (1958) 2082.
- 9) P. W. Selwood, *Chemisorption and Collective Paramagnetism* (Academic Press, New York, 1962) p. 177.
- 10) S. Wagener, *J. Phys. Chem.* **61** (1957) 267.
- 11) O. Beeck, A. E. Smith and A. Wheeler, *Proc. Roy. Soc. (London) A* **177** (1940) 62.
- 12) B. M. W. Trapnell, *Proc. Roy. Soc. (London) A* **218** (1953) 566.
- 13) P. M. Gundry, in: *Actes 2ème Congr. Catalyse*, Paris (1960), Vol. 1, p. 1083.
- 14) P. M. Gundry, J. Haber and F. C. Tompkins, *J. Catalysis* **1** (1962) 363.
- 15) O. Beeck, *Advan. Catalysis* **2** (1950) 151.
- 16) J. C. P. Mignolet, *Discussions Faraday Soc.* **8** (1950) 105.
- 17) T. Günzler, Thesis, Braunschweig (1956).
- 18) R. Suhrmann and G. Wedler, *Z. Elektrochem.* **63** (1959) 748.
- 19) G. Ehrlich and F. G. Hudda, *J. Chem. Phys.* **35** (1961) 1421.
- 20) H. H. Madden and H. E. Farnsworth, *J. Chem. Phys.* **34** (1961) 1186.
- 21) L. H. Germer and A. U. MacRae, *J. Chem. Phys.* **36** (1962) 1555.
- 22) R. P. Eischens and J. Jacknow, in: *Proc. Third Intern. Congr. Catalysis*, Amsterdam, (1964) p. 627.
- 23) A. Ravi, D. A. King and N. Sheppard, *Trans. Faraday Soc.* **64** (1968) 3358.
- 24) D. A. King, *Surface Sci.* **9** (1968) 375.
- 25) A. M. Bradshaw and J. Pritchard, *Surface Sci.* **19** (1970) 198.
- 26) A. M. Bradshaw and O. Vierle, *Ber. Bunsenges. Physik. Chem.* **74** (1970) 630.
- 27) R. Bouwman, H. P. van Keulen and W. M. H. Sachtler, *Ber. Bunsenges. Physik. Chem.* **74** (1970) 198.
- 28) R. Bouwman and W. M. H. Sachtler, *Surface Sci.* **24** (1971) 140.
- 29) A. Korb, Thesis, Technical University Berlin (1952).
- 30) R. Vanselow, *Phys. Status Solidi* **4** (1964) 697.
- 31) A. J. Melmed, *J. Appl. Phys.* **36** (1965) 3691.
- 32) R. Vanselow, *Phys. Status Solidi* **21** (1967) 69.
- 33) R. Lewis and R. Gomer, *Surface Sci.* **12** (1968) 157.
- 34) T. Engel and R. Gomer, *J. Chem. Phys.* **50** (1969) 2428.
- 35) M. Drechsler and E. Henkel, *Z. Angew. Phys.* **6** (1954) 341.
- 36) W. P. Dyke and W. W. Dolan, *Advan. Electron. Electron Phys.* **8** (1956) 89.
- 37) A. A. Holscher, Thesis, Leiden University (1967).
- 38) H. F. Winters, D. E. Horne and E. E. Donaldson, *J. Chem. Phys.* **41** (1964) 2766.
- 39) H. F. Winters, *J. Chem. Phys.* **44** (1966) 1472.
- 40) W. J. M. Rootsart, L. L. van Reijen and W. M. H. Sachtler, *J. Catalysis.* **1** (1962) 416.
- 41) G. Ehrlich, *Advan. Catalysis* **14** (1963) 255.
- 42) J. Frenkel, *Z. Physik.* **26** (1924) 117.
- 43) J. H. de Boer, *Advan. Catalysis* **8** (1956) 17.
- 44) J. H. de Boer, *Vacuum* **16** (1966) 309.
- 45) S. Kruyer, *Proc. Kon. Ned. Acad. Wetenschappen B* **58** (1955) 73.
- 46) L. A. Pétermann, *Nuovo Cimento, Suppl.* **5** (1967) 364.

- 47) H. U. D. Wiesendanger, *J. Catalysis* **2** (1963) 538.
- 48) A. E. Morgan and G. A. Somorjai, *Surface Sci.* **12** (1968) 405.
- 49) K. D. Rendulic and Z. Knor, *Surface Sci.* **7** (1967) 205.
- 50) A. van Oostrom, *Appl. Phys. Letters* **17** (1970) 206.
- 51) R. T. Lewis and R. Gomer, *Surface Sci.* **26** (1971) 197.
- 52) J. W. Coleman and F. A. Inkley, in: *Proc. Fourth Intern. Vacuum Congr.* (1968) p.159.
- 53) D. D. Eley, D. M. Moran and C. H. Rochester, *Trans. Faraday Soc.* **64** (1969) 2168.
- 54) J. Müller and A. Regner, *Coll. Czech. Chem. Commun.* **30** (1965) 3399.

Chapter III

ADSORPTION OF NITROGEN ON SINGLE CRYSTAL FACES OF IRIIDIUM, STUDIED BY FIELD EMISSION MICROSCOPY

B. E. NIEUWENHUYS, D. Th. MEIJER and W. M. H. SACHTLER

Gorlaeus Laboratoria, Rijksuniversiteit, Leiden, The Netherlands

Received 15 January 1973; revised manuscript received 7 May 1973

The adsorption of nitrogen on iridium was studied with a field emission microscope equipped with a probe-hole assembly to enable emission experiments on individual emitter regions. The adsorption of nitrogen is markedly face-specific. Temperature programmed desorption reveals three binding states: γ_1 on the (100) face with a maximum heat of adsorption of 7-8 kcal/mole, γ_2 on the regions around (110) with a maximum heat of adsorption of 10-11 kcal/mole and γ_3 on the roughest tip regions (210), (320), (531) and (731) with a maximum heat of adsorption of 13-14 kcal/mole. Nitrogen adsorbed in the γ_1 and γ_3 states causes a decrease, but in the γ_2 state a small increase, in the work function. These results are discussed in relation with data on nickel, palladium, platinum and rhodium. While nitrogen is only weakly adsorbed on all these metals there is a marked difference in the nature of the pertinent adsorption complex.

1. Introduction

Nitrogen is only weakly adsorbed on the transition metals nickel, palladium, platinum, iridium and rhodium^{1,2}). Crystal face-specificity for these adsorption systems has been assumed by Van Hardeveld et al.^{3,4}) who studied nitrogen adsorption on supported metals. Also results obtained from studies on nickel samples cleaned in ultra-high vacuum seem to indicate crystal face-specific adsorption^{5,6}). On platinum, our FEM results showed a face-specific change in work function due to adsorbed nitrogen, but the heat of adsorption was found to be almost equal for different crystallographic regions⁷).

A systematic study of the adsorption of nitrogen on these metals is desirable in order to understand the nature of the nitrogen adsorption bond and the differences in behaviour of nitrogen on these metals.

The present work describes the system nitrogen on iridium as studied with field emission microscopy, a technique which provides information about the adsorption of gases on well defined single crystals.

2. Experimental

The apparatus used has been described previously⁷). It consists of a probe-

hole field emission tube, with a shielded hemispherical electron collector and a movable emitter. Tip temperatures were measured with thermocouples. Any desired tip temperature in the range 80–300 K was obtained within a few seconds. The iridium wire with 0.10 mm diameter was obtained from Johnson, Matthey and Co., London, and was stated to be 99.98% pure. The emitters were prepared by electrolytic etching in an aqueous 30 wt% CrO_3 solution at an alternating current varying between 1.5 and 0.5 A. Emitter cleaning was performed by field desorption and evaporation at room temperature, alternated with prolonged heating periods to 1000 K. In this way also the environment of the emitting surface was cleaned so that no diffusion of contaminants from the shank to the tip can occur in the temperature range 80–300 K where the experiments have been carried out.

3. Determination of the work functions

Work functions from individual tip regions were obtained by means of the Fowler–Nordheim equation written as

$$\ln(i/V^2) = \ln A - B\Phi^3/V, \quad (1)$$

where i is the emission current from the probed region at an applied voltage V , $\ln A$ is the field independent pre-exponential term and B a term containing the field–voltage proportionality constant C :

$$B = 6.8 \times 10^7/C. \quad (2)$$

B is considered to be constant for the different tip regions and is generally determined by measuring the slope $B\Phi^3$ of $\ln(i/V^2)$ versus $1/V$ plots for a tip area with known work function or for the total tip if an average work function is known.

Unfortunately, no reliable value of the work function of a single iridium crystal plane is available, as the only published value, 5.79 eV for a (111) plane⁸), obtained by the thermionic emission method, is open to doubt because the annealing conditions used did not warrant the absence of surface contaminations.

The work function values obtained by thermionic emission of polycrystalline samples scatter between 4.57 and 5.4 eV^{9–12}) and are, thus, not useful for an appropriate field emission average value. Arthur and Hansen¹³) obtained an average field emission value of 4.65 eV, using the Bradley and d'Asaro method of evaluating the dependence of emission current on applied voltage¹⁴). This value is, however, suspiciously low when compared to recent values of iridium films obtained in our institute with photo-electron emission¹⁵).

A value of 5.0 eV is used throughout this work for the average value of the work function of the total tip emission. This value emerged from a systematic comparison of photo-electric work function values of iridium films sintered at different temperatures¹⁵⁾ with work function values of other metals for which appropriate average field emission values are known. It should be noted that the uncertainty in Φ has only a small influence on the values for $\Delta\Phi$, the change in work function by gas adsorption. Even if the uncertainty in Φ would be as large as 0.3 eV, all values for $\Delta\Phi$ caused by nitrogen adsorption as collected in table I remain unchanged. For the same reason any actual deviation of B for an individual crystal plane from the assumed constant value would be of negligible influence on the $\Delta\Phi$ values for individual crystal faces.

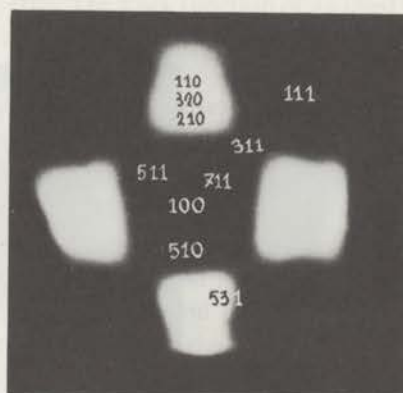


Fig. 1. Field emission pattern of a clean field evaporated iridium tip and the disposition of some crystal faces on it.

TABLE I

Work functions (Φ) of different tip areas, changes in work function ($\Delta\Phi$) and Fowler-Nordheim pre-exponentials ($\Delta \log A$) by nitrogen adsorption at a temperature of 80 K at full coverage and maximum heats of adsorption (Q_{ads})

Tip region	Φ (eV)	$\Delta\Phi$ (eV)	$\Delta \log A$	Q_{ads} (kcal/mole)
Total emission	5.00	-0.08*	-1.0	
(111)	5.79*	-0.2	-1.1	
(100)	5.67*	-0.7	-1.3	7-8
Around (110)	5.0	+0.1	-1.3	10-11
(311)-(211)	5.4			
(510)-(310)	5.4			
(210)	5.0	-0.3	-1.0	13-14
(731)	4.9	-0.1	-1.1	13-14

* The experimental error is 0.05 eV.

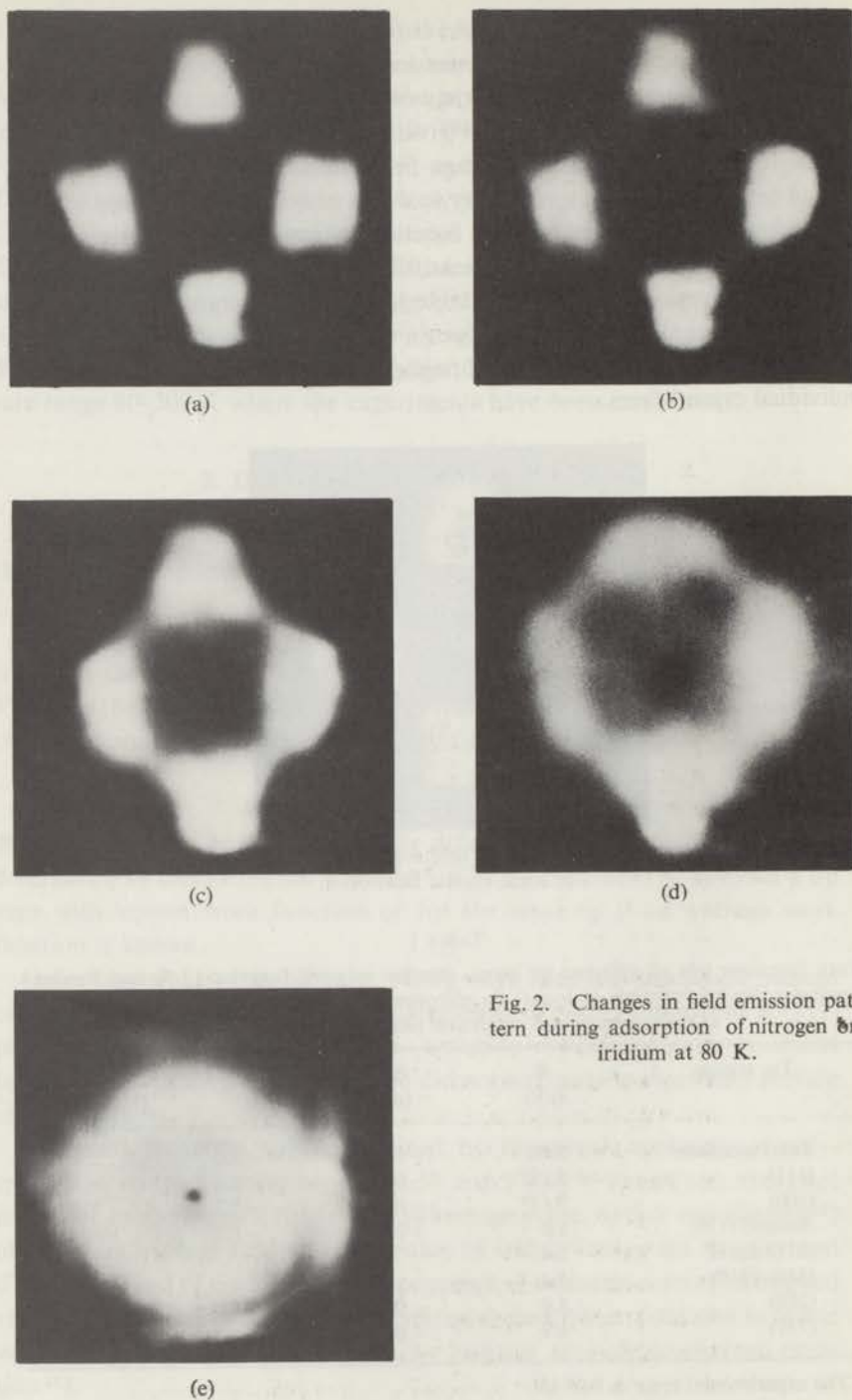


Fig. 2. Changes in field emission pattern during adsorption of nitrogen on iridium at 80 K.

4. Results

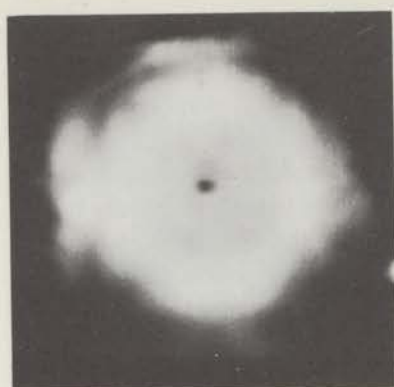
Fig. 1 shows the field emission pattern of a clean field evaporated iridium tip and the disposition of the principal crystal faces on it.

The values for the work function of some tip areas, calculated from eq. (1), are listed in table 1. The accuracy of these values is limited, besides by the experimental errors, by the choice of 5.00 eV for the average work function and by our neglecting any variation of B with the tip region. The value for the (111) tip region is very close to that found by Zandberg and Tondegode⁸). It should be noted that a tip region (hkl) does not necessarily correspond to the smooth crystal face (hkl) as the region may include terraces around the (hkl) face. The (110) face on a field evaporated tip, e.g., never shows up as a well defined dark area. The work function of an ideal (110) plane is presumably much closer to that of the (100) region than the measured value of the (110) region.

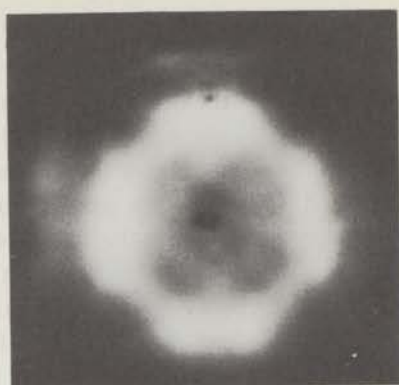
The changes in field emission pattern observed when exposing the tip to a low-pressure stream of nitrogen (10^{-8} Torr) at 80 K are illustrated by fig. 2. Adsorption of nitrogen lowers the total electron emission. The pictures were taken at a constant current of 1×10^{-8} A, thus the voltage between screen and tip had to be raised during the adsorption process.

The relevant results of the visual observations are: First the emission contrast between the regions around (311)–(211) and (210)–(320) becomes less prominent. The regions around the (110) poles become more distinguishable than in the clean pattern. The emission from the central (100) face and surroundings becomes more intense with respect to the high index faces. For high coverage with nitrogen the pattern shows a much more uniform emission than the clean tip. Only the (111) faces and the (110) poles are clearly observable.

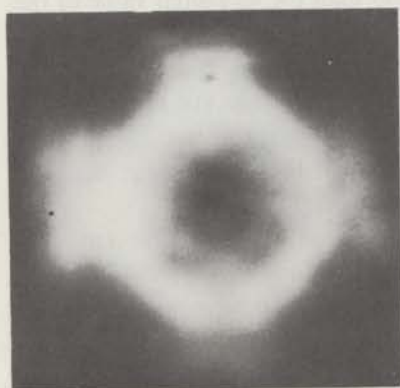
Qualitative information on the crystallographic specificity of the heat of adsorption is obtained by recording the emission pattern with increasing tip temperatures as is shown in fig. 3. Again, a constant emission current was maintained by adjusting the voltage. All images in this figure are reversible upon changes in tip temperature. When, for instance, the temperature of the tip partly covered with nitrogen at 185 K (fig. 3e) is lowered to 165 K, the image changes again to that of fig. 3d. This proves that a surface equilibrium distribution of the adsorbate is established at all temperatures used in these experiments. All changes occurring by temperature increase have therefore to be attributed to a denuding of some tip regions. At 125 K the (100) area is darkened with respect to the (210)–(731) regions. At 155 K the overall contrast has been increased. The (110) faces are still better observable than in the clean pattern. Increasing the tip temperature to 165 K increases the emission



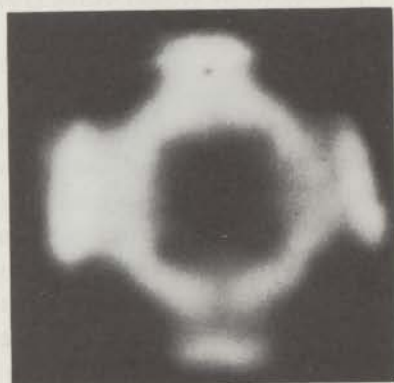
(a)



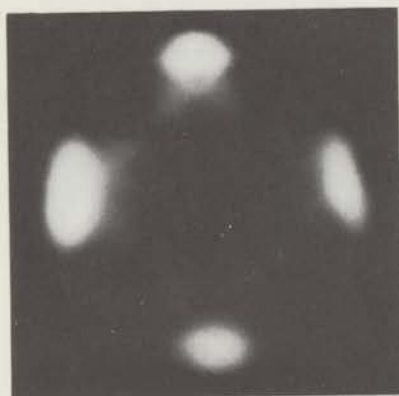
(b)



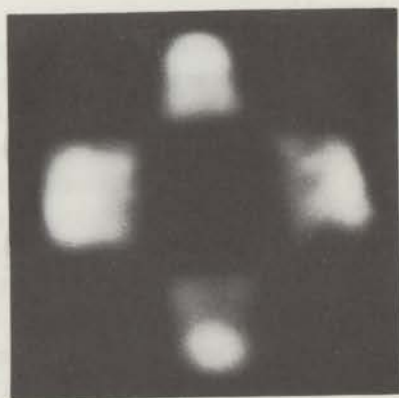
(c)



(d)



(e)



(f)

Fig. 3a-3f

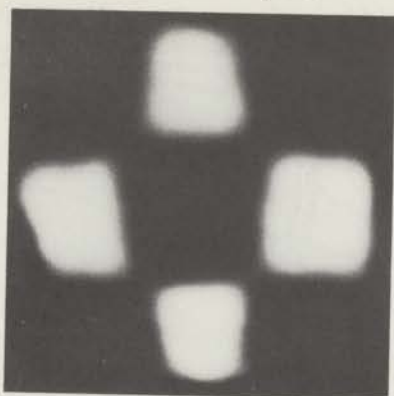


Fig. 3g

Fig. 3. Changes in field emission pattern during thermal desorption of nitrogen from iridium. Tip temperature at: (a) 90 K, (b) 125 K, (c) 155 K, (d) 165 K, (e) 185 K, (f) 195 K, (g) 210 K.

around the (110) faces visibly. It appears therefore, that these regions are denuded at this temperature while the (210) and (731) faces remain covered with nitrogen. At 185 K the emission is mainly due to the regions around (110). At 195 K the emission contrast between (110) and (210)–(731) areas decreases while at 210 K the original clean pattern is restored.

The above-mentioned results show that the adsorption of nitrogen on iridium is strongly face-specific: both the heat of adsorption and the change in work function depend on the substrate structure. More quantitative information is obtained by measuring the probed electron current of several tip regions.

Fig. 4 shows the effect of nitrogen admission on the emission currents of some crystal faces at constant voltage. In table 1 the changes in work function and Fowler–Nordheim pre-exponentials are given for nitrogen exposure at 80 K. The total current and the probed currents at constant voltage from the bright regions such as (210), (531), (320) or (731) as well as from the darker (110) region initially decrease strongly by nitrogen adsorption (see fig. 4). This decrease is strongest for the (110) regions. For the total current a very shallow minimum occurs at high coverage. This is, clearly, due to the emission from the (100) face where the emission markedly increases after an initial small decrease. The effect of nitrogen on the (111) face, the most densely packed face of the fcc lattice, is comparatively small.

Surprisingly, the Fowler–Nordheim plots reveal that the work function for all tip regions except (110) is decreased by nitrogen adsorption, in spite of the decrease in emission. On most areas, the change in work function is small: -0.1 eV for the (731) and -0.3 eV for the (210) region, with an

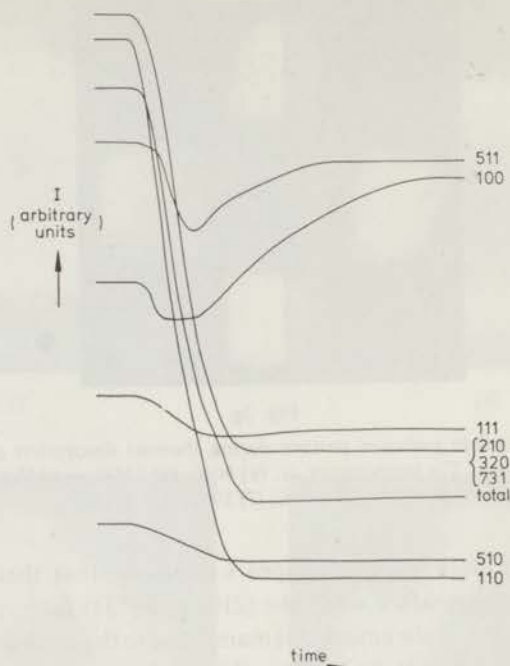
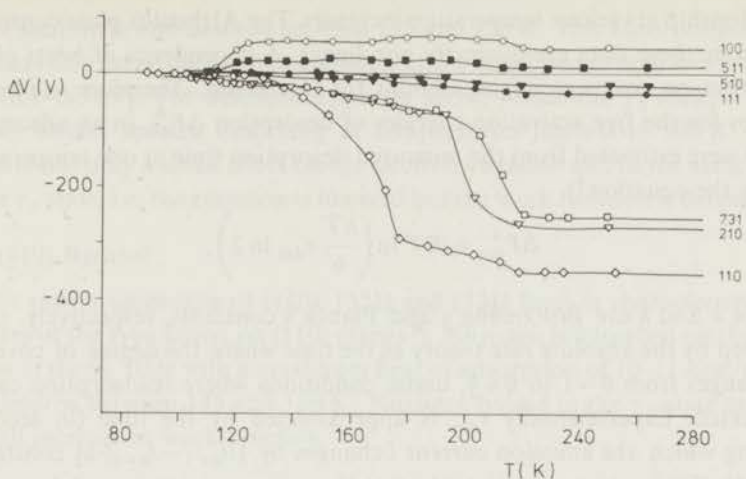


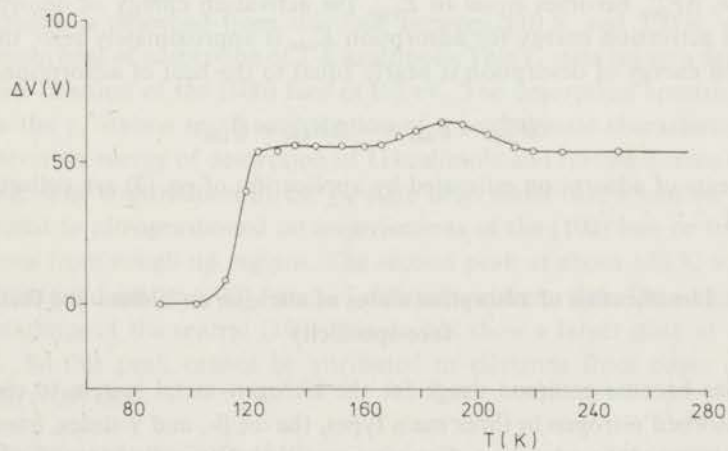
Fig. 4. Changes in field emission currents from individual tip regions at constant field strength during adsorption of nitrogen at 80K.

experimental error of 0.1 eV. The work function of the (100) faces is reduced much more, viz. 0.7 ± 0.1 eV in accordance with the increase in emission from this face. Only for the (110) regions the decrease in emission is accompanied by a small increase in work function. The average work function of the total tip is reduced by 0.08 ± 0.05 eV. But the physical meaning of this average change in work function is debatable as the relative contribution of the individual regions is different from the clean and covered tip surface.

The occurrence of different binding states of nitrogen on iridium is clearly confirmed in heating experiments, shown in fig. 5a for different tip regions and in fig. 5b at an enlarged scale for the (100) face. These figures were obtained by heating a nitrogen covered tip by a few degrees to a temperature T ; after 60 sec the voltage required to maintain the original electron current of the probed tip region was determined. The temperature was then again increased by a few degrees and the voltage adjusted, etc. These experiments were continued up to temperatures where an additional temperature increase does not influence the emission currents while the voltages required for the fixed emission current of the probed regions are identical to that of the original clean tip region.



(a)



(b)

Fig. 5. (a) Variation in voltages required for constant emission currents from individual tip regions during thermal desorption of nitrogen. (b) Variation in voltage required for constant emission current of the (100) face during thermal desorption of nitrogen.

The results confirm the striking differences between various tip regions. Desorption of nitrogen causes a marked decrease in emissivity of the (100) face but the emissivity increases on the areas (110), (210), (531), (320), (731) and (510). The temperature of the largest changes in emissivity and, hence, the activation energy of desorption increases in the sequence (100), (110) and the rough faces (210), (531), (320) and (731).

Values for the activation energy of desorption from rate data can be obtained by measuring the time required to attain a given current-voltage

relationship at various temperature increases. The Arrhenius plots constructed from these data are distinctly non-linear. A dependence of heats of adsorption on coverage might account for this result. Therefore, numerical values for the free activation energies of desorption ΔF_{des}^\ddagger in an adsorption state were estimated from the measured desorption time at one temperature, using the equation⁷⁾

$$\Delta F_{des}^\ddagger = RT \ln \left(\frac{kT}{h} \tau_{des} \ln 2 \right), \quad (3)$$

where k and h are Boltzmann's and Planck's constants, respectively. τ_{des} is defined by the absolute rate theory as the time where the degree of coverage θ changes from $\theta=1$ to $\theta=\frac{1}{2}$, under conditions where readsorption can be neglected. Experimentally τ_{des} is approximated by the time (in seconds) during which the emission current i changes by $\frac{1}{2}|i_{\theta=1} - i_{\theta=0}|$ at constant T and V . If the assumption is made that the activation entropy of desorption is zero, ΔF_{des}^\ddagger becomes equal to E_{des} , the activation energy of desorption. As the activation energy for adsorption E_{ads} is approximately zero, the activation energy of desorption is nearly equal to the heat of adsorption.

$$\Delta F_{des}^\ddagger \sim E_{des} = -\Delta H_{ads} = Q_{ads}. \quad (4)$$

The heats of adsorption estimated by application of eq. (3) are collected in table 1.

5. Identification of adsorption states of nitrogen on iridium and their face-specificity

It has become common usage for the nitrogen-metal system to classify the adsorbed nitrogen in three main types, the α -, β -, and γ -states, based on the stability of the adsorbate. For nitrogen on tungsten the heats of adsorption for the three states are roughly 20, 75 and 10 kcal/mole, respectively. On iridium the heats of adsorption reveal that nitrogen is only bound in the γ -state. The presence of three distinct binding states, each associated with a different range of heats of adsorption is clearly demonstrated in the previous section by fig. 5 and table 1. We shall refer to these states as the γ_1 -, γ_2 - and γ_3 -state in ascending order of their heats of adsorption in analogy with literature's nomenclature for nitrogen on nickel⁵⁾.

5.1. TIP REGION OF THE (210), (531), (320) AND (731) FACES

This region, the roughest of the whole tip, is characterized by the presence of many B_6 -sites⁷⁾. B_5 -sites are also present on the faces (731) and (320). Nitrogen is bound on this region with a maximum heat of adsorption of

13–14 kcal/mole and desorbs between 195 and 220 K. This adsorption state, γ_3 , leads to a large decrease in emission and a small decrease in work function (0.1–0.3 eV). The desorption spectra show, beside the γ_3 state, a very weakly bound species, desorbing at temperatures just above 100 K. This ad-state has only a small effect on the electron emission and in the same sign as the γ_3 state, i.e. the emission is lowered but the work function is decreased.

5.2. (110) REGION

This region consisting of (110), (551) and (331) faces is characterized by B₅-sites of the type found on (110) planes³. Nitrogen is adsorbed on this tip region in the γ_2 state with a maximum heat of adsorption of 10–11 kcal/mole and desorbs between 145 and 180 K. Nitrogen bound in the γ_2 state causes a small increase in work function.

5.3. (100) AREA

Nitrogen is desorbed from this face between 110 K and 130 K with a maximum heat of adsorption of 7–8 kcal/mole. This γ_1 state causes a decrease in work function of the (100) face of 0.7 eV. The desorption spectra show beside the γ_1 state a small contribution of a second state characterized by an activation energy of desorption of 11 kcal/mole and further a trace of the γ_3 state. The contribution of the γ_3 state is so small that it can be safely attributed to nitrogen bound on imperfections of the (100) face or to stray electrons from rough tip regions. The second peak at about 180 K was invariably found on the (100) faces of different iridium tips. The immediate surroundings of the central (100) face do not show a larger peak at about 180 K. So this peak cannot be attributed to electrons from edges of the smooth (100) face.

5.4. REGION AROUND (510)–(310)

In this tip region B₆-sites are present on the edges of (100) terraces. Nitrogen bound on this region desorbs mainly in the temperature range corresponding to the γ_3 -state. Also nitrogen present in the γ_1 -state is found. The total change in emission by nitrogen adsorption or desorption is, however, very small.

5.5. REGION AROUND (711)–(511)

This region is characterized by B₅-sites of the type found on (311) planes³ and by terraces of the (100) face. On this tip region the γ_1 -state is found. Also the state corresponding with an activation energy of desorption of 11 kcal/mole, previously described at the (100) face and the γ_3 -state can be observed. The total change in emission by adsorption or desorption is small.

5.6. (111) REGION

The effect of nitrogen on the emission of this most densely packed face of the fcc lattice is small. The desorption plot does not show clear maxima or minima. A small effect observed at higher temperatures (corresponding to the γ_3 -state) is attributed to electrons originating from rough faces, as the efficiency of electron collection from (111) is limited by the large angle between the [111] direction and the central [100] direction. (All our iridium tips exhibit four-fold symmetry.)

The effect on the electron work function and the Fowler-Nordheim pre-exponential is, however, appreciable: -0.2 eV and 1.1. These changes indicate that nitrogen is certainly adsorbed on a smooth (111) face. It appears that the effect of the decrease in work function on the emission is completely compensated by the large decrease in pre-exponential. At 160 K and a pressure of 2×10^{-9} Torr the work function is only -0.1 eV below the clean value. So it appears that nitrogen adsorbed on the (111) face has a heat of adsorption below that of the γ_3 -state.

6. General discussion

Strong chemisorption of nitrogen on iridium is absent¹⁶). In this respect iridium resembles platinum and other metals of the platinum group. Adsorption of nitrogen on iridium is more markedly face-specific than on platinum; both the activation energy of desorption and the change in work function depend on the crystal region. The emission changes caused by temperature programmed desorption reveal three distinct states: γ_1 on the (100) faces, desorbing between 110 and 130 K with a maximum heat of adsorption of 7–8 kcal/mole, γ_2 on the regions around (110) desorbing between 145 and 180 K and with a maximum heat of adsorption of 10–11 kcal/mole and γ_3 on the rough tip regions desorbing between 195 and 220 K with a maximum heat of adsorption of 13–14 kcal/mole.

Two publications are known where adsorption of nitrogen on silica-supported iridium is studied. Ravi et al.¹⁷) found an infra-red absorption band at 2185 cm^{-1} . The same absorption band was observed by Van Hardeveld⁴) on a catalyst with a mean particle size between 15 and 70 Å in agreement with his previous results on nickel, palladium and platinum³). In both articles the infra-red band was assigned to nitrogen adsorbed on B_5 -sites present on (110) and other rough planes.

The present results show, however, significant differences in heat of adsorption as well as in the change of work function between regions containing B_5 -sites, e.g. between the (110) tip regions and (511) or (320). To the extent that

a comparison of the field emission results with the infra-red results is valid, it would appear that the simple hypothesis that all nitrogen molecules adsorbed on B₅-sites on iridium are equally bound, needs further refinement.

The most strongly bound nitrogen on iridium, the γ_3 -state, is mainly found on the most strongly emitting areas of a clean tip: (531), (210), (320) and (731) faces. These tip regions are the roughest of the whole tip surface with a high concentration of B₆-sites⁷). This fact may indicate that for a tight bond with nitrogen molecules either surface iridium atoms with many available free orbitals are required or atoms with good electron donating properties (low work function) or sites where nitrogen molecules can contact many iridium atoms (B₆-sites).

γ_3 -Nitrogen causes a small decrease in work function but the large decrease in the Fowler-Nordheim pre-exponential term $\log A$ overcompensates this so that the emission is lowered. A similar effect has been observed for nitrogen on tungsten^{6, 18}), rhenium^{19, 20}) and nickel⁶). While on tungsten this decrease in $\log A$ has been attributed to corrosive chemisorption¹⁸), this explanation is not applicable on iridium, platinum or nickel because of the much lower heat of adsorption. When considering other general explanations which have been advanced in the literature^{21, 22}) for the change in $\log A$ by adsorption, it appears that the model by Menzel and Gomer²¹) has the advantage that qualitative predictions are possible which can be faced with the experimental data. These authors ascribe the changes in $\log A$ to a polarization of the adsorbate by the applied electric field. This induced dipole moment of the adsorbed layer results in a work function increment:

$$\Delta\Phi_F = 4\pi N\alpha F/\epsilon \quad (5)$$

In this equation α stands for the polarizability of the adsorbate, N is the number of adsorbed nitrogen molecules per square centimeter and ϵ an effective dielectric constant of the adlayer. The work function after adsorption in the presence of the electric field is then

$$\Phi_F = \Phi_{F=0} + 4\pi N\alpha F/\epsilon_s \quad (6)$$

If the second term in eq. (6) is small compared to $\Phi_{F=0}$ the approximation

$$\Phi_F^{\frac{3}{2}} = (\Phi_{F=0} + 4\pi N\alpha F/\epsilon)^{\frac{3}{2}} \sim \Phi_{F=0}^{\frac{3}{2}} (1 + 6\pi N\alpha F/\epsilon\Phi_{F=0}) \quad (7)$$

can be used, which, after insertion in the Fowler-Nordheim equation (1) results in an apparent change in $\log A$,

$$\Delta \log A = \frac{-0.55 \times 10^{-15} \alpha N \Phi^{\frac{3}{2}}}{\epsilon} \quad (8)$$

(α in \AA^3 and Φ in volts). In this approximation the slope of the Fowler-Nordheim plot remains constant and gives the value $\Delta\Phi$ at zero field. In view of the relatively small polarizability of nitrogen, ϵ in the denominator of eq. (8) is ~ 1 . Assuming $N = 1 \times 10^{15}$ molecules/cm² and putting $\alpha = 1.9 \text{\AA}^3$, $\Phi = 4.9$ V, the value of the (731) region, we get $\Delta \log A = -2.3$ which differs from the experimental value by a factor of two roughly. In view of the uncertainty in N and the approximation $\epsilon \sim 1$, we conclude that the large decrease in $\log A$ can be satisfactorily understood on the basis of the polarization model of Menzel and Gomer.

A remarkable finding is that the local changes in work function differ not only in magnitude but even in sign. A similar behaviour has been found for nitrogen on tungsten^{18, 23-25}); but to our knowledge such a pronounced crystallographic face specificity has never been observed for such a weak adsorption as nitrogen on iridium. No explanation is offered at present for this observation which we found reproducible and not caused by experimental errors. It might be mentioned, however, that recent photo-electric measurements²⁶) in this laboratory seem to indicate that nitrogen can be adsorbed on unsintered rhodium and nickel films in both an electropositive and an electronegative form.

The nature of the adsorption of nitrogen on the metals of group VIIIb and VIIIc of the periodic system is subject to some disagreement in the literature. It was described as weak chemisorption by Eischens²⁷), King⁵) and Ehrlich²⁸) and as physical adsorption by Van Hardeveld³). In Van Hardeveld's model the relatively high heat of adsorption Q_{ads} was attributed to the sum of the London contribution Q_L and a Debye contribution Q_P resulting from an interaction of strong surface electric fields at rough crystal faces and the induced dipoles in the nitrogen molecules:

$$Q_{\text{ads}} = Q_L + Q_P. \quad (9)$$

Q_P and the change in work function $\Delta\Phi$ are then related by

$$Q_P = \frac{1}{2} \Delta\Phi^2 / (4\pi N)^2 \alpha. \quad (10)$$

According to eq. (10) a relation between the heat of adsorption and the change in work function is predicted. The present results are, however, at variance with such a relation. It would, therefore, appear that the polarization of nitrogen molecules by surface electric fields does not form a large contribution to the nitrogen-iridium bond.

Indeed, all data available now seem to indicate that the nature of the nitrogen adsorption on group VIII metals depends in a very specific way of subtle differences of their chemical properties. FEM results now available for nitrogen on nickel⁶), platinum⁷), rhodium²⁸) and iridium show that

nitrogen adsorption differs on these metals with respect to the following phenomena:

- (a) Changes due to adsorption in the visual FEM patterns are different.
- (b) Average work function changes: $\Delta\Phi_{\text{Pt-N}_2} = -0.65$ V, $\Delta\Phi_{\text{Ir-N}_2} = -0.08$ V, $\Delta\Phi_{\text{Ni-N}_2} < -0.1$ V.
- (c) Maximum heat of adsorption $Q_{\text{Ir-N}_2} = 13$ kcal/mole, $Q_{\text{Rh-N}_2} = 11$ kcal/mole, but $Q_{\text{Pt-N}_2} = 9$ kcal/mole.
- (d) Face specificity of Q_{ads} : no detectable specificity for Pt, but large specificity on iridium.
- (e) Anisotropy in the change in work function on different tip regions: on platinum the largest decrease in work function occurs on the rough tip regions but on iridium on the smooth (100) face.

The differences in adsorption of nitrogen show that the interaction is a chemical one, comparable perhaps to the adsorption of CO although the total energy gain is much smaller. In this view the nitrogen adsorption would be caused by a donation of electrons into vacant d-orbitals of the metal and stabilization of the metal-nitrogen bond by back donation of electrons from filled d-orbitals on the metals into vacant antibonding π orbitals on the nitrogen molecule.

In summarizing, the results show that the nitrogen molecule is a sensitive probe for detecting subtle differences in the chemical behaviour of these metals which are geometrically very similar and, moreover, are part of the same sub groups of the periodic table. When seen in this light, it might be hoped that further investigation of nitrogen adsorption by these metals will also help to understand the marked differences in catalytic selectivity of the same metals in hydrocarbon reactions.

Acknowledgements

The investigations were supported by the Dutch Foundation for Chemical Research (S.O.N.) with financial aid from the Dutch Organization for the Advancement of Pure Research (Z.W.O.).

References

- 1) B. M. W. Trapnell, Proc. Roy. Soc. (London) A **218** (1953) 566.
- 2) G. C. Bond, *Catalysis by Metals* (Academic Press, New York, 1962).
- 3) R. van Hardeveld and A. van Montfoort, Surface Sci. **4** (1966) 396.
- 4) R. van Hardeveld and F. Hartog, Advan. Catalysis **22** (1972) 75.
- 5) D. A. King, Surface Sci. **9** (1968) 375.
- 6) G. Ehrlich and F. G. Hudda, J. Chem. Phys. **35** (1961) 1421.
- 7) B. E. Nieuwenhuys and W. M. H. Sachtler, Surface Sci. **34** (1973) 317.
- 8) E. Ya. Zandberg and A. Ya. Tondegode, Soviet Phys.-Solid State **12** (1970) 878.

- 9) D. A. Wright, Radio Section (1952), paper 1404.
- 10) B. Ch. Dyubua and B. N. Popov, Radio Eng. Electron 7 (1962) 1454.
- 11) R. G. Wilson, J. Appl. Phys. 37 (1966) 3170.
- 12) E. Ya. Zandberg and A. Ya. Tondegode, Soviet Phys.-Tech. Phys. 13 (1968) 550.
- 13) J. R. Arthur and R. S. Hansen, J. Chem. Phys. 36 (1962) 2062.
- 14) R. C. Bradley and L. A. d'Asaro, J. Appl. Phys. 30 (1959) 226.
- 15) R. Bouwman and W. M. H. Sachtler, Surface Sci. 24 (1971) 140, and unpublished values.
- 16) V. J. Mineault and R. S. Hansen, J. Phys. Chem. 70 (1966) 3001.
- 17) A. Ravi, D. A. King and N. Sheppard, Trans. Faraday Soc. 64 (1968) 3358.
- 18) A. A. Holscher, Thesis, Leiden University, 1967.
- 19) R. Klein and J. W. Little, Surface, Sci. 6 (1967) 193.
- 20) K. Ishizuka, J. Res. Inst. Catalysis, Hokkaido Univ. 15 (1967) 95.
- 21) D. Menzel and R. Gomer, J. Chem. Phys. 41 (1964) 3311.
- 22) C. B. Duke and M. E. Alferieff, J. Chem. Phys. 46 (1967) 923.
- 23) T. Oguri, J. Phys. Soc. Japan 19 (1964) 83.
- 24) A. A. Holscher, J. Chem. Phys. 41 (1964) 579.
- 25) A. G. J. van Oostrom, J. Chem. Phys. 47 (1967) 761.
- 26) B. E. Nieuwenhuys, O. G. van Aardenne and W. M. H. Sachtler, Thin Solid Films 17 (1973) S7.
- 27) R. P. Eischens and J. Jacknow, in: *Proc. 3rd Intern. Congr. Catalysis*, Amsterdam, 1964, Eds. W. M. H. Sachtler et al. (North-Holland, Amsterdam, 1965) p. 627.
- 28) G. Ehrlich, Technical Report General Electric S-68-1125 (1968).

Chapter IV

Short Communication

Photoelectric determination of the changes in work function of nickel, rhodium and platinum films by nitrogen adsorption

B. E. NIEUWENHUYS, O. G. VAN AARDENNE AND W. M. H. SACTLER

Gorlaeus Laboratories, State University of Leiden, Leiden (The Netherlands)

(Received April 10, 1973; accepted April 19, 1973)

While nitrogen adsorption on nickel has been studied by several authors (for references see Ref. 1), much less attention has been paid to nitrogen adsorption on the other metals of Group VIII b and c of the Periodic System: rhodium, iridium, palladium and platinum. On all these metals nitrogen is only weakly adsorbed^{2,3}. Results obtained with field emission microscopy show that the interaction is of a chemical nature, as is concluded from the heat of adsorption and from the crystal face specificity of nitrogen adsorption, two properties for which the metals in this group were found to differ markedly⁴. In particular, measurements on different emitter regions of platinum and iridium, performed with the field emission probe hole technique, show that the change in work function by nitrogen adsorption is specific for the crystal face and the metal studied⁴.

In the present note, we report on studies of nitrogen adsorption on films of nickel, platinum and rhodium, carried out with the photoelectric technique. While field emission provides information on well-defined crystal faces, the present data on sintered and unsintered films provide information on the influence of surface imperfections on adsorption. In the literature, only work function changes on nickel films are reported; data on platinum and rhodium films are lacking.

Experimental

The films were prepared by evaporation on a glass substrate in a vacuum of 10^{-10} torr and they were subsequently heated to various temperatures in a phototube, identical to the one described by Bouwman and Sachtler⁵. The nickel and platinum wires, obtained from Johnson Matthey & Co., London, were stated to be spec. pure; the rhodium wire has a stated purity of 99.98%. Nitrogen with an impurity level lower than 0.001% was further purified before entering the phototube by the use of freshly deposited nickel films in the supply system.

Results and discussion

The effect of nitrogen admission on the photocurrent, at constant wavelength, of nickel, rhodium and platinum films is shown in Figs. 1, 2 and 3. The films were annealed at different temperatures and were subsequently cooled to 78 K at which temperature the adsorption experiments had been carried out.

With unsintered nickel films the following phenomena are observed (Fig. 1):

(1) After admission of nitrogen, the photocurrent increases from the clean film value A to a maximum value B. When nitrogen admission is stopped at this stage no further change in the photocurrent occurs.

(2) When admission of nitrogen is continued the photocurrent decreases to a minimum value C which is obtained at a pressure of about 10^{-4} Torr.

(3) Upon pumping to 10^{-7} – 10^{-6} Torr, a small increase in emission current occurs (D). This effect is reversible, subsequent nitrogen readmission to 10^{-4} Torr causing the photocurrent to decrease to a value E equal to C.

Nickel films sintered at room temperature show a much less pronounced maximum B than is observed with unsintered films (Fig. 1(b)). No maximum in the photocurrent during nitrogen admission can be observed on nickel films annealed at 373 K (Fig. 1(c)).

The changes in the photocurrents of rhodium films, annealed at different temperatures, brought about by nitrogen adsorption are almost identical to those of nickel films (Fig. 2). On platinum, however, no decrease in photocurrent during nitrogen adsorption can be observed, either for unsintered or for annealed films. The maximum B in the photocurrent *versus* exposure time curve is completely absent (Fig. 3).

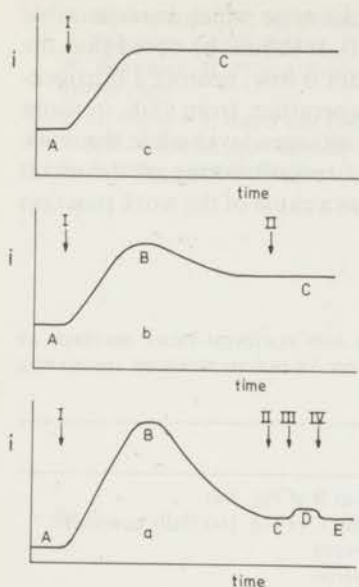
Some values for the photoelectric work function of nickel, rhodium and platinum films, sintered at different temperatures, and the changes in work function brought about by nitrogen adsorption at 78 K have been compiled in Table I. The values for platinum films have been published earlier¹.

The photoelectric work function values of nickel films are in fair agreement with values of Suhrmann and Wedler⁶ and those of platinum films with data of Suhrmann and Wedler⁶ and Bouwman *et al.*⁷. Work function values of rhodium films have not been published yet in the literature. Bouwman and Sachtler predicted a value of 5.1–5.2 eV for a film annealed at 373 K from a systematic comparison of the work function values of Group VIII metals⁵. The present value of 5.11 eV confirms their prediction.

The change in work function of platinum films caused by nitrogen adsorption decreases with increasing annealing temperature. During annealing, closely packed stable crystal faces grow at the expense of high index faces. So it appears that the change in work function is larger on high index faces than on low index faces. This result agrees completely with our previous results obtained with field emission microscopy¹.

On nickel and rhodium, contrary to platinum, the change in work function increases with annealing temperature. Obviously, the decrease in work function is larger on closely packed than on less densely packed crystal faces.

Using a contact potential difference method, Gundry, Haber and Tompkins⁸ found for nitrogen on nickel a change in work function of -0.22 eV, in agreement with Mignolet's value⁹ of -0.21 eV and the photoelectric value of Suhrmann and Wedler¹⁰ of -0.20 eV. These values are in reasonable agreement with the value of -0.18 eV which we found for films sintered at 373 K, so that we may conclude that the films used by the authors had a state of annealing comparable to our films sintered at 373 K.



- I admission of nitrogen,
 II nitrogen pressure is 10^{-4} – 10^{-3} Torr,
 III pumping off the nitrogen to 10^{-6} Torr,
 IV readmission of nitrogen to 10^{-4} Torr,
 A photocurrent of the clean film,
 B maximum in the photocurrent during nitrogen adsorption,
 C photocurrent of the film fully covered with nitrogen,
 D photocurrent at a pressure of 10^{-6} Torr,
 E photocurrent after readmission of nitrogen to 10^{-4} Torr.

Fig. 1. Change in photocurrent i of nickel, at constant wavelength, during adsorption of nitrogen at 78 K. i in arbitrary units. (a) Unsintered film, $\lambda = 256$ nm; (b) film annealed at 293 K, $\lambda = 238$ nm; (c) film annealed at 373 K, $\lambda = 226$ nm.

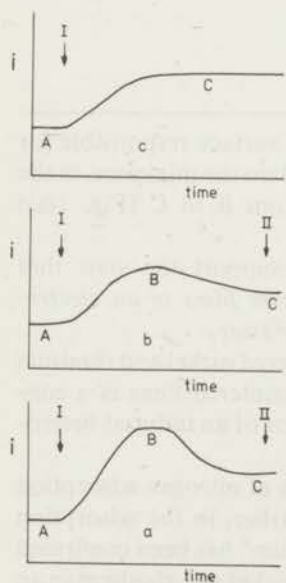


Fig. 2. Change in photocurrent i of rhodium, at constant wavelength, during adsorption of nitrogen at 78 K. (a) Unsintered film, $\lambda = 260$ nm; (b) film annealed at 293 K, $\lambda = 246$ nm; (c) film annealed at 373 K, $\lambda = 246$ nm.

For the meaning of I, A, B and C, see legend to Fig. 1.

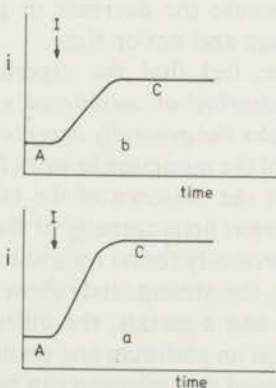


Fig. 3. Change in photocurrent i of platinum, at constant wavelength, during adsorption of nitrogen at 78 K. (a) Unsintered film, $\lambda = 200$ nm; (b) film annealed at 293 K, $\lambda = 204$ nm. For the meaning of I, A and C, see legend to Fig. 1.

In discussing the causes of the work function decrease which is responsible for the rise in photocurrent in Fig. 1(a) (see Table I), it should be noted that the heat of adsorption of nitrogen on nickel and rhodium is low: heating a nitrogen-covered nickel film, previously sintered at room temperature, from 78 K to room temperature results in a complete desorption of the nitrogen layer while the work function returns to the original value. Therefore, a reconstruction of the metal surface during nitrogen adsorption can be excluded as a cause of the work function minimum.

TABLE I

THE PHOTOELECTRIC WORK FUNCTION ϕ OF NICKEL, RHODIUM AND PLATINUM FILMS, SINTERED AT DIFFERENT TEMPERATURES T_s , AND THE CHANGES IN WORK FUNCTION $\Delta\phi$ DUE TO NITROGEN ADSORPTION AT 78 K

Metal	T_s (K)	ϕ (eV)	$\Delta\phi$ (eV)	Remarks
Ni	78	4.56	-0.07	$\Delta\phi$ at point B of Fig. 1(a)
			-0.03	$\Delta\phi$ at point C of Fig. 1(a) (fully covered)
	293	4.95	-0.17	Fully covered
	373	5.10	-0.18	Fully covered
Rh	78	4.87	-0.02	Fully covered
	293	5.06	-0.15	Fully covered
	373	5.11	-0.17	Fully covered
	Pt	78	5.45	-0.51
293		5.63	-0.30	Fully covered

It is also easy to show that diffusion from the front surface responsible for the photoelectric emission to the inner surface cannot explain the minimum in the work function because the decrease in photocurrent from B to C (Fig. 1(a)) depends on coverage and not on time.

We, therefore, feel that the experimental results support the view that nitrogen can be adsorbed on unsintered nickel and rhodium films in an electronegative state besides the generally accepted electropositive state.

The absence of the minimum in work function on sintered nickel and rhodium films suggests that the presence of the two states on unsintered films is a consequence of an *a priori* heterogeneity of the surface and not of an induced heterogeneity, just as previously found on iridium⁴.

Summarizing, the present study shows the complexity of nitrogen adsorption on Group VIII b and c metals; the difference, stated earlier, in the adsorption complex of nitrogen on platinum and on nickel and rhodium⁴ has been confirmed and it has been argued that nitrogen can be adsorbed on nickel and rhodium in an electronegative adsorbed state besides the generally accepted electropositive state.

1 B. E. Nieuwenhuys and W. M. H. Sachtler, *Surface Sci.*, **34** (1973) 317.

2 B. M. W. Trapnell, *Proc. Roy. Soc. A*, **218** (1953) 566.

3 G. C. Bond, *Catalysis by Metals*, Academic Press, New York, 1962.

4 B. E. Nieuwenhuys, D. Th. Meyer and W. M. H. Sachtler, submitted to *Surface Sci.*

- 5 R. Bouwman and W. M. H. Sachtler, *Surface Sci.*, 24 (1971) 140.
- 6 R. Suhrmann and G. Wedler, *Z. angew. Phys.*, 14 (1962) 70.
- 7 R. Bouwman, H. P. van Keulen and W. M. H. Sachtler, *Ber. Bunsenges. physik. Chem.*, 74 (1970) 198.
- 8 P. M. Gundry, J. Haber and F. C. Tompkins, *J. Catalysis*, 1 (1962) 363.
- 9 J. C. P. Mignolet, *Disc. Faraday Soc.*, 8 (1950) 105.
- 10 R. Suhrmann and G. Wedler, *Z. Elektrochem.*, 63 (1959) 748.

It has been shown that the polymerization of styrene in the presence of a small amount of a monofunctional monomer leads to a linear polymer with a narrow molecular weight distribution. The polymerization of styrene in the presence of a small amount of a difunctional monomer leads to a crosslinked polymer with a broad molecular weight distribution. The polymerization of styrene in the presence of a small amount of a trifunctional monomer leads to a highly crosslinked polymer with a very broad molecular weight distribution. The polymerization of styrene in the presence of a small amount of a tetrafunctional monomer leads to a highly crosslinked polymer with a very broad molecular weight distribution.

Table I

Summary of the experimental conditions and results for the polymerization of styrene in the presence of a small amount of a difunctional monomer. The values in parentheses are the values for the polymerization of styrene in the presence of a small amount of a monofunctional monomer.

Run	[M] ^a	[I] ^b	[D] ^c	Conversion (%)	\bar{M}_w/\bar{M}_n	Notes
1	1.0	0.01	0.00	100	1.05	Linear polymer
2	1.0	0.01	0.01	100	1.10	Linear polymer
3	1.0	0.01	0.02	100	1.15	Linear polymer
4	1.0	0.01	0.05	100	1.25	Linear polymer
5	1.0	0.01	0.10	100	1.40	Linear polymer
6	1.0	0.01	0.20	100	1.60	Linear polymer
7	1.0	0.01	0.50	100	1.80	Linear polymer
8	1.0	0.01	1.00	100	2.00	Linear polymer
9	1.0	0.01	2.00	100	2.20	Linear polymer
10	1.0	0.01	5.00	100	2.50	Linear polymer
11	1.0	0.01	10.00	100	2.80	Linear polymer
12	1.0	0.01	20.00	100	3.20	Linear polymer
13	1.0	0.01	50.00	100	4.00	Linear polymer
14	1.0	0.01	100.00	100	5.00	Linear polymer
15	1.0	0.01	0.01	100	1.05	Linear polymer
16	1.0	0.01	0.02	100	1.10	Linear polymer
17	1.0	0.01	0.05	100	1.20	Linear polymer
18	1.0	0.01	0.10	100	1.30	Linear polymer
19	1.0	0.01	0.20	100	1.40	Linear polymer
20	1.0	0.01	0.50	100	1.60	Linear polymer
21	1.0	0.01	1.00	100	1.80	Linear polymer
22	1.0	0.01	2.00	100	2.00	Linear polymer
23	1.0	0.01	5.00	100	2.20	Linear polymer
24	1.0	0.01	10.00	100	2.40	Linear polymer
25	1.0	0.01	20.00	100	2.60	Linear polymer
26	1.0	0.01	50.00	100	2.80	Linear polymer
27	1.0	0.01	100.00	100	3.00	Linear polymer
28	1.0	0.01	0.01	100	1.05	Linear polymer
29	1.0	0.01	0.02	100	1.10	Linear polymer
30	1.0	0.01	0.05	100	1.20	Linear polymer
31	1.0	0.01	0.10	100	1.30	Linear polymer
32	1.0	0.01	0.20	100	1.40	Linear polymer
33	1.0	0.01	0.50	100	1.60	Linear polymer
34	1.0	0.01	1.00	100	1.80	Linear polymer
35	1.0	0.01	2.00	100	2.00	Linear polymer
36	1.0	0.01	5.00	100	2.20	Linear polymer
37	1.0	0.01	10.00	100	2.40	Linear polymer
38	1.0	0.01	20.00	100	2.60	Linear polymer
39	1.0	0.01	50.00	100	2.80	Linear polymer
40	1.0	0.01	100.00	100	3.00	Linear polymer

It has been shown that the polymerization of styrene in the presence of a small amount of a difunctional monomer leads to a linear polymer with a narrow molecular weight distribution. The polymerization of styrene in the presence of a small amount of a trifunctional monomer leads to a crosslinked polymer with a broad molecular weight distribution. The polymerization of styrene in the presence of a small amount of a tetrafunctional monomer leads to a highly crosslinked polymer with a very broad molecular weight distribution.

It has been shown that the polymerization of styrene in the presence of a small amount of a difunctional monomer leads to a linear polymer with a narrow molecular weight distribution. The polymerization of styrene in the presence of a small amount of a trifunctional monomer leads to a crosslinked polymer with a broad molecular weight distribution. The polymerization of styrene in the presence of a small amount of a tetrafunctional monomer leads to a highly crosslinked polymer with a very broad molecular weight distribution.

It has been shown that the polymerization of styrene in the presence of a small amount of a difunctional monomer leads to a linear polymer with a narrow molecular weight distribution. The polymerization of styrene in the presence of a small amount of a trifunctional monomer leads to a crosslinked polymer with a broad molecular weight distribution. The polymerization of styrene in the presence of a small amount of a tetrafunctional monomer leads to a highly crosslinked polymer with a very broad molecular weight distribution.

It has been shown that the polymerization of styrene in the presence of a small amount of a difunctional monomer leads to a linear polymer with a narrow molecular weight distribution. The polymerization of styrene in the presence of a small amount of a trifunctional monomer leads to a crosslinked polymer with a broad molecular weight distribution. The polymerization of styrene in the presence of a small amount of a tetrafunctional monomer leads to a highly crosslinked polymer with a very broad molecular weight distribution.

^a [M] = 1.0 M, [I] = 0.01 M, [D] = 0.00 M, [T] = 0.00 M, [Tetra] = 0.00 M, [Solvent] = 1.0 M, [Temp] = 60°C, [Time] = 24 h.
^b [M] = 1.0 M, [I] = 0.01 M, [D] = 0.00 M, [T] = 0.00 M, [Tetra] = 0.00 M, [Solvent] = 1.0 M, [Temp] = 60°C, [Time] = 24 h.
^c [M] = 1.0 M, [I] = 0.01 M, [D] = 0.00 M, [T] = 0.00 M, [Tetra] = 0.00 M, [Solvent] = 1.0 M, [Temp] = 60°C, [Time] = 24 h.

Chapter V

THE CHANGES IN WORK FUNCTION OF GROUP Ib AND VIII METALS BY XENON ADSORPTION, DETERMINED BY FIELD ELECTRON AND PHOTOELECTRON EMISSION*

by

B.E. Nieuwenhuys, R. Bouwman** and W.M.H. Sachtler

Gorlaeus Laboratoria, Rijksuniversiteit, Leiden, Netherlands

A b s t r a c t

The surface potentials of xenon on Ni, Pd, Pt, Rh, Ir, Ru, Fe, Cu, Ag and Au films were determined by photoelectron emission as a function of the temperature of previous annealing. On Pd, Ir, Rh, Ru and Ag films, vapour quenched at 78 K, the surface potential does not change significantly up to an annealing temperature of 400 K, but on Au and Ni it decreases with annealing. The xenon surface potential is face-specific, as appears from measurements with a field emission microscope equipped with a probe-hole assembly. On Ir the largest surface potentials are found on the (111) and (100) tip regions. The variation in the surface potential on a polycrystalline film with the annealing temperature may be attributed to the change in the contribution of the various crystal faces on the film surface.

* Thin Solid Films 21 (1974) 55

** present address: Koninklijke/Shell-Laboratorium, Amsterdam, Netherlands

1. Introduction

Since Mignolet's discovery¹ in 1950 that Xe is adsorbed on a nickel film with a large positive surface potential (s.p.), i.e. a decrease in work function, a large number of s.p. values of Xe on various metals have been published. Most studies were carried out on polycrystalline metal films¹⁻¹⁰ while information of Xe on single crystal planes is limited to the Pd (100) plane¹¹ and to some crystal planes of Cu¹², Ag¹² and W^{13,14}. It appears that the s.p. at monolayer coverage depends besides on the metal also on the evaporation and/or subsequent annealing conditions of the film. A decrease in the s.p. of Xe with higher temperatures of annealing the films prior to admitting Xe at low temperatures has been reported for films of Ni^{4,5}, Cu^{6,8}, Fe⁸ and Ag^{9,12}. It has, therefore, been proposed that the Xe s.p. is larger on rough crystal planes than on close-packed planes¹⁵. A different interpretation, brought forward by Klemperer and Snaith⁸, suggests that the s.p. arises mainly from polarization of Xe atoms adsorbed at asperities where the surface electric field would be particularly large. Annealing of the films would result in a reduction of the number of effective asperities and, thus, to a lowering of the s.p.. However, on Ru films the s.p. remains constant up to an annealing temperature of 537 K⁷ and s.p. data on individual faces of W measured with the field electron probe-hole technique show that the s.p. on the closest-packed (110) face is much larger than on the (210), (100), (111) and (211) faces^{13,14}. In view of this rather confusing situation we decided to measure the s.p. of Xe on

- several metal films - Ni, Pd, Pt, Rh, Ir, Ru, Fe, Cu, Ag and Au - as a function of the annealing temperature, in order to investigate the possible significance of surface asperities on the s.p.;
- individual crystal faces of Ir and Pt.

The techniques used were photoelectron emission for films and field electron microscopy for single crystal faces. A comparison of the results obtained with these two techniques should enable us to understand the cause of the variation of the s.p. on films with the temperature of previous annealing.

2. Experimental

Spec.pure wires of Ni, Pt, Fe, Cu, Ag and Au, wires of Ir, Rh and Pd with a stated purity of 99.98% and spec.pure Ru sponge were supplied by Johnson, Matthey & Co., Ltd. London. The Ru sponge was molten in an argon

arc to pellets with a diameter of 0.1 - 0.2 mm. Pt, Ru, Cu, Ag and Au films were evaporated from beads of these metals which had been premelted in vacuum onto multi-hair-pin filaments of W wires. Ni, Pd, Rh, Ir and Fe films were evaporated from coils of these metal wires. All these metals were evaporated on a glass substrate cooled at 78 K. The gas pressure during evaporation was kept below 3×10^{-10} Torr.

Ir and Pt field emitters were obtained by electrolytic etching of wires with 0.10 mm diameter in an aqueous solution of CrO_3 and CaCl_2 , respectively. Emitter cleaning was performed by alternate heating to 1000 K and field evaporation in a vacuum below 1.10^{-10} Torr.

Xe with a stated purity of 99.997% was supplied by Air Liquide. Before entering the measuring tubes it was further purified with the aid of freshly evaporated Ni getter films in the supply system. The maximum Xe pressures used were 10^{-7} Torr for the field emission and 10^{-3} Torr for the photoelectron emission experiments. All adsorption measurements were carried out at 78 K.

For the photoelectric measurements a narrow light beam monochromatized by a grating monochromator, equipped with a high pressure mercury lamp was directed by a mirror system either onto the phototube containing the metal film or to a calibrated Ta reference tube. The phototube used was described earlier¹⁶.

The field emission apparatus has also been described previously¹⁷. It consists of a probe-hole field emission tube with as most essential parts a movable emitter which can be cooled to 78 K, an electrically conducting and fluorescent screen with in its centre a hole of 1.0 mm diameter and a shielded hemispherical electron collector behind the hole.

The s.p. values were determined with the aid of the Fowler-Nordheim equation in field emission and of the Fowler equation in photoemission. All details have been given earlier¹⁶⁻¹⁸.

3. Results

A. The s.p. of Xe on various metal films as a function of the temperature of previous annealing.

Table I summarizes some results for films of group VIII and Table II of group Ib metals. The variations of the s.p. with the temperature at which the films were annealed prior to admission of Xe at 78 K are shown in

Table I

The work function (ϕ) of a film annealed at a temperature T_s , the surface potential (s.p.) of Xe and the change in emission constant (Δm) by Xe adsorption

metal	T_s (K)	ϕ (eV)	s.p. (V)	$\Delta \log m$
Fe	78	4.06	0.50	- 0.11
	293	4.36	0.46	- 0.12
Ru	78	4.50	0.95	- 0.16
	293	4.71	0.98	- 0.26
	373	4.76	0.98	- 0.28
	473	4.82	1.00	- 0.36
	573	4.89	0.98	- 0.38
Rh	78	4.88	1.09	- 0.09
	293	4.98	1.08	- 0.09
	373	5.11	1.07	- 0.13
	458	5.18	1.01	- 0.11
Ir	78	5.17	1.05	- 0.14
	293	5.33	1.03	- 0.13
	373	5.36	1.01	- 0.16
	473	5.38	0.94	- 0.16
Ni	78	4.56	1.01	- 0.18
	293	4.90	0.85	- 0.15
	406	5.11	0.73	- 0.05
	589	5.16	0.6	- 0.11
Pd	78	4.90	1.12	- 0.16
	293	5.12	1.08	- 0.15
	383	5.20	1.06	- 0.14
	483	5.22	1.03	- 0.14
	583	5.22	0.96	- 0.11
Pt	373	5.69	0.90	- 0.03
	473	5.70	0.85	- 0.05
	573	5.72	0.65	- 0.21

Table II

The work function (ϕ) of a film annealed at a temperature T_s , the surface potential (s.p.) of Xe and the change in emission constant (Δm) by Xe adsorption

metal	T_s (K)	ϕ (eV)	s.p. (V)	$\Delta \log m$
Cu	78	4.19	0.55	- 0.1
	293	4.52	0.63	- 0.1
Ag	78	4.18	0.75	- 0.25
	293	4.33	0.71	- 0.21
	378	4.35	0.74	- 0.20
	485	4.37	0.73	- 0.21
Au	78	5.06	0.59	- 0.21
	293	5.28	0.52	+ 0.06
	373	5.31	0.51	+ 0.05
	498	5.32	0.51	+ 0.05
	573	5.34	0.51	+ 0.05

figures 1 and 2. The s.p. values in these figures were obtained from measurements on at least two different films of each metal except for Ir and Pd for each of which one film was used.

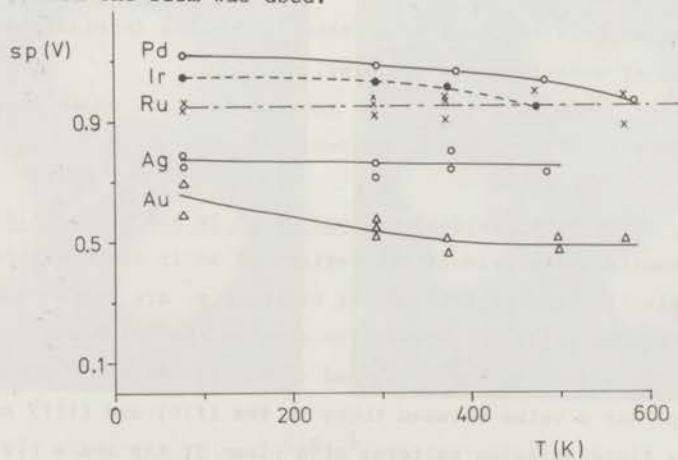


Fig. 1

The influence of previous annealing on the surface potential of Xe on Pd, Ir, Ru, Ag and Au films

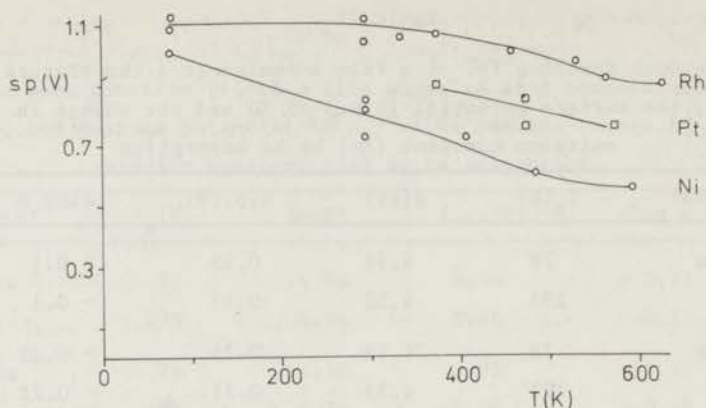


Fig. 2

The influence of previous annealing on the surface potential of Xe on Rh, Pt and Ni films

The relevant results are:

- 1) The work function of all films increases significantly by annealing, in agreement with results of Bouwman and Sachtler¹⁹.
- 2) The s.p. of Xe on Au and Ni films decreases when the vapour-quenched films, deposited at 78 K, are annealed. This decrease is strongly dependent on the annealing temperature but not on the annealing time.
- 3) The s.p. of Xe on Pd, Ir and Rh films does not change significantly by annealing up to a temperature of about 400 K and decreases only slightly at higher annealing temperatures.
- 4) The s.p. of Xe on Ru and Ag films remains constant up to an annealing temperature of 573 and 485 K, respectively.

B. The s.p. of Xe on individual regions of an Ir and a Pt field emitter.

The results on individual tip regions of an Ir field emitter are given in Table III. The highest values of the s.p. are found on the closest-packed tip regions (111) and (100). The s.p. on the (110) region is only one-half of the values on the (111) and (100) regions. At the rough (210) area the s.p. has a value between those on the (110) and (111) and (100) regions. The field emission patterns of a clean Ir tip and a tip saturated with Xe at 78 K are shown in Fig. 3. The decrease in emissivity of the (110) region in respect to e.g. the (210) region is clearly visible. The emission of the tip saturated with Xe is mainly originated from the regions

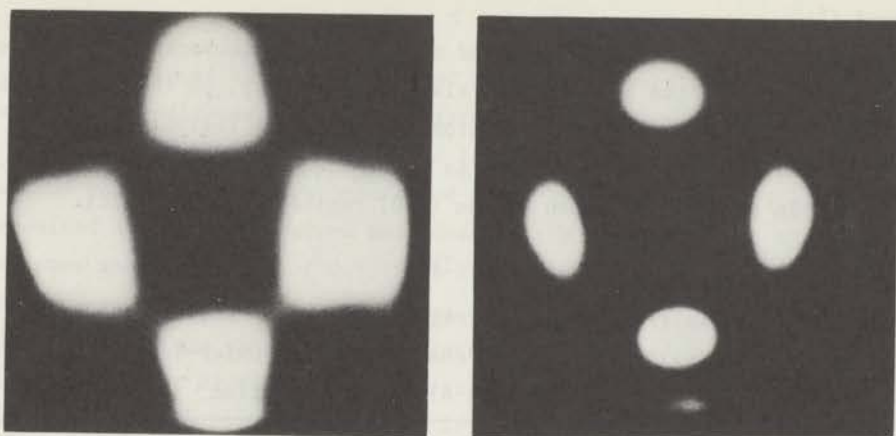


Fig. 3

Field emission from Ir before and after Xe adsorption at 78 K

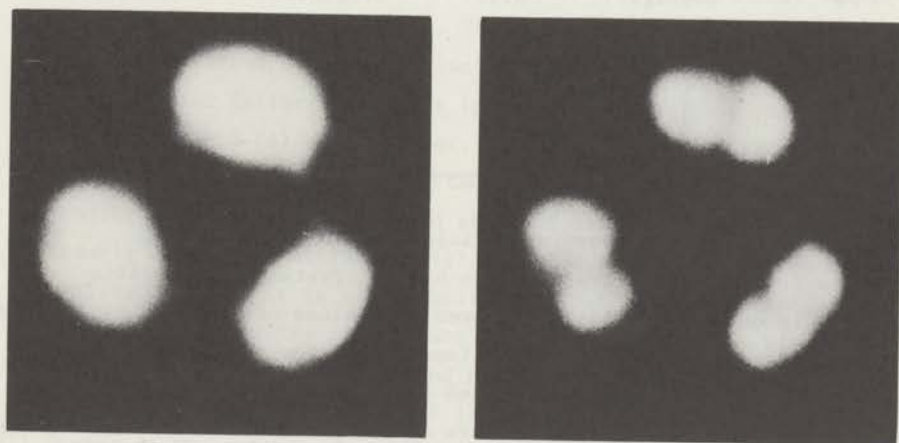


Fig. 4

Field emission from Pt before and after Xe adsorption at 78 K

around (210).

The pattern of a clean Pt tip and of the same tip covered with Xe are shown in fig 4. It can be seen that also on Pt the s.p. on the (110) region is smaller than on the surrounding atomically rougher regions as around (210). The s.p. on the (100) region is about the same as the average s.p. over the tip and is lower than on the (210) region (See Table III).

Table III

Work functions (ϕ) of some tip regions of Ir and Pt, surface potentials (s.p.) of Xe and the changes in the Fowler-Nordheim pre-exponentials ($\Delta \log A$) by Xe adsorption

metal	tip region	ϕ (eV)	s.p.(V)	$\Delta \log A$
Ir	average	5.00	1.18±0.03	-0.42±0.05
	(111)	5.79	1.8	-1.9
	(100)	5.67	1.6	-1.8
	around (110)	5.0	0.8	-0.0
	(210)	5.0	1.3	-0.5
	(331)	5.4	1.1	-0.4
	(321)	5.4	1.0	-0.0
Pt	average	5.32	0.95±0.02	-0.64±0.04
	(100)	5.8	0.96	
	(210)	5.2	1.1	
	(321)	5.4	0.9	
	(311)	5.5	0.9	

In summarizing, the pertinent field emission results are:

- 5) The s.p.'s of Xe on Ir and Pt are highly crystal face specific.
- 6) There is no direct relation between the values of the Xe s.p. and the atomic roughness, i.e. the work function of the tip regions. Large s.p.'s are found on closest-packed tip regions as Ir (111), Ir (100) and Pt (100) but also on some more open high-index faces as the (210) region. On the rather close-packed (110) regions low s.p. values are found.
- 7) The s.p.'s of Xe on Ir are larger than on Pt.

4. Discussion

Comparison of our s.p. values of Xe on polycrystalline films with literature data indicates that there exists no unique picture of these values on polycrystalline films. On Ag, for instance, Knapp and Stiddard⁹ report maximum values of 0.6 V on unannealed films and 0.45 to 0.49 V on films deposited at room temperature and subsequently annealed up to 453 K whereas we found maximum values of 0.7 - 0.8 V on unannealed as well as on films annealed up to 485 K. Possible causes of this diversity in s.p. values are differences in the abundances of crystal faces in the outer surface of the film as a result of different evaporation and/or subsequent annealing circumstances, and other contamination levels.

For some metal films annealing prior to admitting Xe at 78 K causes the s.p. of Xe to decrease. This has also been observed by other authors: on Ni^{4,5}, Fe⁸, Cu^{6,8} and Ag^{9,12} films. Possible causes for this decrease are:

- I) Contamination of the film during the annealing process. Although this possibility cannot be entirely excluded, it appears rather improbable to us, as the annealing time has no large influence on the s.p. (result 2).
- II) Reduction of the number of surface asperities by annealing, as proposed by Klemperer and Snaith⁸. The correlation between the s.p. of Xe and the latent heat of sublimation (or melting point) as suggested by Hall²⁰ and Müller¹⁵ would be in agreement with this proposal. Results (3) and (4) can, however, not be reconciled with this view. For instance, the number of surface asperities must be considerably smaller for an Ag film annealed at 485 K than for the very rough film freshly evaporated at 78 K, still the s.p. is not changed by the annealing process. It is also significant that our s.p. values do not confirm the suggested correlation^{20,15} between the Xe s.p. and the melting point: Au with a melting point of 1336 K displays a lower s.p. than Ag with a melting point of 1234 K.
- III) Change in the relative contribution of various crystal faces on the film surface by annealing. Result (5) shows that this view can be a valid explanation for the variation of the s.p. on some metal films with the annealing conditions.

The surface structure of a film is changed during annealing. The resulting abundance of crystal faces on the surface depends on many variables as rate and temperature of evaporation, film thickness, the substrate, rate of temperature increase, and, of course, on the annealing temperature²¹. The contribution of (111) and (100) faces will certainly be higher on thick well-annealed films than on rough films. The simplest explanation for the lowering of the s.p. upon previous annealing in terms of model III is, therefore, the suggestion¹⁵ that the s.p. on rough crystal faces should be larger than on close-packed faces. However, if this were correct, annealing should always cause an increase in work function and a decrease in s.p.. Results (3) and (4) show that such a general relation of changes in work function and s.p. upon annealing does not exist. The increase in work function (result 1) is, undoubtedly, a result of a larger contribution of close-packed crystal faces. We, therefore, conclude that a relative increase in the contribution of smooth crystal faces does not unequivocally cause a decrease in s.p.. This is further confirmed by the field emission result (6). A high s.p. was also found on a macroscopic Pd (100) plane by Palmberg¹¹. On Ir the s.p. decreases in the order (111), (100), (210) and (110) faces. It is, therefore, clear that the dependence of the s.p. on the atomic roughness of a face is not straightforward. It remains valid, however, that the s.p. of Xe on a metal film and its change upon annealing are determined by

- (a) the crystal face distribution on the surface;
- (b) the s.p.'s on the individual crystal faces of the metal.

In conclusion we can state that the dependence of the surface potential of Xe on the state of previous film annealing can be rationalized in terms of the relative contribution of crystal faces to the total surface. The individual surface potentials on each crystal face are, however, not sufficiently determined by their atomic packing. Upon annealing the surface potential therefore changes in a more complicated way than the work function of the pure metal does.

Acknowledgements

The investigations were supported by the Netherlands Foundation for Chemical Research (S.O.N.) with financial aid from the Netherlands Organization for the Advancement of Pure Research (Z.W.O.).

References

1. J.C.P. Mignolet, *Disc. Faraday Soc.* 8 (1950) 105.
2. J.C.P. Mignolet, *J. Chem. Phys.* 21 (1953) 1298.
3. J.C.P. Mignolet, in "Chemisorption" (W.E. Garner, ed.), Butterworths, London, 1957, p. 118.
4. R. Suhrmann, E.A. Dierk, B. Engelke, H. Hermann and K. Schulz, *Naturwissenschaften* 43 (1956) 127.
5. R. Suhrmann, E.A. Dierk, B. Engelke, H. Hermann and K. Schulz, *J. Chim. Phys.* 54 (1957) 15.
6. J. Pritchard, *Trans. Faraday Soc.* 59 (1963) 437.
7. R. Bouwman and W.M.H. Sachtler, *Ber. Bunsenges. physik. Chem.* 74 (1970) 1273.
8. D.F. Klemperer and J.C. Snaith, *Surface Sci.* 28 (1971) 209.
9. A.G. Knapp and M.H.B. Stiddard, *J. Chem. Soc., Faraday Trans. I*, 68 (1972) 2139.
10. Th.G.J. van Oirschot and W.M.H. Sachtler, *Ned. Tijdschrift Vacuümtechniek* 8 (1970) 96.
11. P.W. Palmberg, *Surface Sci.* 25 (1971) 598.
12. M.A. Chesters, M. Hussain and J. Pritchard, *Surface Sci.* 35 (1973) 161.
13. J. Nikliborc and Z. Dworecki, *Acta Physica Polonica* 32 (1967) 1023.
14. T. Engel and R. Gomer, *J. Chem. Phys.* 52 (1970) 5572.
15. J. Müller, *Chem. Commun.* (1970) 1173.
16. R. Bouwman, H.P. van Keulen and W.M.H. Sachtler, *Ber. Bunsenges. physik. Chem.* 74 (1970) 198.
17. B.E. Nieuwenhuys and W.M.H. Sachtler, *Surface Sci.* 34 (1973) 317.
18. B.E. Nieuwenhuys, D.Th. Meijer and W.M.H. Sachtler, *Surface Sci.*, 40 (1973) 125.
19. R. Bouwman and W.M.H. Sachtler, *Surface Sci.* 24 (1971) 350.
20. P.G. Hall, *Chem. Commun.* (1966) 877.
21. P.E.C. Franken, R. Bouwman, B.E. Nieuwenhuys and W.M.H. Sachtler, *Thin Solid Films* 20 (1974) 243.

Chapter VI

CRYSTAL FACE SPECIFICITY OF XENON ADSORPTION ON IRIDIUM FIELD EMITTERS*

by

B.E. Nieuwenhuys and W.M.H. Sachtler

Gorlaeus Laboratoria, Rijksuniversiteit, Leiden, Netherlands

A b s t r a c t

Fundamental problems of the adsorption of noble gas atoms on metal surfaces are discussed on the basis of new data of xenon adsorption on well-defined crystal faces of iridium. These data include surface potentials (= changes in work function), heats of adsorption and their decrease with increasing coverage; they have been obtained by using a field emitter probe-hole assembly. It is found that the heat of adsorption Q_{hkl} is not simply additive in the number of Ir atoms contacting a Xe atom on a given site; in particular for the close-packed faces, Q_{111} and Q_{100} are relatively too high. Apparently, strong bonding is favoured by high work function of the adsorbing crystal face. This proves a significant contribution of a charge-transfer no-bond interaction to the adsorption bond.

A model of Xe polarization by an electric surface field is rejected, as it predicts the wrong sign for the adsorption dipole.

While at low coverage adsorption is confined to sites determined by the atomic topography of the adsorbing surface, several possibilities exist for high coverages. Either a two-dimensional close-packed layer is formed with little or no epitaxial relation to surface topography, or adsorption remains confined to certain sites. The present data favour the former possibility for atomically smooth faces in agreement with recent LEED results. For atomically rough faces however, the smallness of the decrease of Q_{hkl} with coverage seems to favour site adsorption even at high coverage. The latter result is of relevance for surface area determinations by means of "physical" adsorption.

* submitted to Surface Science

1. Introduction

Adsorption of inert gases has been used over many years in order to determine the surface areas of polycrystalline metal samples. It was assumed in early work that the inert gas atoms do not encounter an influence of the geometry of the surface. The packing in the adsorbed layer would resemble the closest-packed layer as is formed in the condensed phase of the particular gas. Field emission experiments revealed, however, that adsorption of Xe, Kr and Ar on W displays a large crystal specificity¹⁻⁴. The heat of adsorption of Xe appeared to be much higher on (411) - (611) regions where the adatoms fit perfectly into the substrate structure, than on (111) faces where Xe is less coordinated^{2,4}. Comparable results were obtained by field emission microscopy for Xe adsorption on Mo⁵, just as W a metal with the b.c.c. structure and also on Re⁶ with the h.c.p. structure. All these results support strongly the view that the adsorption of inert gases on metals is a true site adsorption. Relevant in this context is also the observation of Ponc and Knor⁷ that the number of adsorbed Xe atoms in a monolayer on a Ni film is in no way smaller than the number of adsorbed Kr atoms on the film, while Xe has a much larger atomic radius than Kr. Brennan and Graham⁸ found that the ratio of the monolayer capacities for these two gases on films of several metals is close to unity. Also these results support the view of site adsorption. More recently Engel and Gomer⁹ have used the field emission probe-hole technique to examine the adsorption of Ar, Kr and Xe on those individual planes of W which are not accessible with the conventional field emission technique. The binding energy appeared to be much larger on the closest-packed face, the (110) face, than on the (210), (100), (211) and (111) faces although the adatoms can be here only in contact with a small number of metal atoms, much smaller than on the other faces. Unfortunately, the region near (411) where the earlier field emission studies had demonstrated a high heat of adsorption, was not examined. Recent LEED observations of Ar on Nb (100)¹⁰, a b.c.c. lattice and of Xe on the f.c.c. crystal faces Pd (100)¹¹, Cu (111), (100) and (110)^{12,13} and Ag (111), (110) and (211)¹³ indicate that at high coverage the adatoms are close-packed on these surfaces. The surface areas per Xe adatom in a complete monolayer is about 17 \AA^2 on each of these surfaces, resembling the area in bulk Xe. It appears, therefore, from the LEED results that the packing of Xe on these surfaces is, at least at monolayer coverage, more governed

by the adatom size than by lattice-packing.

The aim of the present study is to investigate the influence of the metal surface structure on the adsorption of Xe. For this purpose the field emission probe-hole technique was chosen because a field emitter is a nearly ideal adsorbent for this study since it is a small almost perfect single crystal simultaneously exposing several crystal faces. The probe-hole device enables us to investigate the adsorption of Xe on all the exposed crystal faces at exactly identical circumstances. Since most of the above mentioned LEED results were obtained on f.c.c. metal surfaces we decided to use Ir, a metal which has the f.c.c. structure and where no special difficulties are encountered in emitter cleaning.

For the probe-hole measurements were selected a number of emitter regions exposing strongly different sites viz. the smooth regions (111) and (100); the region around (110), the rough region around (210), the regions around (531), consisting of (210) areas alternated by small (111) terraces, the (321) region which is basically a (531) plane with larger (111) terraces and the (511) region, possessing large (100) terraces.

The results are also of interest for a better understanding of the nature of the bond between inert gases and metal surfaces. The classical picture which regards inert gas adsorption as due entirely to the dispersion interaction, appeared to be unable to explain the observed large surface potentials of adsorbed noble gases¹⁴ and the relative ordering of the binding energies on the crystal planes of W^9 .

2. Experimental

Iridium field emitters were prepared from 0.10 mm wires, spot-welded to 0.25 mm diameter loops of Ir. The Ir wires had a stated purity of 99.98%. The tips were sharpened by electrolytic etching in an aqueous solution of CrO_3 . Emitters were cleaned by field desorption and field evaporation at room temperature in a vacuum below 1.10^{-10} Torr, alternated with prolonged heating periods to 1000 K. In this way also the tip shanks were cleaned sufficiently so that no diffusion of contaminants to the tip took place in the temperature range 78 to 296 K where the experiments have been carried out.

Xenon with a stated purity of 99.997% was further purified with the aid of freshly evaporated Ni getter films in the supply system. In the

field emission tube the equilibrium pressure of Xe was $< 1.10^{-7}$ Torr.

The field emission apparatus has been described previously¹⁵. It consists of a field emission probe-hole tube connected to a bakeable ultra-high vacuum system, equipped with a gas-dosing ultra-high vacuum line to the Xe ampulla. The most essential parts of the tube are a movable emitter which can be cooled to 78 K and heated to any desired temperature, an electrical conducting and fluorescent screen with in its centre the probe-hole of 1.0 mm diameter and a shielded hemispherical electron collector behind the probe-hole.

Tip temperatures were determined by measuring the heating current through the loop. The temperature-current relation was preliminary calibrated with the aid of chromel-alumel thermocouple wires. Any desired temperature in the range 78 - 300 K could be obtained within a few seconds.

Measurements were made by positioning the tip such that the emission beam from the desired region was directed to the probe-hole. After the necessary calibration measurements were carried out, the tip was cleaned and the Fowler-Nordheim work function of the tip area was measured. Hereafter Xe was admitted in the tube while the temperature of the tip was 78 K. When the emission current remains stable the change in work function was measured. After this the tip temperature was gradually increased, and the behaviour of the adlayer was followed at continually higher temperatures by measuring the emission voltage necessary to maintain a constant emission current of the probed region. When depletion of the tip area considered was complete, data for a Fowler-Nordheim plot were collected at this temperature in order to check the cleanliness of the tip area. Hereafter the tip was repositioned in order to repeat the measurements on other tip regions.

3. Determination of the surface potential of Xe on the different tip regions.

The electron currents I_{hkl} from a probed region (hkl) at applied voltages V were plotted as $\ln I_{hkl}/V^2$ versus $1/V$ which produces a straight line according to the Fowler-Nordheim equation:

$$\ln \frac{I_{hkl}}{V^2} = \ln A_{hkl} - B\phi_{hkl}^{3/2}/V \quad (1)$$

In this equation ϕ_{hkl} stands for the work function of the tip region (hkl), $\ln A_{hkl}$ for the field independent pre-exponential term and B for a term

containing the field (F)-voltage proportionality constant C

$$B = 6.8 \times 10^7 / C \quad (2)$$

and

$$F = CV \quad (3)$$

The change in C and thus in B by adsorption is usually so small that it may be neglected. Comparison of the slopes m_{hkl} of the Fowler-Nordheim plots for a clean and a Xe covered tip region yields therefore

$$s.p._{hkl} = \frac{-\Delta\phi}{e} = \frac{\phi_{clean} - \phi_{Xe}}{e} = \frac{\phi_{clean}}{e} \left\{ 1 - \left(\frac{m_{hkl}(Xe)}{m_{hkl}(clean)} \right)^{2/3} \right\} \quad (4)$$

Insertion of the value $\phi_{hkl}(clean)$, which determination has been described previously¹⁶, in equation (4) yields the surface potential $s.p._{hkl}$ on the tip region (hkl).

4. Determination of the heat of adsorption.

Values for the free activation energies of desorption ΔF_{des}^* can be estimated by following the desorption at a temperature T, using the equation

$$\Delta F_{des}^* = RT \ln \left\{ \frac{kT}{h} \tau_{des} \ln 2 \right\} \quad (5)$$

where k and h are Boltzmann's and Planck's constants, respectively.

τ_{des} is defined by the absolute rate theory as the time where the degree of coverage θ changes from $\theta = 1$ to $\theta = \frac{1}{2}$ under conditions where readsorption can be neglected. Experimentally τ_{des} is approximated by the time (in seconds) during which the electron current changes by $\frac{1}{2} |I_{\theta=1} - I_{\theta=0}|$ at constant T and V. If the assumption is made that the activation entropy of desorption is zero, ΔF_{des}^* becomes equal to the activation energy of desorption E_{des} . As will appear in the next section the activation energy for adsorption is zero, hence, the estimated activation energy of desorption is equal to the heat of adsorption:

$$\Delta F_{des}^* \sim E_{des} = -\Delta H_{ads} = Q_{ads} \quad (6)$$

The desorption behaviour of Xe on Ir on each region (hkl) cannot be described by using one single value of Q_{ads} . Therefore, three isothermal heats of adsorption were considered, viz. Q_{hkl}^{min} , the heat of adsorption at high coverage; Q_{hkl} , the heat of adsorption calculated at a temperature where the temperature programmed desorption plot exhibits a maximum rate of desorption (see next section); and Q_{hkl}^{max} , the maximum heat of adsorption.

The experimental error in the Q_{hkl} 's is mainly determined by the accuracy in the loop current - tip temperature calibration. The experimental

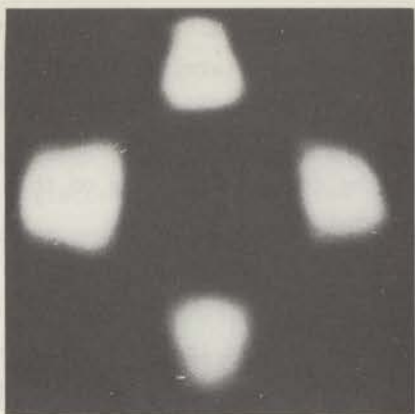
error in T is about 4° corresponding with an experimental error in Q of only 0.3 kcal/grat. The actual error is, of course, determined by limitation of the procedure followed. For our purpose it is sufficient to know exactly the relative heats of adsorption on the various tip regions. The estimated error in the differences between the comparable Q_{hkl} 's on the different tip regions is less than 0.2 kcal/grat.

5. Results.

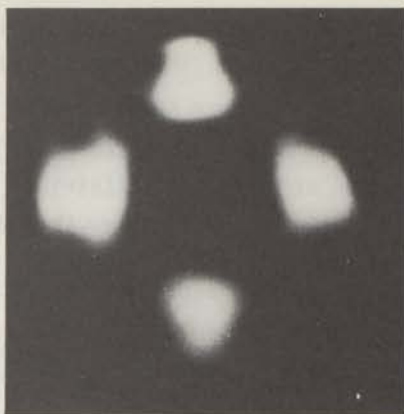
The changes in field emission pattern when an Ir tip at 78 K is exposed to Xe at a pressure of 10^{-8} Torr are shown in Fig. 1. The adsorption causes a large increase in emission. All the pictures were taken at a constant total current of 1.10^{-8} A. The applied voltage between fluorescent screen and tip had to be diminished steadily during the adsorption process to maintain a constant current. Xe adsorption affects the field emission image in a very characteristic way. In the early stage of adsorption the areas around (321), which are dark in the clean pattern, are strongly brightened (Fig. 1b - c). After longer exposure times these bright areas grow into the direction of the (320) - (210) poles (Fig. 1d - e). In a later stage the bright areas shrink to the direction of (320) - (210) (Fig. 1f - g). At saturation most of the emission is, as in the clean pattern, mainly originated from regions around (320) - (210) (Fig. 1h). The emissivity of the region around (110) is appreciably decreased in respect to the (320) - (210) regions.

The local changes in work function by Xe adsorption at monolayer coverage, which can be found in Table I, reveal that Xe adsorption has also a surprisingly large effect on the emission from the dark densely-packed regions (111) and (100). The largest changes in work function are found just there.

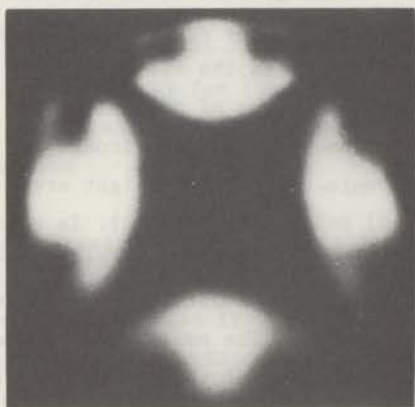
The nature of the changes in field emission image during adsorption is clarified by observing the course of the emission patterns with increasing tip temperature, as shown in Fig. 2. The Xe pressure during the experiments was 3.10^{-8} Torr. Again a constant emission current was maintained by adjusting the voltage. The first changes can be observed to occur near 102 K (Fig. 2b). At 114 K the image resembles the clean image except around the (321) poles, where the emissivity is still much higher than on the bare tip (Fig. 2f). At 116 K the emission intensity of the (321) regions is also visibly reduced (Fig. 2g) while at 123 K the original clean



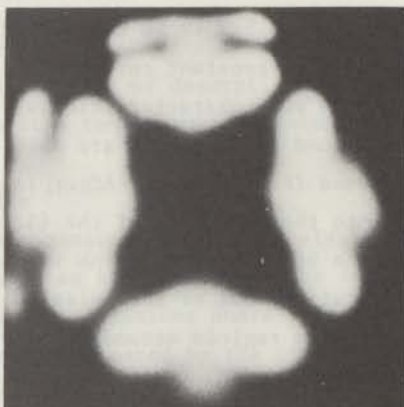
a



b



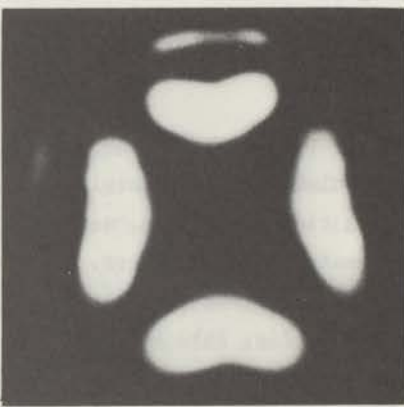
c



d



e

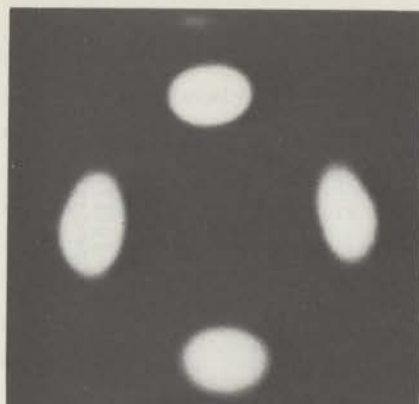


f

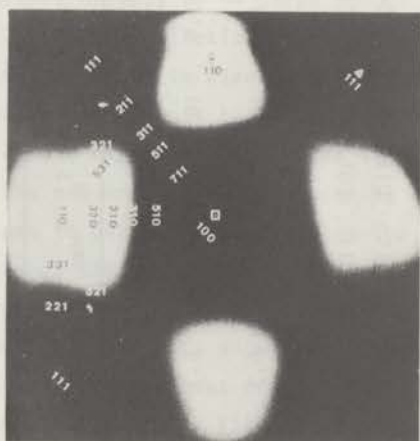
Fig. 1a - 1f



g



h



i

Fig. 1

Change in field emission pattern by Xe adsorption at 78 K.

a : clean Ir tip

b-h: increasing coverage

h : monolayer coverage

i : orientation diagram

TABLE I

Work function (ϕ), the maximum surface potential of Xe (s.p.), the change in Fowler-Nordheim pre-exponential ($\Delta \log A$) by Xe adsorption and the heats of adsorption (Q) calculated from the desorption times at temperatures T , on different tip regions

Tip region	ϕ (eV)	s.p. (V)	$\Delta \log A$	T_{\min}	T_n	T_{\max}	Q_{\min} (kcal/mole)	Q_n (kcal/mole)	Q_{\max} (kcal/mole)
total emission	5.00	1.18 ± 0.03	-0.42 ± 0.05						
(111)	5.79 ± 0.05	1.8	-1.9	103	111	118	6.5	7.0	7.5
(100)	5.67 ± 0.05	1.6	-1.8	103	109	118	6.5	6.9	7.5
around (110)	5.0	0.8	-0.0	99	103	110	6.3	6.5	7.0
(210)	5.0	1.3	-0.5	105	110	115	6.7	7.0	7.2
(321)	5.4	1.0	-0.0	110	119	124	7.0	7.6	7.8
(511)				103	107	115	6.5	6.8	7.2
(531)-(731)	4.9			106	110	115	6.7	7.0	7.2

pattern is restored (Fig. 2h).

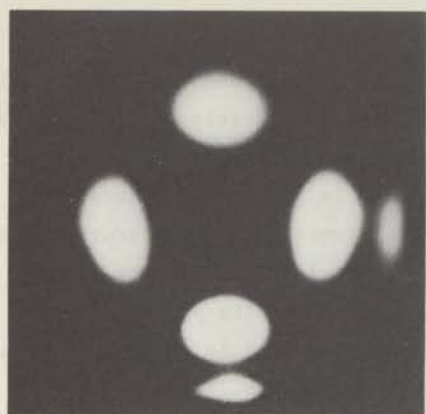
Obviously the sequence of emission patterns observed during gradually increasing the tip temperature (Fig. 2) is completely the reversal of the series of pictures observed during increasing the Xe coverage at 78 K (Fig. 1). Further, it appeared that all images in Fig. 2 are reversible upon changes in tip temperature. When, for instance, the temperature of the tip partly covered with Xe at 114 K (Fig. 2f) is lowered to 112 K, the image changes again to that of Fig. 2e. These two results prove that

(a) a surface equilibrium distribution of the adsorbed Xe can be established at all the temperatures used in our experiments.

(b) the activation energy of adsorption is approximately zero.

All changes occurring by temperature increase have, therefore, to be attributed to a denuding of certain tip regions. Even at 78 K the diffusion rate of Xe over the tip surface appears to be large enough for the establishment of a diffusional equilibrium distribution of Xe over the whole tip surface. So we conclude that the increase in electron emission around (321) in the early stage of adsorption corresponds to an enhancement of the Xe concentration on this area at the expense of areas as (210), (311) and (511). In other words, both the sequence of pictures during adsorption at 78 K (Fig. 1) and the changes in pattern by increasing the tip temperature (Fig. 2) point to a higher binding energy of Xe on the (321) regions with respect to their surroundings.

The above-mentioned results show that the adsorption of Xe on Ir is crystal face specific: both the heat of adsorption and the surface potential depend on the surface structure. Figures 1 and 2, however, do not give information of the heat of adsorption on the two most densely-packed regions where the surface potentials are the largest. Therefore, the change in emission of various tip regions covered with Xe were recorded during temperature programmed desorption: the temperature of a tip completely covered with Xe, was increased by a few degrees to temperature T . After 60 seconds the voltage required to maintain the original electron current of the probed region was determined. The temperature was then again increased by a few degrees. The voltage was adjusted after 60 seconds, etc.. The Xe pressure during these experiments was 3.10^{-8} Torr. The results of this procedure carried out on various tip regions are shown in Fig. 3. In Fig. 4 the first derivatives of the desorption plots of Fig. 3 are given. It appeared that on the flat parts of the desorption plots, thus in the begin-



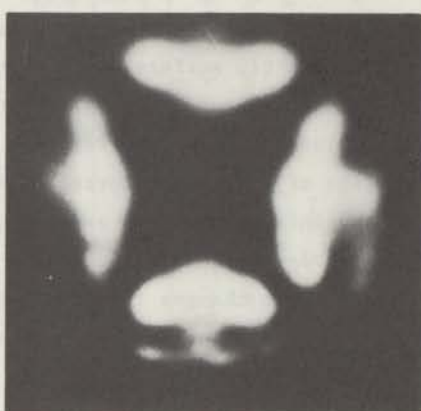
a



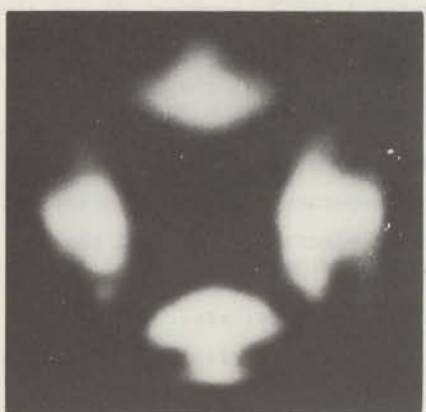
b



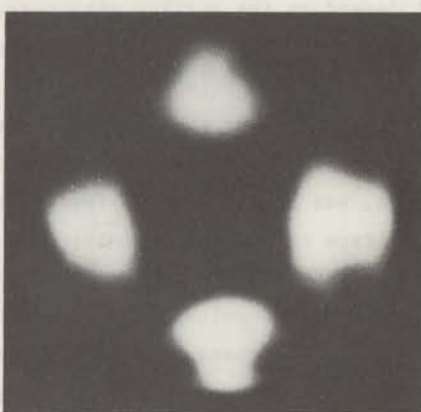
c



d

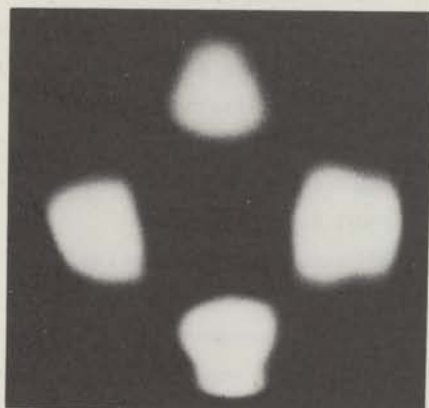


e

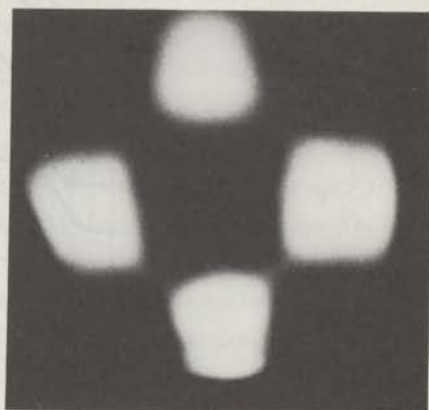


f

Fig. 2a - 2f



g



h

Fig. 2

Thermal desorption of Xe from Ir. $p \approx 3 \cdot 10^{-8}$ Torr.

a) T = 90 K.	Voltage	required	for	a	total	current	of	$1 \cdot 10^{-8}$ A:	1422 V
b) T = 102 K.	"	"	"	"	"	"	"	"	: 1500 V
c) T = 105 K.	"	"	"	"	"	"	"	"	: 1654 V
d) T = 110 K.	"	"	"	"	"	"	"	"	: 1749 V
e) T = 112 K.	"	"	"	"	"	"	"	"	: 1858 V
f) T = 114 K.	"	"	"	"	"	"	"	"	: 1894 V
g) T = 116 K.	"	"	"	"	"	"	"	"	: 1916 V
h) T = 123 K.	"	"	"	"	"	"	"	"	: 1935 V

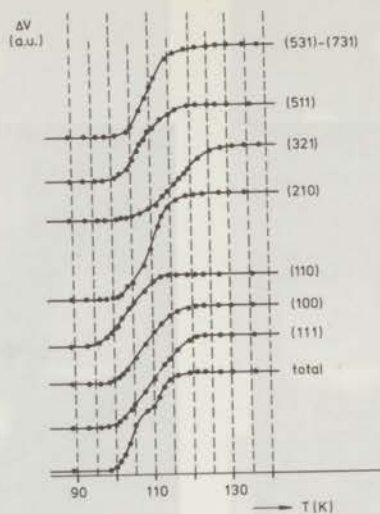


Fig. 3

Variation in voltages required for constant emission currents from individual tip regions during thermal desorption of xenon.

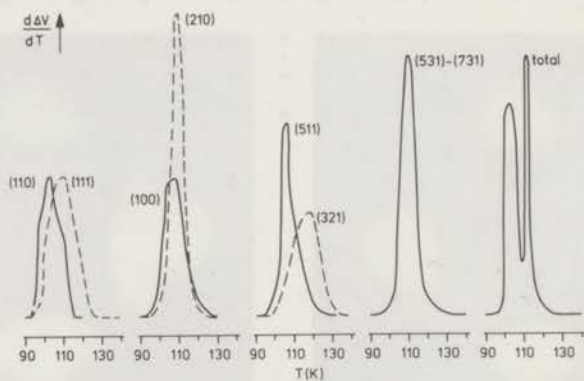


Fig. 4

The first derivatives of the desorption plots of Fig. 3.

ning and in the end of the plots the time interval of 60 sec. was large enough for the attainment of a constant emission. A decrease in temperature again causes an enhancement of the emission. So a new adsorption equilibrium situation was again established within 60 sec. In the steep part of the desorption plots, however, the time intervals between the successive temperature rises were too short to attain an equilibrium situation. We conclude from these observations that the adsorbed Xe at monolayer coverage on a tip region cannot be represented by one single value for the heat of adsorption but that the heat of adsorption decreases with increasing coverage.

The function of the heat of adsorption versus coverage is characterized by three numerical values for the heats of adsorption on each of a number of tip regions. They were determined by measuring the desorption times at three temperatures, starting at monolayer coverage and at a low residual Xe pressure ($\sim 10^{-9}$ Torr), so that the contribution of readsorption is small. The three characteristic temperatures are:

- I A temperature T_n at which the largest effect on the emission occurs, hence the temperature at which the plots of Fig. 4 exhibit a maximum.
- II A temperature T_{max} just high enough to desorb all the adsorbed Xe.
- III A temperature T_{min} high enough to desorb the most loosely bound Xe and to bring about a new adsorption equilibrium situation while the more firmly bound Xe cannot be desorbed.

From equations (5) and (6) the corresponding heats of adsorption were estimated. The results are inserted in Table I. Q_n corresponds approximately to the heat of adsorption with which most of the adsorbed Xe is bound on the surface. Q_{max} is the maximum heat of adsorption, hence the heat of adsorption at low coverage. Q_{min} corresponds roughly to the minimum heat of adsorption, hence to the heat of adsorption at high coverage.

The initial heat of adsorption decreases in the sequence (321); (111) and (100); (531)-(731) and (210); and (110). This order was found to be reproducible on each of the three tips used for the Xe adsorption experiments.

Summarizing, the relevant results are

- (1) the mobility of adsorbed Xe is high enough, even at 78 K, for the attainment of an adsorption equilibrium between the different tip regions.
- (2) Xe adsorption is crystal face specific. Both the heat of adsorption and the surface potential vary with the tip region.
- (3) There is no direct relation between the heat of adsorption and the

surface potential of Xe at monolayer coverage on the different tip regions.

- (4) the maximum heat of adsorption decreases in the sequence (321); (111) and (100); (531) - (731) and (210); and (110).
- (5) the heat of adsorption decreases with increasing coverage. This decrease is much smaller on the (210) and (531) regions than on (111) and (100).

6. Discussion.

First it has to be examined whether the electric field necessary to obtain electron emission might have influenced the obtained results. It may be argued that this field effect is negligible since

- a. no deviation from linearity of the Fowler-Nordheim plots could be observed.
- b. the values for the surface potential and the heat of adsorption do not differ significantly from values obtained by means of photo-electron emission^{17,18}.
- c. the results are also in line with the surface potential of 0.94 V and the isosteric heat of adsorption decreasing from 7.6 to 6.4 kcal/mole on a macroscopic Pd (100) plane, as measured by Palmberg¹¹.
- d. the decrease of the heat of adsorption - $\frac{1}{2}eF^2$ - due to depolarization at the fields applied - $\sim 0.2 \text{ V/\AA}$ - should amount to $\sim 0.2 \text{ kcal/mole}$ which is within the error of our experiments and, therefore, may be neglected.

6a. Adsorption at low coverage.

It has been realized by a number of authors^{14,19,20,2,9} that Van der Waals' forces alone are insufficient to understand the Xe-metal bond. Especially the large surface potential of Xe and the high heat of adsorption on a W(110) plane⁹ are incompatible with the general view of interaction by dispersion forces. Yet it cannot be excluded a priori that these forces may have a significant, perhaps even a predominant part in the bonding of Xe to the metal. Strong interaction by these dispersion forces can be expected when the adsorbate atoms are in close contact to a large number of atoms of the adsorbent²¹, at interatomic distances such that the orbitals do not overlap. This interaction would favour an adsorption in definite sites on the surface. The high heat of adsorption on (411) regions of a W tip could be understood with this model. For a rationalization of the observed differen-

TABLE II

The coordination of Xe atoms adsorbed on sites above the centres B_n at a crystal plane (hkl)

a = number of direct contacting metal atoms

b = total number of neighbour atoms at a distance $< 0.4 \text{ \AA}$ from the adatom

c = number of neighbour atoms at a distance between 0.4 and 0.9 \AA from the adatom

crystal face	site	<u>a</u>	<u>b</u>	<u>c</u>
111	B_3	$3(C_9)$	$3(C_9)$	$3(C_9)$
100	B_4	$4(C_8)$	$4(C_8)$	-
110	B_5	$4(C_7)$	$4(C_7)$	$1(C_{11})$
210	B_6	$3(C_6)$	$5(3C_6+2C_9)$	$1(C_{11})$
	B_3	$3(2C_6+1C_8)$	$4(3C_6+1C_8)$	-
321	B_6^*	$3(2C_6+1C_9)$	$6(2C_6+2C_8+1C_9+1C_{10})$	$2(1C_6+1C_{11})$
	B_4	$3(1C_6+1C_8+1C_9)$	$4(2C_6+1C_8+1C_9)$	$1(C_{10})$
	B_3 type*1	$3(1C_6+1C_8+1C_9)$	$4(1C_6+1C_8+1C_9+1C_{10})$	$3(2C_6+1C_8)$
	B_3 type 2	$3(1C_6+1C_8+1C_9)$	$4(2C_6+1C_8+1C_9)$	$2(1C_8+1C_{10})$
	B_3 type 2	$3(1C_6+1C_8+1C_9)$	$3(1C_6+1C_8+1C_9)$	$2(1C_8+1C_{10})$
311	B_5	$3(C_7)$	$3(C_7)$	$4(2C_7+2C_{10})$
	B_3	$3(C_7)$	$4(3C_7+1C_{10})$	$2(C_7)$
211	B_5	$3(2C_7+1C_9)$	$5(2C_7+1C_9+2C_{10})$	$2(C_9)$
	B_3 type 1	$3(1C_7+2C_9)$	$4(1C_7+2C_9+1C_{10})$	$3(C_7)$
	B_3 type 2	$3(1C_7+2C_9)$	$3(1C_7+2C_9)$	$3(2C_7+1C_{10})$
	B_3 type 3	$3(2C_7+1C_9)$	$3(2C_7+1C_9)$	$2(C_9)$
531	B_6^{**}	$3(2C_6+1C_8)$	$6(3C_6+2C_8+1C_{10})$	$1(C_{11})$
	B_4^{**}	$3(2C_6+1C_8)$	$4(2C_6+1C_8+1C_{10})$	-
	B_3^{**}	$3(2C_6+1C_8)$	$4(2C_6+1C_8+1C_{10})$	$2(1C_6+1C_8)$
331	B_5	$4(2C_7+2C_9)$	$5(3C_7+2C_9)$	$1(C_{11})$
	B_3 type 1	$3(1C_7+2C_9)$	$3(1C_7+2C_9)$	$5(4C_7+1C_{11})$
	B_3 type 2	$3(2C_7+1C_9)$	$3(2C_7+1C_9)$	$2(C_9)$
310	B_6	$3(2C_6+1C_8)$	$5(2C_6+1C_8+2C_9)$	$1(C_{11})$
	B_4	$4(1C_6+2C_8+1C_9)$	$5(2C_6+2C_8+1C_9)$	-
	B_3	$3(2C_6+1C_8)$	$3(2C_6+1C_8)$	-
320	B_6	$3(1C_6+2C_7)$	$5(1C_6+2C_7+2C_9)$	$1(C_{11})$
	B_5	$4(2C_6+2C_7)$	$4(2C_6+2C_7)$	$1(C_{11})$
	B_3	$3(2C_6+1C_9)$	$4(2C_6+1C_7+1C_9)$	-

* These sites are nearly identical for Xe.

ces in the maximum heats of adsorption on the tip regions studied, it is, therefore, interesting to examine the packing of a Xe adatom in the available sites on the different tip regions.

In Table II is given the coordination of Xe atoms adsorbed above sites B_n for the important crystal faces (hkl). The symbol B_n emanated from Van Hardeveld and Van Montfoort²² is used to distinguish the different sites present on one crystal face. The index n denotes the number of lattice atoms with which an adatom with the same diameter as the metal atom is in direct contact. For a Xe atom which diameter is 1.6 times larger than an Ir atom, the number of direct contacting metal atoms (a) is in many cases much smaller than n. In the third column of Table II a is given. The individual metal atoms on the surface are distinguished by the symbol C_m in order to examine the influence of coordinative unsaturation on the heat of adsorption; m stands for the number of first neighbour metal atoms. The number of missing first neighbours is, therefore, expressed by $12 - m$. An inspection shows that the observed order in the maximum heats of adsorption cannot be explained by the difference in a on the tip regions studied.

It is relevant to refine the model by including further neighbour atoms. Adding up all lattice atoms intersecting a circle with radius 2.6 \AA around the centre of the hard sphere, representing a Xe atom (radius 2.2 \AA), yields the number of neighbours b given in the fourth column. Because of the uncertainty of the hard sphere model all atoms in this column should be considered, in first approximation, as being equivalent. The number of neighbours (c) at a distance between 0.4 and 0.9 \AA from the hard sphere representing the Xe adatom can be found in the fifth column. Their contribution to the bonding is, according to Lennard-Jones r^{-6} attractive potential, much smaller than that of the b close neighbours, but cannot be neglected.

It appears from the fourth and fifth columns that if close-packing with the metal lattice would be the only condition for strong interaction, the heat of adsorption would decrease in the order (321); (531); (331) \sim (210) \sim (320) \sim (310); (110); (100); (111). The experimentally determined sequence is, thus, correctly predicted except for the position of the (111) and (100) regions. It is also clear from the Table that the principle of maximum coordination is more important than the coordinative unsaturation of the metal atoms, just as previously found on W^4 .

The rather high heat of adsorption on the close-packed tip regions (111) and (100) implies that other forces than mere dispersion forces have a part in the interaction between Xe and the metal. We assume that the additional interaction term is due to the same causes which are responsible for the large surface potential of Xe on the metal surface. This assumption is supported by the high value of the surface potential on the (111) and (100) regions. As to the origin of the large surface potentials two explanations have been proposed^{14,19} and are still under discussion^{20,23,24}:

- (a) polarization of the adsorbate by an electric surface field which is caused by the Helmholtz double layer at the metal surface, and
- (b) charge-transfer no-bond interaction stabilizing an electron transfer from Xe to the metal.

It is clear that the electron transfer to the metal, as required in C.T.N.B. bonding, is favoured by a high work function of the adsorbing surface. The large heat of adsorption of Xe on the (111) and (100) regions can thus easily be rationalized in the charge-transfer no-bond model. This cannot be said for the polarization model as it is generally assumed that certainly on smooth faces as (111) and (100), the electric double layer, conventionally ascribed to a "spill-over" of electrons has its negative sign at the outside. The Smoluchowsky smoothening which is important for atomically rough faces, where it decreases the double layer potential, is unlikely to be important for the smooth faces (111) and (100). Once it is accepted that on close-packed faces the electric double layer has its negative pole at the outside, it would be incompatible with the basic principles of electrostatics to postulate that this double layer polarizes a big adsorbed molecule such as Xe in such a way that a positive surface potential results for the adsorbate. We therefore would prefer the C.T.N.B. model. While refraining from further discussion of the physical nature of the adsorption bond, we can conclude from the results of the present work that strong bonding of Xe is favoured by

- 1) large coordination of Xe atoms with metal atoms,
- 2) high work function of the crystal plane.

6b. Adsorption at high coverage.

The high heat of adsorption on the (321) regions where Xe adatoms above B_6 sites have better coordination than on other examined regions,

illustrates the existence of site adsorption at low coverage. The adsorbed atoms will jump rapidly from site to site, even at 78 K, until they have found the most favourable sites where their time averaged residence is much larger than on other sites. At higher coverage one may imagine two processes:

- I The adsorption is finished when all favourable sites have been occupied. The observed decrease in heat of adsorption with increasing coverage may then only be attributed to repulsion between the adatoms. The Xe layer will in most cases be appreciably less densely packed than in bulk Xe.
- II The formation of a two-dimensional close-packed Xe layer. When all favourable sites have been occupied, Xe adsorption proceeds via less favourable sites. Usually the formation of a close-packed layer will require a rearrangement of the already adsorbed Xe atoms so that a part of the Xe atoms must leave their low-energy sites. The experimentally found decrease in heat of adsorption with increasing coverage may be caused by repulsive interaction between Xe adatoms, occupation of less favourable sites and by "saturation" of the metal atoms already interacting with other Xe atoms as in chemisorption. These causes can be classified as a priori heterogeneity on one crystal plane or induced heterogeneity.

LEED results indicate the formation of a close-packed Xe layer on a number of smooth crystal planes¹¹⁻¹³). We have, therefore, examined whether our results can better be rationalized in terms of a close-packed Xe layer or a site adsorption model even at high coverage. Relevant for this examination is the observed order in the difference $\Delta Q = Q_{\max} - Q_{\min}$ on the different tip regions.

Desorption from the (210) regions is characterized by a very small ΔQ . A close-packed layer might be formed by occupation of all sites above B_6 . The resulting area per adatom would be 14.8 \AA^2 compared with 17 \AA^2 for bulk Xe, so that a considerable Xe-Xe repulsion must be expected which is incompatible with the observed extreme small ΔQ_{210} . Hence we expect that only a part of the sites are occupied, resulting in a very large area per adatom. The decrease in Q indicates that the interaction between Xe is repulsive.

A somewhat different situation exists on a (531) plane. When all sites above B_6 have been occupied, a rather close-packed layer will result

with a large adatom area of 21 \AA^2 entailing a small Xe-Xe repulsion. The observed small ΔQ_{531} supports this model.

On (321) planes a close-packed Xe layer can only be formed when other sites than B_6 and B_4 are occupied, sites where the packing with the metal is worse. These sites are by no way unique for this face, identical sites are found on other faces. It appears, however, that not only Q_{\max} but also Q_n and Q_{\min} are higher than on other regions. We therefore conclude that no low-energy sites are occupied on these planes, i.e., the formation of a close-packed Xe layer is unlikely. The most probable packing of Xe is the occupation of B_6 sites, the packing in one dimension is then reasonably close, causing a larger Xe-Xe repulsion than on (210).

As shown in the previous section a localization of the adatoms at single sites is less favourable on the smooth regions (111), (100) and (110) than on rougher regions, so that process II is more likely on the smooth planes. Here ΔQ is larger than on rougher regions. On a (111) face a nearly close-packed layer can be formed by occupation of B_3 sites. The area per adatom would be then 19 \AA^2 . The field emission technique cannot indicate whether this arrangement exists or that a closer-packed layer is formed as on Ag (111)¹³. On the (100) and (110) faces a close-packed layer can only be formed if a part of the adatoms leave the sites above B_4 and B_5 centres which were preferred at low coverage. LEED results on Pd (100)¹¹, Cu (100) and (110)¹³ and on Ag (110)¹³ strongly support that a close-packed layer will also be formed on Ir (110) and (100). This would explain the large decrease of the heat of adsorption with coverage.

In conclusion we can state that the field emission probe-hole technique remains a powerful method for the examination of the influence of the surface structure on adsorption processes. The possibility of measuring the desorption behaviour of a gas on the different regions of the tip at exactly the same conditions, enables us to measure the relative binding energies of an adsorbate on these surfaces. These data yield indirectly information of adsorbate-adsorbate interaction, the influence of packing conditions with the lattice and the importance of coordinative unsaturation of metal atoms. In the case considered, the adsorption of Xe on Ir, the combined results of the present study and those of LEED by Chesters et al.¹³ and Palmberg¹¹ show that

- (1) at low coverage site adsorption is preferred at least on faces exhibiting sites where good coordination with the metal atoms is possible.

(2) at high coverage there is a tendency to the formation of a closer-packed Xe layer. On low index faces this can result in a closest-packed Xe layer eventually without true site adsorption but often in registry with the substrate. But on faces where favourable sites are available, large coordination of the Xe atoms with metal atoms is preferred to the formation of a close-packed Xe layer.

References

1. G. Ehrlich, T.W. Hickmott and F.G. Hudda, *J. Chem. Phys.* 28 (1958) 977.
2. G. Ehrlich and F.G. Hudda, *J. Chem. Phys.* 30 (1959) 493.
3. R. Gomer, *J. Chem. Phys.* 29 (1958) 441.
4. W.J.M. Rootsart, L.L. van Reijen and W.M.H. Sachtler, *J. Catalysis* 1 (1962) 416.
5. G. Ehrlich, *J. Appl. Phys.* 15 (1964) 349.
6. K. Ishizuka, *J. Res. Inst. Catalysis, Hokkaido Univ.* 15 (1967) 95.
7. V. Ponec and Z. Knor, *Coll. Czech. Chem. Comm.* 27 (1962) 1091.
8. D. Brennan and M.J. Graham, *Phil. Trans. Roy. Soc. London A* 258 (1965) 325.
9. T. Engel and R. Gomer, *J. Chem. Phys.* 52 (1970) 5572.
10. J.M. Dickey, H.H. Farrell and M. Strongin, *Surface Sci.* 23 (1970) 448.
11. P.W. Palmberg, *Surface Sci.* 25 (1971) 598.
12. M.A. Chesters and J. Pritchard, *Surface Sci.* 28 (1971) 460.
13. M.A. Chesters, M. Hussain and J. Pritchard, *Surface Sci.* 35 (1973) 161.
14. J.C.P. Mignolet, *Discussions Faraday Soc.* 8 (1950) 105.
15. B.E. Nieuwenhuys and W.M.H. Sachtler, *Surface Sci.* 34 (1973) 317.
16. B.E. Nieuwenhuys, D.Th. Meijer and W.M.H. Sachtler, *Surface Sci.* 40 (1973) 125.
17. B.E. Nieuwenhuys, R. Bouwman and W.M.H. Sachtler, *Thin Solid Films*, 21 (1974) 55.
18. B.E. Nieuwenhuys, O.G. van Aardenne and W.M.H. Sachtler, to be published.
19. J.C.P. Mignolet, in "Chemisorption" (W.E. Garner ed.) p. 118, Butterworths, London, 1957.
20. P.M. Gundry and F.C. Tompkins, *Trans. Faraday Soc.* 56 (1960) 846.
21. J.H. de Boer and J.F.H. Custers, *Z. physik. Chem.* B 25 (1934) 225.
22. R. van Harveld and A. van Montfoort, *Surface Sci.* 4 (1966) 396.
23. Th.G.J. van Oirschot and W.M.H. Sachtler, *Ned. Tijdschr. Vacuum Techniek* 8 (1970) 96.
24. A. Schram, in "Adsorption - Desorption Phenomena", (F. Ricca ed.) p. 57, Acad. Press, London and New York, 1972.

Chapter VII

ADSORPTION OF XENON ON PLATINUM, STUDIED BY FIELD EMISSION MICROSCOPY

by

B.E. Nieuwenhuys, D.Th. Meijer and W.M.H. Sachtler
Gorlaeus Laboratoria, P.O. Box 75, Leiden, The Netherlands

S u m m a r y

The adsorption of Xe on Pt was investigated with a field emission microscope, equipped with a probe-hole assembly. The initial heat of adsorption decreases in the order $(321) > (111) \sim (100) > (210) > (110)$. At low coverage Xe is adsorbed in surface sites providing a maximum coordination of the adatom with metal atoms. The heat of adsorption decreases with coverage, in particular on the smooth regions (111) and (100), where a close-packed Xe layer is apparently formed at high coverage. On the rough areas (321) and (210), however, site adsorption is preferred to the formation of a close-packed Xe layer; by consequence the heat of adsorption decreases only little with coverage. The crystal face dependence of Xe adsorption on Pt is virtually identical to that found for Ir. When data reported for Xe on W are also included the general conclusion is drawn that strong bonding of Xe on transition metals is favoured by (1) a large coordination of adatoms with metal atoms and (2) a high work function of the adsorbing crystal plane.

Z u s a m m e n f a s s u n g

Die Adsorption von Xe auf Pt wurde mit Hilfe eines Feldelektronenmikroskopes mit Lochblende untersucht. Die initiale Adsorptionswärme auf den verschiedenen Kristallflächen nimmt ab in der Reihenfolge (321) > (111) ~ (100) > (210) > (110). Bei geringer Bedeckung wird Xe auf Oberflächenplätzen mit maximaler Umringung des Adatoms durch Metallatome adsorbiert. Die Adsorptionswärme sinkt mit steigender Bedeckung insbesondere auf den glatten Gebieten (111) und (100), wo bei hoher Bedeckung anscheinend eine dichtgepackte Xe-Schicht ausgebildet wird. Auf den rauhen Gebieten (321) und (210) dagegen bleibt die Adsorption auf bestimmten Gitterplätzen auch bei hohem Bedeckungsgrad günstiger als die Bildung einer dichtgepackten Schicht.

Infolgedessen nimmt die Adsorptionswärme hier nur wenig ab mit zunehmender Bedeckung. Die Abhängigkeit der Xe-Adsorption von der Kristallfläche ist für Pt praktisch identisch mit der für Ir gefundenen. Werden auch die für W publizierte Werte mitberücksichtigt, so folgt, dass allgemein eine starke Bindung zwischen Xe mit einem Übergangsmetall begünstigt wird durch:

- 1) hohe Umringung des Adatoms mit Metallatomen;
- 2) hohe Austrittsarbeit der adsorbierenden Kristallfläche.

1. Introduction

Recently we described the adsorption of Xe on various tip regions of an Ir field emitter¹. By performing probe-hole measurements on the tip regions under exactly identical conditions the variation of the heat of adsorption with the tip region was determined. It appeared that strong bonding of Xe on Ir is favoured by:

- (1) large coordination of Xe atoms with lattice atoms;
- (2) high work function of the adsorbing crystal plane.

Adsorption measurements on evaporated films of different metals indicate that the heat of adsorption and the surface potential of Xe depend strongly on specific properties of the metals^{2,3}. On Au films, for instance, the heat of adsorption and the surface potential are much lower than on Pt films while the work function and the lattice parameters differ only slightly. All these data suggest a significant contribution of a charge-transfer no-bond interaction to the adsorption bond in addition to dispersion forces. This contribution is particularly important on crystal faces with high work function. A model of Xe polarization by a hypothetical electric surface field⁴ was rejected as it appears to predict the wrong sign for the adsorption dipole.

In order to ascertain these conclusions it is important to investigate the crystal face dependence of Xe adsorption on several metals. The purpose of the present paper is to check whether conclusions (1) and (2) are of general validity. This question is not a trivial one since Ehrlich⁵ had reported that for the b.c.c. metals W and Ta, although differing in lattice parameters only by 6%, the distribution of the heat of adsorption was significantly different. These measurements have, however, been carried out with a field emission microscope without a probe-hole assembly, they therefore provided merely qualitative results. For f.c.c. metals no systematic study of the adsorption of inert gases has been published to our knowledge. In the present paper we report a study of the adsorption of Xe on Pt. The noble metals Pt and Ir are neighbours in the periodic system of elements. Yet, there are some specific differences in adsorption behaviour on these metals. Nitrogen which just like Xe is only weakly adsorbed on Ir and Pt reveals distinct differences between these two metals⁶. A comparative study of the adsorption of Xe on these metals is, therefore, of particular interest. Pt and Ir have both the f.c.c. structure, their lattice constants differ only by 2%. If a difference in variation of the heat of adsorption

with tip region is observed it would, therefore, be impossible to ascribe it to differences in the relative contribution of dispersion forces.

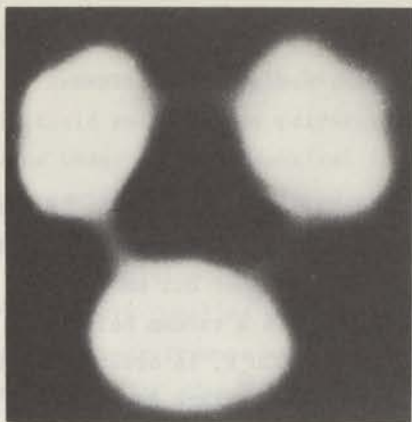
2. Experimental

The measurements were performed with a field emission probe-hole tube described previously⁷, which yields information about all exposed crystal faces. The Pt tips fabricated from spec. pure Pt wires of 0.1 mm diameter were cleaned by field desorption and field evaporation in a vacuum below $1 \cdot 10^{-10}$ Torr, alternated by prolonged heating periods to 1000 K, in order to avoid diffusion of contaminants from the shank to the tip surface during the measurements. Xe with an impurity level lower than 0.003% was further purified by use of freshly deposited Ni getter films. All details concerning the determination of the relative heats of adsorption and the surface potentials of Xe have been given earlier¹.

3. Results and Discussion

The change in field emission pattern occurring during the exposure of a Pt tip to a low pressure of Xe (1×10^{-8} Torr) at a tip temperature of 78 K is shown in fig. 1. The pictures were taken at a constant emission current of 1×10^{-8} A. Xe adsorption causes a continuous increase in emission; therefore the voltage had to be diminished steadily during the adsorption process. First, the emission from the region around (321) is much enhanced (fig. 1 b). After longer exposure times the regions around (110) become blurred as compared to their surroundings, while the (210) - (310) regions brighten up (fig. 1 d-e). At a later stage of adsorption the most emitting areas grow towards (110) (fig. 1 f-g). Once the tip has been saturated with Xe the regions around (320) - (210) are again the brightest regions in the emission pattern (fig. 1 g). The area around (110) is darker than for the clean tip.

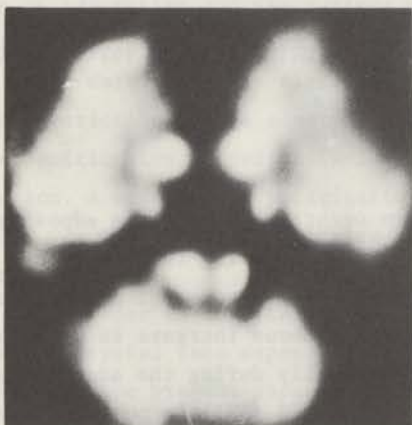
A gradual increase of the temperature of the tip saturated with Xe gives rise to the sequence of images shown in fig. 2. These images are equal to the pictures of fig. 1 but they appear in reversed order. This reversibility proves that the changes in the emission pattern by Xe adsorption are due to differences in heat of adsorption. With respect to surface diffusion equilibrium over the whole tip is evidently established at each temperature used. It seems safe to conclude that the heat of adsorption of Xe



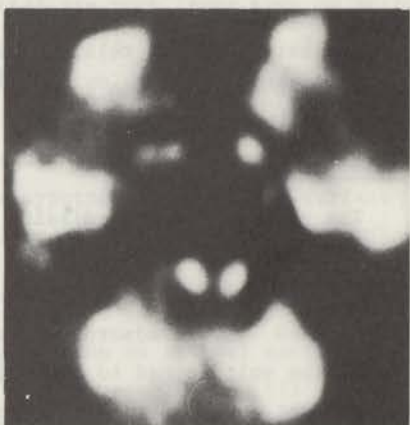
a



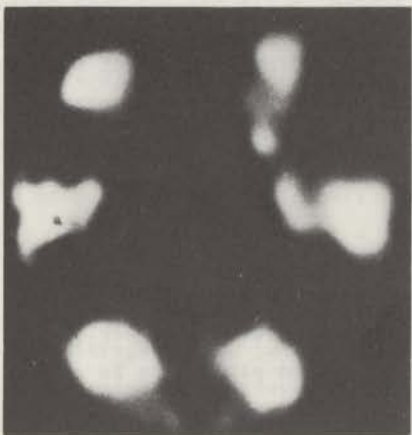
b



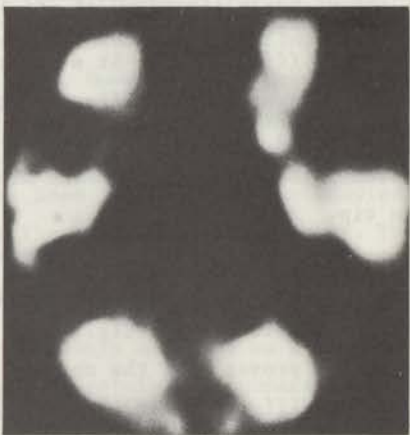
c



d

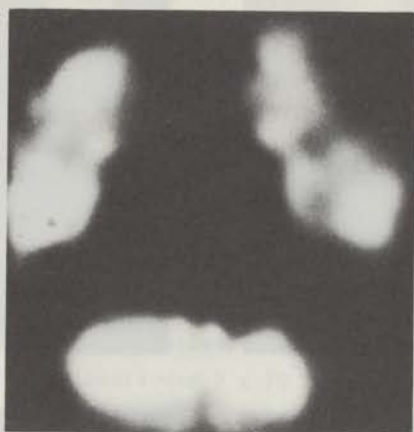


e



f

Fig. 1a - 1f



g

Fig. 1a - 1g

Change in field emission pattern by Xe adsorption at 78 K

a : clean tip

b-g: increasing coverage

g : monolayer coverage

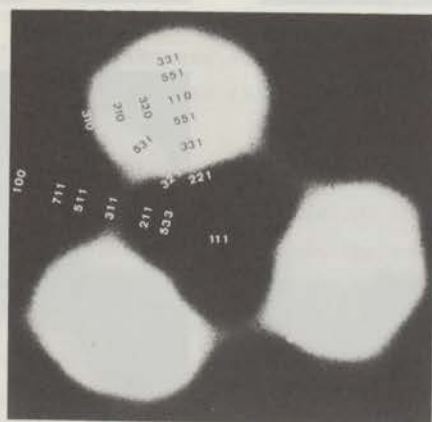


Fig. 1h

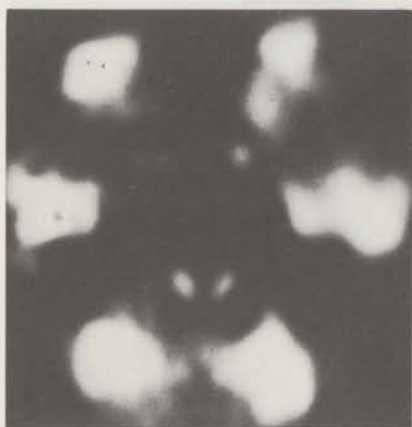
Orientation diagram



(a) $T = 90 \text{ K}$



(b) $T = 105 \text{ K}$



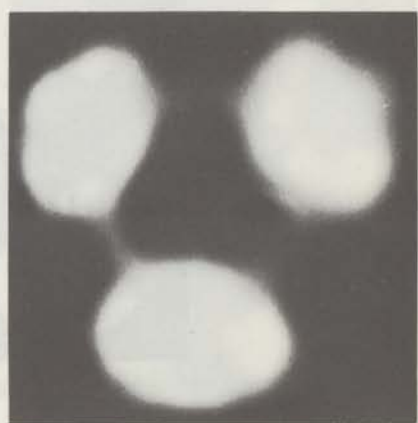
(c) $T = 110 \text{ K}$



(d) $T = 115 \text{ K}$



(e) $T = 120 \text{ K}$



(f) $T = 130 \text{ K}$

Fig. 2 Thermal desorption of Xe from Pt. $p \approx 3 \cdot 10^{-8}$ Torr

on the different tip regions decreases in the order (321), (210) and around (110). The behaviour of Xe on other tip regions is clarified by measuring the changes in emission from the individual regions during a stepwise increase of the tip temperature. In fig. 3 are shown the desorption plots of Xe from the smooth regions (111) and (100); the region around (110); the atomical rough region (210); and the region (321) which consists of edges of the (210) configuration alternated by (111) terraces. The plots were obtained by recording the voltage required to maintain a constant electron current from the probed region while the temperature was increased in steps. Sixty seconds after increasing the temperature to a new value the voltage was adjusted and measured, then the temperature was raised again. The Xe pressure during these experiments was 3×10^{-8} Torr. Fig. 3 shows that the maximum heat of adsorption increases in the sequence (110); (210); (100) and (111); and (321). Experiments were performed on three different tips and this order was found to be reproducible. In fig. 4 the first derivatives of the desorption plots are shown.

Numerical values for the heat of adsorption and the surface potential of Xe on some tip regions are compiled in Tables I and II. Q_n is the heat of adsorption estimated from the desorption time at the temperature T_n , where the corresponding plot in fig. 4 exhibits a maximum. Q_{\max} and Q_{\min} approximate the maximum and the minimum heat of adsorption, respectively. The procedures followed for the estimation of these values have been described in detail elsewhere¹. The estimated error in the differences between the comparable Q_{hkl} 's on the different tip regions is less than 0.2 kcal/mole. As appears from Table II, the difference ΔQ between Q_{\max} and Q_{\min} is very small on (210), it is larger on the regions (321) and (110) and much larger on the smooth areas (111) and (100).

If dispersion forces would form the main contribution to the bonding of Xe on the metal, the coordination of Xe adatoms in the possible adsorption sites would be decisive for the differences in the heat of adsorption on the tip regions studied. The heat of adsorption should then decrease in the sequence (321), (210), (110), (100) and (111)¹. This order agrees with the results except for the position of the (111) and (100) regions. Evidently, other forces than dispersion forces also contribute to the bonding. This additional interaction term is, presumably, responsible for the large surface potential of Xe on metals which has been attributed to induced polarization in the electric double layer at the surface⁴ and alternatively to charge-transfer no-bond interaction^{8,9}. Apparently, a high work function

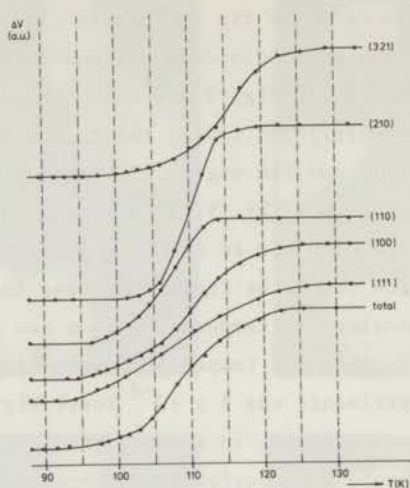


Fig. 3

Variation in voltages required for constant emission currents from individual tip regions during thermal desorption of Xe.

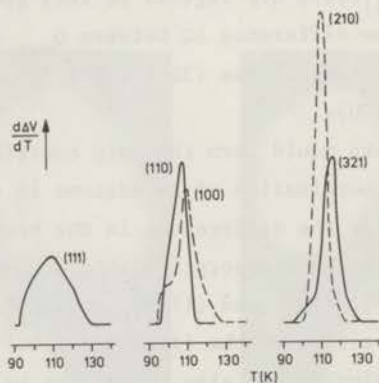


Fig. 4

The first derivatives of the desorption plots of fig. 3.

Table I
Adsorption of Xe on Pt at 78 K

Tip region	ϕ (eV)	s.p.(V)	$\Delta \log A$
average	5.32	0.95±0.02	-0.64±0.04
(111)	5.9		
(100)	5.8	1.0	
(210)	5.2	1.1	
(321)	5.4	0.9	
(311)	5.5	0.9	

Q : clean work function of the tip region (hkl)

s.p.: surface potential of Xe at full coverage

$\Delta \log A$: change in Fowler-Nordheim pre-exponential factor by Xe adsorption

Table II
The heat of adsorption of Xe on Pt and Ir (in kcal/mole)

Tip region	platinum			iridium		
	Q_{\min}	Q_n	Q_{\max}	Q_{\min}	Q_n	Q_{\max}
(111)	6.3	7.0	7.6	6.5	7.0	7.5
(100)	6.4	7.0	7.5	6.5	6.9	7.5
around (110)	6.4	6.8	7.1	6.3	6.5	7.0
(210)	6.8	7.0	7.2	6.7	7.0	7.2
(321)	6.9	7.4	7.8	7.0	7.6	7.8

Q_{\min} and Q_{\max} approximate the maximum and minimum heat of adsorption. Q_n is the heat of adsorption calculated from the desorption time at a temperature T_n where the desorption plot in fig. 4 exhibits a maximum.

favours this interaction.

The high heat of adsorption on the (321) region shows that Xe adsorption at low coverage prefers sites with a very favourable atomic topography. Only on the high work function faces (111) and (100) adsorption needs not to be confined to special sites. For high coverages two possibilities are conceivable:

- a) The formation of a two-dimensional close-packed Xe layer with little or no epitaxial relation to surface topography, as observed on Pd (100)¹⁰ and on some low-index faces by Cu and Ag¹¹ by LEED studies.
- b) Adsorption remains confined to certain favourable sites.

In order to decide between these two models the information obtained from the observed decrease in heat of adsorption ΔQ which is significantly different on the different tip regions appears relevant. In this analysis we shall label each adsorption site with the symbol B_n , where n denotes the number of metal atoms with which an adatom with the same diameter as the metal atom is in direct contact (see ref. 12).

It is unlikely that on (321) planes other sites than the centers above B_6 are occupied since not only Q_{\max} but also Q_n and Q_{\min} are higher than on other tip regions. When all these sites are filled the Xe-Xe distance approaches that of a close-packed layer in one dimension only. The observed decrease of Q with coverage indicates that the interaction between Xe adatoms in one Xe row is repulsive.

ΔQ is very small on the (210) region. This indicates a very small repulsion between the Xe adatoms of the highest coverages of our experiments i.e. the Xe layer is not densely packed on this region. This suggests that only part of the sites above the B_6 centers become occupied. A complete filling of all these sites would cause a considerable repulsion, as the Xe-Xe distance would then be smaller than in crystalline Xe.

A close-packed Xe layer is presumably formed on the regions (111) and (100) as here ΔQ is large. We cannot exclude, however, some site adsorption on the (111) planes because the spacing of the sites above B_3 is such that it would be consistent with a rather large ΔQ . Still, a close-packed layer on both (111) and (100) appears more probable in view of the almost equal ΔQ values for these two planes. If adsorption were confined to B_3 sites on (111) the ΔQ value should be considerably smaller for (111) than for (100). A closer-packed layer without true site adsorption has also been reported for Xe on Ag (111)¹¹ where the geometrical situation is virtually

identical to Pt (111).

Summarizing, the present results indicate that:

- (1) site adsorption is preferred at low coverage, certainly on faces exhibiting sites where Xe atoms fit well with the metal lattice. The initial heat of adsorption on these areas is relatively large.
- (2) an interaction by forces other than dispersion contributes to the Xe-metal bonding and is important on high work function faces. This additional interaction can be described as a CTNB bonding.
- (3) at high coverage a close-packed Xe layer is formed on the smooth faces.

On the faces possessing suitable sites for Xe, site adsorption is, however, preferred to the formation of a close-packed layer even at the highest coverages observed under the conditions of our experiments.

In Table II the heats of adsorption of Xe on several tip regions of Pt are faced with those on the same regions of Ir. This confrontation clearly shows that the distribution of the heat of adsorption and its dependence on coverage over the different tip regions of Ir and Pt is identical. It is further interesting to compare adsorption of Xe on the f.c.c. metals Pt and Ir with Xe adsorption on the b.c.c. metal W, the only system from which sufficient data on the crystal face dependence are available in the literature. Early studies with a field emission microscope without probe-hole device revealed a high heat of adsorption on regions around (411) where Xe adatoms fit perfectly into the kinked lattice edges^{13,14}. A later study by Engel and Gomer¹⁵ by the field emission probe-hole technique showed, however, that the heat of adsorption is still higher on the closest-packed (110) face (which upon mere visual observation seemed to remain empty) than on the lower work function faces (100), (111) and (210). Also in this case, the highest work function face displays an astonishingly high heat of adsorption. This result is, hence, in line with the present findings. Hence, we may conclude that all these field emission studies on Pt, Ir and W consistently show: strong binding of Xe is favoured by

- A) large coordination of Xe adatoms with metal atoms;
- B) high work function of the adsorbing crystal plane.

References

- 1) B.E. Nieuwenhuys and W.M.H. Sachtler, submitted to Surface Sci.
- 2) B.E. Nieuwenhuys, R. Bouwman and W.M.H. Sachtler, Thin Solid Films 21 (1974) 55.
- 3) B.E. Nieuwenhuys, O.G. van Aardenne and W.M.H. Sachtler, to be published.
- 4) J.C.P. Mignolet, Disc. Faraday Soc. 8 (1950) 105.
- 5) G. Ehrlich, J. appl. Phys. 15 (1964) 349.
- 6) B.E. Nieuwenhuys, D.Th. Meijer and W.M.H. Sachtler, Surface Sci. 40 (1973) 125.
- 7) B.E. Nieuwenhuys and W.M.H. Sachtler, Surface Sci. 34 (1973) 317.
- 8) J.C.P. Mignolet, in Chemisorption (W.E. Garner ed.) p. 118, Butterworths, London, 1957.
- 9) P.M. Gundry and F.C. Tompkins, Trans. Faraday Soc. 56 (1960) 846.
- 10) P.W. Palmberg, Surface Sci. 25 (1971) 598.
- 11) M.A. Chesters, M. Hussain and J. Pritchard, Surface Sci. 35 (1973) 161.
- 12) R. van Hardeveld and A. van Montfoort, Surface Sci. 4 (1966) 396.
- 13) G. Ehrlich and F.G. Hudda, J. Chem. Phys. 30 (1959) 493.
- 14) W.J.M. Rootsaert, L.L. van Reijen and W.M.H. Sachtler, J. Catalysis 1 (1962) 416.
- 15) T. Engel and R. Gomer, J. Chem. Phys. 52 (1970) 5572.

Chapter VIII

ADSORPTION OF XENON ON GROUP VIII AND IB METALS, STUDIED BY PHOTOELECTRON EMISSION

by

B.E. Nieuwenhuys, O.G. van Aardenne and W.M.H. Sachtler

Gorlaeus Laboratoria, P.O. Box 75, Leiden, Netherlands

S u m m a r y

The heat of adsorption of Xe and the change in work function by Xe adsorption have been investigated on Cu, Au, Ni, Pt and Rh films using the photoelectron emission technique. The surface potential of Xe appears to be directly related to the heat of adsorption: a large heat of adsorption is accompanied by a large surface potential. These results are discussed on the basis of various models for physical adsorption of inert gases on metals. The heats of adsorption found experimentally can satisfactorily be correlated with the measured surface potentials upon considering the interaction between Xe and the transition metal as charge transfer-no bond interaction. An alternative explanation for the large decrease in work function by Xe adsorption, the classical polarization model, can be rejected since it is unable to explain the high heats of adsorption on group VIII metals and it fails to describe the observed interdependence of the heat of adsorption and the surface potential. These conclusions are in agreement with earlier results obtained by studying the adsorption of Xe on several well defined crystal faces of Pt and Ir by field emission microscopy.

1. Introduction

Mignolet's discovery in 1950 that inert gas adsorption produces a large decrease in the work function of transition metals¹, showed the inadequacy of the classical picture which assumed the bonding between the inert gas atoms and the metal to be entirely due to dispersion forces. The additional interaction responsible for the high surface potential (i.e. decrease in work function) was ascribed either to the polarization of the adatoms in a hypothetical electrostatic surface field¹, or alternatively to a charge transfer-no bond interaction stabilizing an otherwise endothermic electron transfer from the adsorbate to the metal².

Some typical examples of surface potential (s.p.) values of Xe are: 0.21 V on Zn², 0.52 V on Au³, 0.85 V on Ni^{2,3} and 1.1 V on Rh films³, all these films being annealed at room temperature. These results illustrate that the s.p. is characteristic for the adsorbing metal. It may therefore be expected that the heat of adsorption depends also on the metal. In principle two limiting cases may be considered:

- 1) Dispersion forces have the largest contribution in the binding of Xe to the transition metal. The variation in heat of adsorption should then be marginal and within the limits for cast by the theories of dispersion forces⁴.
- 2) The total heat of adsorption is largely determined by the additional interaction term. In this case the variation in heat of adsorption should be entirely different from that predicted by the dispersion forces theories.

An example to be further elaborated on in the Discussion of this paper shows that the heats of adsorption of Xe should be nearly equal on Au and on Rh if the dispersion forces prevail. If, however, the additional interaction predominates, these heats should be markedly different, as the s.p.'s of Xe on these two metals differ by a factor of two³.

Another challenging question is which of the two different models for explaining the large s.p. is correct. It appears that either of them predicts a different relationship between the heat of adsorption and the s.p., as will be shown in the Discussion chapter of this paper.

It may therefore be concluded that a systematic comparison of the heats of adsorption and the s.p.'s of an adsorbed rare gas on a number of clean metals is likely to provide important information on the fundamental nature of the adsorption bond of noble gases on metals. This is the purpose of the present paper.

The heats of adsorption of Xe were determined on films of transition metals from the adsorption isosteres. Upon assuming that a constant s.p. corresponds to a constant coverage, the $\ln p$ versus $1/T$ plots at constant coverages were constructed and the heats of adsorption calculated from their slopes (p corresponds to the equilibrium pressure of Xe and T to the temperature of the adsorbing metal). The transition metals examined in this way are the group VIII metals Ni, Rh and Pt and the IB metals Cu and Au.

2. Experimental

Spec. pure wires of Ni, Pt, Cu and Au, and wires of Rh with a stated purity of 99.98% were supplied by Johnson, Matthey & Co., London. Pt, Cu and Au were evaporated from beads of these metals - which had been premelted in a hydrogen atmosphere - onto multi-hair-pin filaments of W wires. Ni and Rh films were deposited on a glass substrate cooled at 78 K. The gas pressure during evaporation was kept below 3×10^{-10} Torr.

Xe with an impurity level below 0.003% was supplied by Air Liquide. Before entering the phototube it was further purified with the aid of freshly evaporated Ni getter films. In order to avoid contamination which might arise from pumping off inert gases by means of ion-getter pumps the Xe pressure in the phototube was reduced with the aid of gettering by metal films cooled to 78 K. In this way very reproducible values for the Xe s.p. were found.

3. Measuring procedure

Work functions were measured using the photoelectric emission technique in a phototube identical to the one designed by Bouwman et al.⁵. A narrow light beam monochromatized by a grating monochromator, equipped with a high pressure mercury lamp was directed by a mirror system either onto the phototube containing the metal film or to a calibrated Ta reference tube. The photoelectron yield J of a metal film was calculated for each of the used frequencies of the incident light from the measured photocurrents I and I_{ref} and the known photoelectron yield J_{Ta} of the calibrated reference tube, according to

$$J = \frac{I}{I_{\text{Ta}}} J_{\text{Ta}} \text{ (electrons/photon)} \quad (1)$$

The work function ϕ of the film was then determined with the aid of the equation of Fowler which can be written, in a good approximation, as

$$J = M \frac{(E - \phi)^2}{2k^2} \quad (2)$$

In this equation E stands for the energy of the incident light, k for the Boltzmann constant and M for the emission constant. A straight line is obtained by plotting $J^{\frac{1}{2}}$ versus E . ϕ can be calculated from the intercept of this plot on the abscissa. By performing this procedure both for the film without and for the film covered with Xe to a degree of coverage θ , the s.p. of Xe was obtained from

$$\text{s.p.}(\theta) = -\Delta\phi(\theta) = \frac{\phi_{\text{clean}} - \phi(\theta)}{e} \quad (3)$$

First the s.p. was determined on a film completely covered with Xe at 78 K. Then the temperature was increased to a constant temperature T . At this temperature a number of s.p.'s was determined at stepwise increasing Xe pressures, until the film was either saturated with Xe or the pressure exceeded the value of 10^{-2} Torr, which is the upper limit tolerable before ion formation due to collisions in the gas phase sets in. This procedure was then repeated at different T . In all cases the s.p. was found to be reversible and a unique function of T and p_{Xe} . The curves obtained by plotting s.p. versus p_{Xe} at constant T are essentially adsorption isotherms since the s.p. is a unique function of θ .

From each set of adsorption isotherms $\ln p$ versus $1/T$ plots were constructed for several constant values of the s.p. and, hence, of ϕ . These plots yield straight lines according to the Clausius-Clapeyron equation:

$$\ln p = -Q_{\theta}/RT - \Delta S_{\theta}/R \quad (4)$$

where R and Q_{θ} are respectively the gas constant and the isosteric heat of adsorption. Q_{θ} was evaluated from the slope of the isosteres using the least-square method. ΔS_{θ} corresponds to the change in differential molar entropy:

$$\Delta S_{\theta} = \tilde{s}_s - \bar{s}_g^0 \quad (5)$$

where \tilde{s}_s is the differential entropy of the adsorbed phase and \bar{s}_g^0 the standard molar entropy of the gas. ΔS_{θ} referred to the standard gas phase at 1 atm. was obtained from the intercept of the isosteres (p in atm.). Between the successive determinations of the adsorption isotherms on one metal film ϕ of the bare metal film at room temperature and also the maximum s.p. at 78 K were determined in order to check the cleanliness of the metal film.

4. Results

It is convenient to define

$$\psi(\theta) = \text{s.p.}(\theta) / \text{s.p.}_{\text{max}} = \Delta\phi(\theta) / \Delta\phi_{\text{max}} \quad (6)$$

where s.p._{max} is the Xe s.p. at monolayer coverage and $\text{s.p.}(\theta)$ the Xe s.p. measured at a temperature T and an equilibrium Xe pressure p . Monolayer coverage is expected to exist at 78 K and $p = 10^{-3}$ Torr. It will be clear that ψ is directly related to θ .

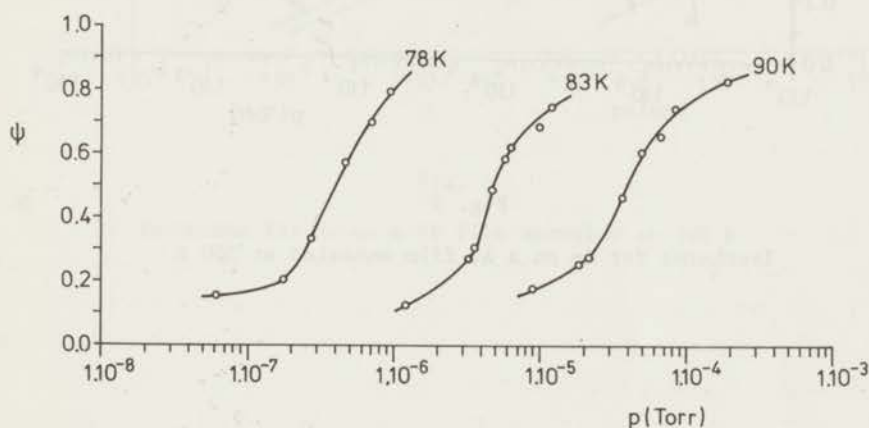


Fig. 1

Isotherms for Xe on a Cu film annealed at 300 K

Figures 1 - 5 display the ψ versus $\ln p$ characteristics ("isotherms") for various values of T , as measured for Xe on Cu, Au, Ni, Pt and Rh films, respectively. All these films had been deposited at pyrex cooled at 78 K and were subsequently annealed at room temperature.

Figure 6 shows the sets of "isotherms" for Xe on a Ni film which had been annealed at 570 K during 30 minutes.

The $\log p$ versus $1/T|_{\text{const.}\psi}$ plots, constructed from Figures 1 - 5 for $\psi = 0.50$ (for Ni $\psi = 0.30$) are shown in Figure 7. In Table I the maximum s.p., the heat of adsorption Q_{t} and the change in entropy ΔS , both at $\psi = 0.50$ (for the Ni film annealed at room temperature $\psi = 0.30$ and for the Ni film annealed at 570 K $\psi = 0.35$) are given for the metal studied. The variation of Q_{t} with ψ in the limited range accessible in Figures 1 - 6 is smaller than 0.4 kcal/mole and is, thus, of the same order as the experimen-

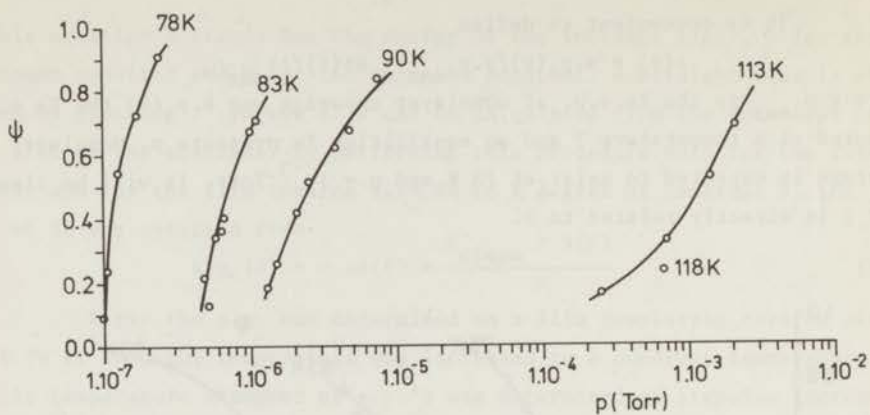


Fig. 2

Isotherms for Xe on a Au film annealed at 300 K

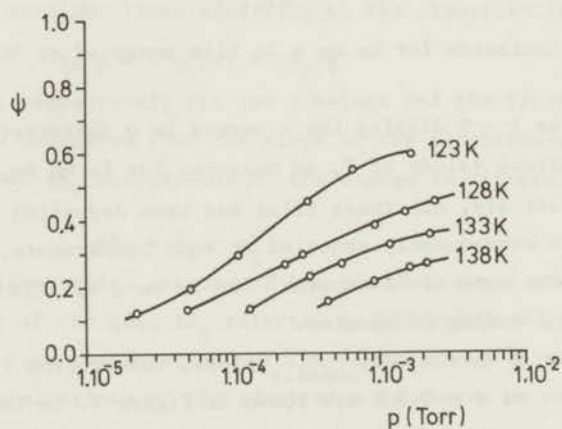


Fig. 3

Isotherms for Xe on a Ni film annealed at 300 K

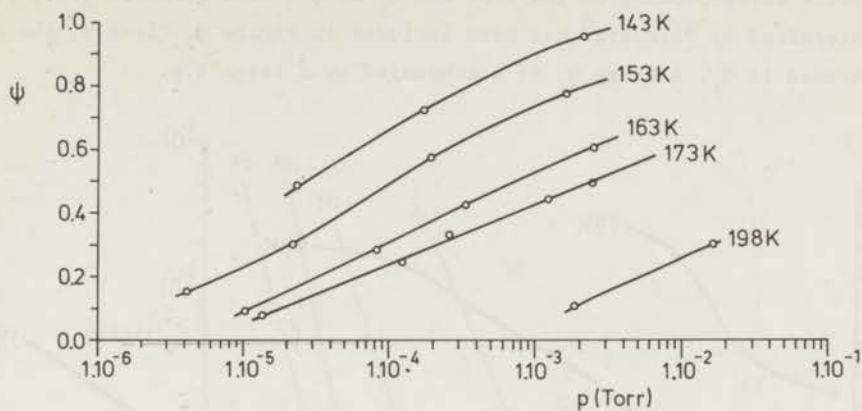


Fig. 4

Isotherms for Xe on a Pt film annealed at 300 K

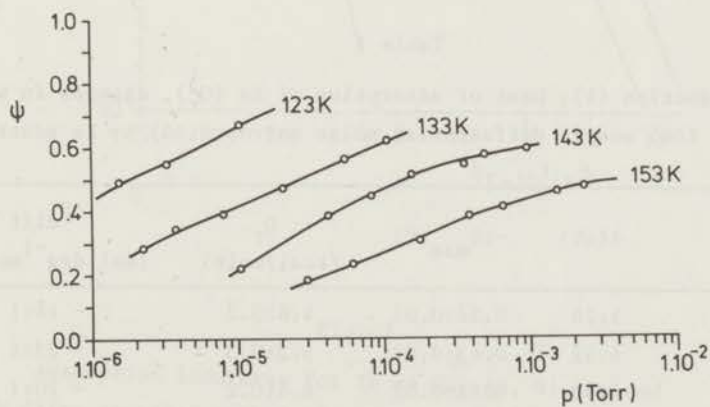


Fig. 5

Isotherms for Xe on a Rh film annealed at 300 K

tal error. The values for Q_t have been plotted versus $s.p._{max}$ in Figure 8. The point corresponding to the s.p. and Q_t at $\psi = 0.50$ for a Pd (100) plane as determined by Palmberg⁶ has been included in Figure 8. Clearly, the s.p. is related to Q_t . A large Q_t is accompanied by a large s.p.

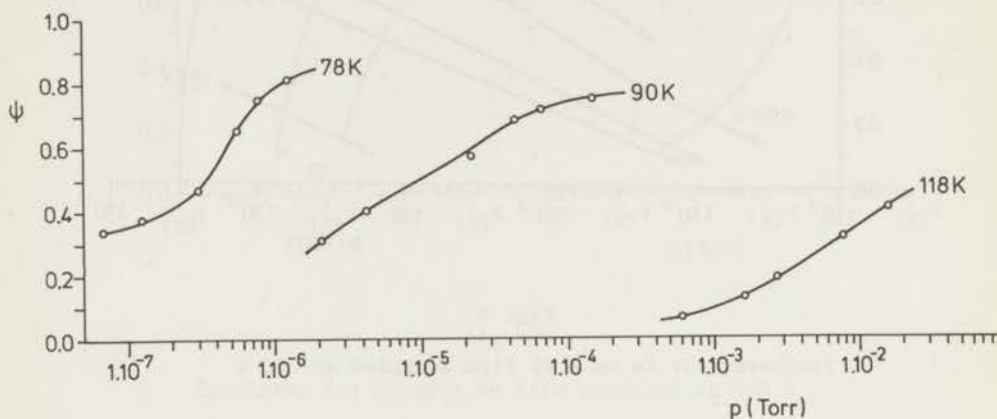


Fig. 6

Isotherms for Xe on a Ni film annealed at 570 K

Table I

Work function (ϕ), heat of adsorption of Xe (Q_t), changes in work function ($\Delta\phi$) and in differential molar entropy (ΔS) by Xe adsorption

metal	ϕ (eV)	$-\Delta\phi_{max}$ (V)	Q_t (kcal/mole)	ΔS_{diff} (cal.deg ⁻¹ mole ⁻¹)
Au	5.28	0.52±0.02	4.6±0.2	- 14±1
Cu	4.52	0.63±0.02	5.2±0.3	- 23±1
Ni	4.90	0.82±0.02	6.4±0.2	- 20±1
Pt	5.62	0.95±0.02	7.6±0.2	- 20±1
Rh	4.98	1.08±0.02	8.7±0.3	- 30±1
Ni(570 K)	5.12	0.65±0.02	5.5±0.3	- 22±1
Pd(100)		0.94	7.2	

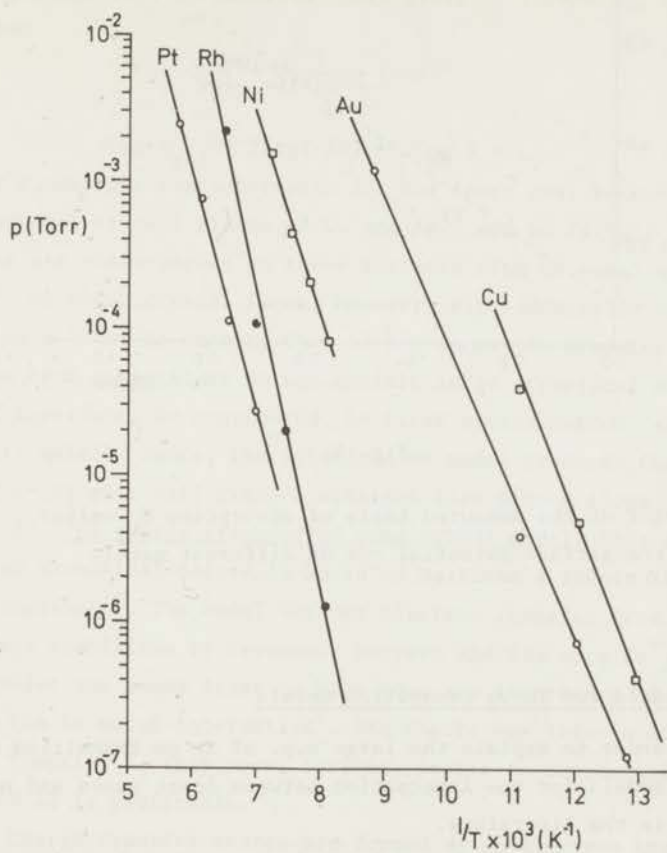


Fig. 7

Adsorption isosteres for Xe on Cu, Au, Ni, Pt and Rh films annealed at 300 K for $\psi = 0.50$ (for Ni $\psi = 0.30$)

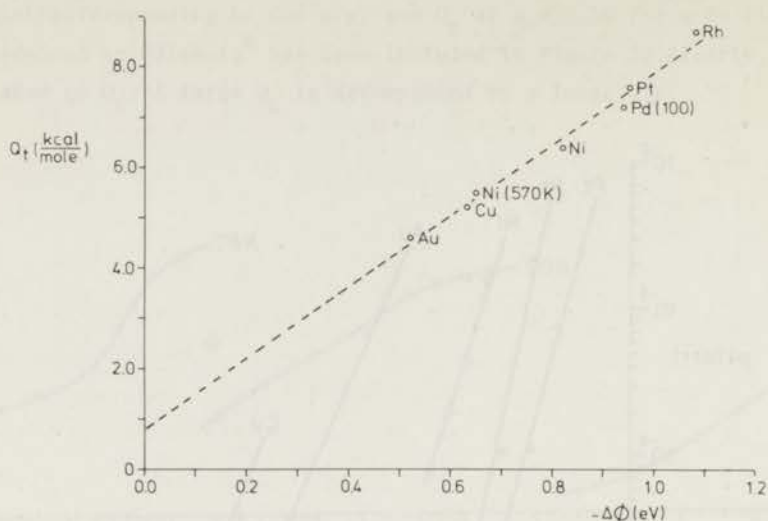


Fig. 8

A plot of the measured heats of adsorption Q_t versus the surface potential $-\Delta\Phi$ on different metals

5. Discussion

A. Bonding models for Xe on transition metals

In order to explain the large s.p. of Xe on transition metals two different models for the interaction between inert gases and metals have been proposed in the literature.

I. The polarization model. It is assumed that an interaction is taking place, in addition to dispersion forces, as a result of a hypothetical surface field $-F$ at the metal surface. According to this model the adatom is strongly polarized at the surface resulting in a dipole moment μ

$$\mu = -\Delta\Phi/4\pi N = \alpha F \quad (7)$$

where α stands for the polarizability of the adatom and N for the number of adsorbed atoms per unit area. The heat of adsorption Q_a arising from the interaction, additional to dispersion force interaction

$$Q_t = Q_{disp} + Q_a \quad (8)$$

is then

$$Q_a = Q_{pol} = \frac{1}{2} \alpha F^2 \quad (9)$$

This classical model, first used by Mignolet¹, is still frequently used to explain the large s.p. of adsorbed inert gases⁷⁻¹⁰. From eq. (7) and (9) it follows that

$$Q_{pol} = \frac{1}{32\pi^2 N^2 \alpha} (-\Delta\phi)^2 \quad (10)$$

Hence,

$$\log Q_{pol} = 2 \log(-\Delta\phi) - 2 \log N + c \quad (11)$$

where c is a constant characteristic for the inert gas. Recent LEED studies of Xe on several crystal planes of Cu and Ag¹¹ and on Pd(100)⁶ show that the adatoms are close-packed on these surfaces with an equal area per adatom of $17 \pm 1 \text{ \AA}^2$. On rough crystal faces, however, site adsorption takes place^{12,13} resulting in a lower Xe density than 17 \AA^2 . It may be expected that the films sintered at room temperature do not exhibit large structural differences. $\log N$ may, therefore, be considered, in first approximation, as being the same for all metals. Hence, the polarization model predicts that a $\log Q_a$ versus $\log(-\Delta\phi)$ plot will yield a straight line with a slope ~ 2 .

II. The charge transfer-no bond (CTNB) model. This explanation of a quantum mechanical nature is based on Mulliken's theory of charge transfer complexes¹⁴. The model assumes electron transfer from Xe to the metal surface stabilized by resonance between the ion core Xe^+ and the metal. It was Mignolet who seems first to have seen the importance of this type of bonding in the Xe metal interaction². The theory was later elaborated by Gundry and Tompkins¹⁵. They were, however, unable to decide which of the two models I and II is preferable.

Charge transfer states are formed by an electron transfer from Xe to a state k in the metal above the Fermi level k_F . We assume that the contribution of charge transfer from a metal state k below k_F to an excited state of Xe may be neglected. In our opinion this is supported by the large positive surface potentials found for Xe on metals.

An approximate wave function Ψ for the adsorbed system is obtained by linearly superimposing the unperturbed wave function ψ_{NB} (Xe, metal) for the "no-bond" state and the unperturbed wave functions ψ_k (Xe^+ , metal) for the charge transfer states:

$$\Psi = B\psi_{NB} + \sum_{k > k_F} C_k \psi_k \quad (12)$$

This form of the wave function was used by Grimley¹⁶ for the calculation of

the heat of adsorption of CO on Ni with the aid of Mulliken's charge transfer theory¹⁴. Following the procedure of Grimley in deriving an appropriate expression for the energy of the system, we arrive at the following equation for the heat of adsorption:

$$Q_{\text{CTNB}} = \sum_k \frac{\beta_k^2}{H_k - H_0} \quad (13)$$

where β_k corresponds to the energy of interaction between the unperturbed, no-bond state and the charge-transfer state; H_0 is the energy of the unperturbed no-bond state and H_k the energy of a charge-transfer state (Xe^+ , metal⁻).

The difference in energy between a charge-transfer and the no-bond state, $H_k - H_0$, can be substituted by the expression:

$$H_k - H_0 = I_g - \phi - e^2/4R + \epsilon = \Delta E + \epsilon \quad (14)$$

This equation follows from the energy balance of a process where an electron is extracted from Xe (which requires an energy equal to the ionization energy I_g of the adsorbate), transferred to the metal (energy gain ϕ) and put there on an unoccupied level with energy ϵ above the Fermi level.

The image energy term $e^2/4R$ represents the electrostatic attraction between the metal and the positive charge at a distance $2R$ between the centre of charge and its image.

Following a suggestion of Van Santen¹⁷ we simplify the summation in (13) by converting it to the following integration:

$$Q_{\text{CTNB}} = 6 \int_0^{\epsilon_{\text{max}}} d\epsilon \frac{\beta^2}{\Delta E + \epsilon} g(\epsilon) \quad (15)$$

where $g(\epsilon)$ is the density of electron states with energy ϵ above the Fermi level and ϵ_{max} is the distance of the top of the metal band involved in the interaction with Xe from the Fermi level. The factor 6 in equation (15) is present because of the threefold degeneracy of the 5p level of Xe.

The same procedure yields an expression for the dipole moment μ of the adsorption band:

$$\mu = eR \left[6 \int_0^{\epsilon_{\text{max}}} d\epsilon \frac{\beta^2}{(\Delta E + \epsilon)^2} g(\epsilon) \right] \quad (16)$$

Equations (15) and (16) may significantly simplified when $\epsilon_{\text{max}} \ll \Delta E$. Then, the integrals may be approximated by the values of the integrand for $\epsilon = 0$ multiplied by ϵ_{max} . We arrive then at the following relation between Q_{CTNB} and μ :

$$Q_{\text{CTNB}} = \mu / eR \cdot \Delta E \quad (17)$$

It follows from equations (17), (7) and (14) that $\Delta\phi$ is related to Q_{CTNB} by

$$Q_{\text{CTNB}} = \frac{I_g - \phi - e^2/4R}{4\pi NeR} (-\Delta\phi) \quad (18)$$

This equation can also be derived from the approximate equations used by Gundry and Tompkins¹⁵.

The validity of equation (18) depends on the width of the unoccupied band involved in the interaction with Xe. For the metals Ni, Pt and Rh the assumption $\epsilon_{\text{max}} \ll \Delta E$ is justified when only the d-band is involved in the interaction. Equation (18) may directly be faced with our experimental results. In order to evaluate our results on the basis of the CTNB model we shall use equation (18) but we must keep in mind that a deviation from equation (18) may be expected, especially for Cu and Au. The limitations and the validity of our approach are now, thus, well-defined.

Equation (18) is written as:

$$\log Q_{\text{CTNB}} = \log (-\Delta\phi) + A \quad (19)$$

with

$$A = \log \frac{I_g - \phi - e^2/4R}{4\pi NeR} \quad (20)$$

Numerical values for A can be found in Table II. It appears that the varia-

Table II

metal	ϕ (eV)	$-\Delta\phi$ (V)	Q_t (kcal/mole)	$R(\text{\AA})$	$\hbar\omega_p$ (eV)	Q_M (kcal/mole)	$Q_{\text{p.s.}}$ (kcal/mole)	A^*
Au	5.28	0.52	4.6	3.62	24.3	2.9	4.0	13.65
Cu	4.52	0.63	5.2	3.46	19.1	2.8	5.8	13.69
Ni	4.90	0.82	6.4	3.43	19.5	2.9	6.3	13.68
Pt	5.62	0.95	7.6	3.56	28.2	3.4	4.6	13.63
Rh	4.98	1.08	8.7	3.52	24.6	3.2	5.0	13.67

$$A^* = \log \frac{I_g - \phi - N_A e^2/4R}{4\pi NeR}$$

tion of A for the metals studied is much lower than that of $\log \Delta\phi$. Hence, it is expected that a $\log Q_{\text{CTNB}}$ versus $\log (-\Delta\phi)$ plot should approximate a straight line with a slope near to 1 and an intercept on the Q axis of about 13.7 (c.g.s. units).

In principle other mechanisms could be imagined. So it could be interesting to apply the theory of the inhomogeneous electron gas by Hohenberg, Kohn and Lang¹⁸⁻²¹ to the adsorption of inert gases on group Ib metals.

This model yields values for the dipole moment of adsorbed alkali atoms which are in quite satisfactory agreement with experimental data²². In this paper only models I and II are discussed on the basis of the present results.

B. Dispersion forces

First, it will be examined which contribution may be expected of dispersion forces to the bonding between Xe and the transition metal. Theories which deal specifically with the dispersion force interaction of a gas with a metal surface were published by Lennard-Jones²³, Margenau and Pollard²⁴, Bardeen²⁵, Prosen and Sachs²⁶ and Mavroyannis²⁷. The most recent theory developed by Mavroyannis derives the following approximate expression for the heat of adsorption:

$$Q_M = \frac{N_A \hbar \omega_p}{m^{1/2}} \frac{\alpha^{1/2} n^{1/2}}{8R^3} \frac{\hbar \omega_p / \sqrt{2}}{\left(\frac{n}{\alpha}\right)^{1/2} \frac{\hbar \omega_p}{\sqrt{m}} + \hbar \omega_p / \sqrt{2}} \quad (21)$$

where n is the number of electrons in the adsorbate atom, N_A the Avogadro constant, \hbar the Planck constant divided by 2π , m the electron mass and ω_p the plasma frequency of the metal. Taking for R the sum of the metallic radius and the Van der Waals' radius of the adsorbate (see Table II), values for Q have been calculated from eq. (21) for He, Ne, Ar and Kr on Pt^{4,27}. They are in reasonable agreement with those found by experiment⁴. For Xe on Au, Cu, Ni, Pt and Rh we have calculated Q_m from eq. (21). The numerical values are given in column 7 of Table II. For $\hbar \omega_p$ the experimental values for the characteristic energy losses in the metals have been used, taken from Lynch and Swan²⁸ and from Klemperer and Shepherd²⁹. The values for Q_{disp} obtained from the older theories by Margenau and Pollard²⁴ and by Bardeen²⁵ are somewhat smaller than those obtained from Mavroyannis' theory. On the other hand, much higher values are obtained by using the equation by Prosen and Sachs (P.S.)²⁶:

$$Q_{P.S.} = \frac{N_A \alpha e^2 k_m^2}{8\pi^2} \frac{\ln(2k_m R)}{R^2} \quad (22)$$

with

$$k_m = (3\pi^2 \rho)^{1/3} \quad (23)$$

ρ being the electron density in the metal.

It appears from Table II that for Xe Q_M is fairly constant on the metals considered and that it is much lower than Q_t . $Q_{P.S.}$ is about equal to Q_t for Xe on Cu, Ni and Au while it is on Pt and Rh 3 kcal/mole lower than Q_t . Upon remembering that the large decrease in ϕ caused by Xe adsorption on

all these metals unequivocally shows that a pronounced interaction must be present between Xe and the metal surface in addition to the dispersion forces, we conclude that the values calculated by eq. (22) are definitely too high. As the values calculated by Mavroyannis' formula are not inconsistent with the experimental values, we shall use eq. (21) for our further discussion.

C. Evaluation of the results

I. The relation between Q and the s.p. It follows from section 5.A. that a $\log Q$ versus $\log (-\Delta\phi)$ plot may possibly serve as a criterion to discriminate between the polarization and the CTNB models: the classical polarization model predicts a slope of 2.0 while according to the CTNB theory a slope roughly equal to 1 may be expected. The predicted intercepts on the Q axis are respectively 15.2 and 13.7 (Q and $\Delta\phi$ in c.g.s. units), when taking $N = 5.8 \times 10^{14}$ atoms per cm^2 , the value obtained from the LEED results^{6,11} and $\alpha = 4.0 \text{ \AA}^3$, the polarizability of an isolated Xe atom while for R the values mentioned in Table II were taken. The problem is that the Q values required for constructing such a graph have to be calculated from the measured Q_t values by applying an appropriate correction. If the polarization model is valid, Q_{disp} has to be subtracted from Q_t . If, however, the bonding is of the CTNB type the contribution of dispersion forces cannot be predicted easily because the CTNB interaction may be considered as a chemical interaction which already involves a great part of interaction called dispersion forces interaction. The relative contribution by dispersion forces would, consequently, become smaller than predicted by eq. (21). After this discussion of the theoretical possibilities it is interesting to face them with the experimental results.

The existence of a correlation between the Xe s.p. and the heat of adsorption is clearly demonstrated by Fig. 8. This relation may be considered, within the experimental accuracy, as linear; the straight line is cutting the Q axis at about 0.8 kcal/mole. This could imply that the dispersion forces are responsible for a very small contribution to the bonding of Xe, say of the order of 1 kcal/mole.

Table III lists the slopes and intercepts of the $\log Q_a$ versus $\log (-\Delta\phi)$ plots obtained by subtracting from Q_t two quite arbitrary values of Q_{disp} 0, 1 and 2 kcal/mole for all metals. The plots are shown in Fig. 9.

Table III

The slopes m and intercepts I for $\log Q_a$ versus
 $\log (-\Delta\phi)$ plots with $Q_t = Q_{\text{disp}} + Q_a$

Q_{disp} (kcal/mole)	Q_a	m	I (c.g.s. units)
0		0.87 ± 0.01	13.72 ± 0.06
1		1.04 ± 0.01	14.09 ± 0.06
2		1.31 ± 0.01	14.67 ± 0.06
Mavroyannis		1.54 ± 0.02	15.17 ± 0.07
	polarization model	2.0	15.2
	CTNB model	1.0	13.7

It appears that both the slope and the intercept are in excellent agreement with the CTNB model. Taking for Q_{disp} the values obtained from eq. (21) a $\log Q_a$ versus $\log (-\Delta\phi)$ plot yields a line (see Fig. 9) with a slope of 1.54 ± 0.02 and an intercept on the Q_a axis equal to 15.17 ± 0.07 (Q and $\Delta\phi$ in c.g.s. units). In conclusion we can state that the observed relation between Q and $\Delta\phi$ can best be understood indeed by considering the interaction as a CTNB bond with a small contribution by dispersion forces which we estimate to be in the order of 1 kcal/mole.

II. Calculation of Q_a from the measured s.p. A different approach is the calculation of absolute values for Q_{CTNB} and Q_{pol} from $\Delta\phi$ using eq. (10) and (18), respectively. In this calculation $\alpha = 4.0 \text{ \AA}^3$ and $N = 5.8 \times 10^{14}$ atoms per cm^2 were used while for R and $\Delta\phi$ the values mentioned in Table II and the experimentally determined values were taken, respectively. The results are given in Table IV. ($Q_{\text{pol}} + Q_m$) and ($Q_{\text{pol}} + Q_{\text{P.S.}}$) are both too small to account for the observed values of Q_t , especially for Pt and Rh. However, ($Q_{\text{CTNB}} + Q_m$) is in satisfactory agreement with the Q_t values. This would confirm our conclusion that the CTNB model is realistic.

Up to this point the lateral interactions between adsorbed Xe atoms have been neglected. It has been observed that Q_{Xe} on Pd^6 , Pt^{13} and Ir^{12} decreases with coverage; it may be expected from these data that Q_t (at $\psi = \frac{1}{2}$) has to be corrected upward by about 0.5 kcal/mole in order to get Q_t at $\theta \sim 0$. Presumably, the correction will be somewhat larger for Ni, Pt and Rh than for Cu and Au. More important is the variation in ϕ with θ as a result of depolarization of an adsorbed atom by the neighbouring adatoms.

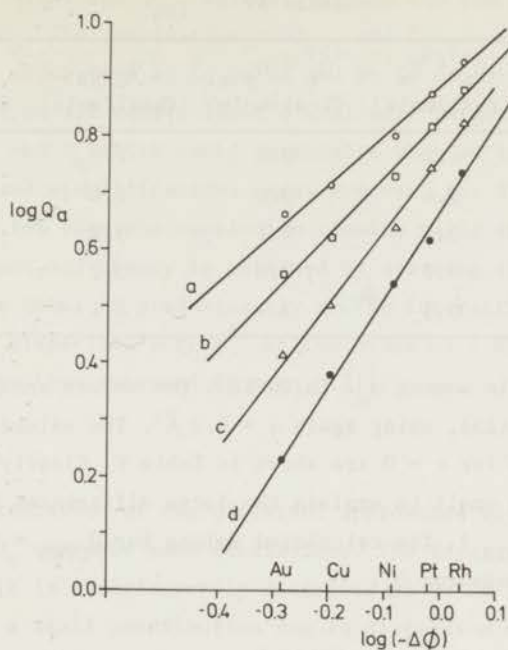


Fig. 9

The correlation between $Q_a = Q_t - Q_{\text{disp}}$ and the surface potential $-\Delta\phi$

- a - $Q_{\text{disp}} = 0$ kcal/mole
- b - $Q_{\text{disp}} = 1$ kcal/mole
- c - $Q_{\text{disp}} = 2$ kcal/mole
- d - $Q_{\text{disp}} = Q_m$

μ_o , the dipole moment normal to the surface in the limit of zero coverage may be estimated from Topping's formula³⁰ for an array of point dipoles³¹:

$$\Delta\phi = \frac{-4\pi\mu_o N}{1+9\alpha N^{3/2}} \quad (24)$$

The second term in the denominator accounts for the depolarization of the adatoms by the field from an array of point dipoles. Eq. (24) may be re-written as

$$\Delta\phi = \frac{\Delta\phi_o}{1+9\alpha N^{3/2}} \quad (25)$$

where $\Delta\phi_o = -4\pi\mu_o N$ is the change in work function resulting if each Xe adatom

Table IV

metal	$-\Delta\phi$ (V)	$Q_t - Q_m$ (kcal/mole)	$Q_t - Q_{p.s.}$ (kcal/mole)	Q_{CTNB} (kcal/mole)	Q_{pol} (kcal/mole)
Au	0.52	1.7	0.6	1.8	0.1
Cu	0.63	2.4	- 0.6	2.6	0.1
Ni	0.82	3.5	0.1	3.2	0.2
Pt	0.95	4.2	3.0	3.2	0.3
Rh	1.08	5.5	3.7	4.1	0.4

would possess a dipole moment μ_o . In Table V the values are given for $\Delta\phi_o$, calculated from eq. (25), using again $\alpha = 4.0 \text{ \AA}^3$. The values for Q_{CTNB} and Q_{pol} calculated thus for $\theta = 0$ are shown in Table V. Clearly the numbers for Q_{pol} are far too small to explain the large differences between Q_t and Q_{disp} (Q_m or even $Q_{p.s.}$). The calculated values for $Q_{CTNB} + Q_m$ are in agreement with the measured Q_t .

Table V

metal	Q_t (kcal/mole)	$-\Delta\phi_o^*$ (V)	Q_{CTNB}^* (kcal/mole)	Q_{pol}^* (kcal/mole)	$-\Delta\phi_o^+$ (V)	Q_{CTNB}^+ (kcal/mole)	Q_{pol}^+ (kcal/mole)
Au	4.6	0.78	2.7	0.2	1.04	3.6	0.2
Cu	5.2	0.95	3.9	0.3	1.26	5.2	0.3
Ni	6.4	1.23	4.8	0.6	1.64	6.4	0.5
Pt	7.6	1.43	4.8	0.8	1.90	6.4	0.7
Rh	8.7	1.62	6.1	1.0	2.16	8.2	0.9

* for $\alpha = 4.0 \text{ \AA}^3$

+ for $\alpha = 8.0 \text{ \AA}^3$

The assumption that the polarizability of adsorbed Xe is equal to that of an isolated Xe atom (4 \AA^3) appears debatable. The only numerical value available for the polarizability of a Xe adatom in close contact with a metal lattice is that for Xe adsorbed on Pd (100) for which Palmberg⁶ had estimated $\alpha = 8 \text{ \AA}^3$, thus twice that of an isolated Xe atom. If we accept this value of $\alpha = 8 \text{ \AA}^3$, the results shown in Table V are obtained for $\Delta\phi_o$,

Q_{CTNB} and Q_{pol} . Still the Q_{pol} values are much too low to explain the difference $Q_t(\theta=0) - Q_m$. The combination of Q_{pol} and $Q_{\text{p.s.}}$ cannot explain the much higher heats of adsorption of Xe on Rh and Pt in comparison with Xe on Au and Cu. Q_{CTNB} is on all metals about 2 kcal/mole larger than the difference between $Q_t(\theta=0)$ and Q_m which looks reasonable when we take into account all approximations and simplifications made. However, the difference between Q_t and Q_{CTNB} is so low that the conclusion remains valid that best agreement between experiment and theory is obtained by assuming the interaction between Xe and the metal as predominantly a CTNB interaction with only a small contribution of dispersion forces*) of the order of 1 kcal/mole and, thus, even much smaller than expected from eq. (21).

6. Conclusions

The confrontation of the different approaches with our experimental data on $\Delta\phi$ and Q_t warrants some conclusions. The interaction between Xe and transition metals is satisfactorily described as being largely a CTNB interaction to which a small contribution due to dispersion forces is added. The latter term appears to be much smaller than predicted by the equation of Prosen and Sachs and is even smaller than the values obtained by Mavroyannis' equation. The alternative explanation for the large s.p. of adsorbed Xe, viz. the classical polarization model can be rejected for two reasons:

- it is unable to account for the high heats of adsorption on Group VIII metals, and
- it fails to describe the observed interdependence of Q and s.p. which is properly given by the CTNB model.

The present work confirms our earlier conclusions based on F.E.M. results of Xe adsorption on several well defined crystal faces of Pt¹³ and Ir¹². In that study it had been found that both the initial heat of adsorption and the s.p. of Xe are larger on the close-packed crystal faces (111) and (100) of Ir than on the rougher faces (110) and (210). On Pt, likewise, the initial heat of adsorption had been found to be higher on (111) and (100) than on (110) and (210). We had reasoned that these results were in agreement with the CTNB model while they were in conflict with the classical polarization model as this model predicts the wrong sign for the adsorption dipole.

*) With a contribution by dispersion forces is meant here each interaction which does not cause a change in work function.

References

- 1) J.C.P. Mignolet, *Disc. Faraday Soc.* 8 (1950) 105.
- 2) J.C.P. Mignolet, in *Chemisorption* (W.E. Garner ed.) p. 118, Butterworths, London, 1957,
- 3) B.E. Nieuwenhuys, R. Bouwman and W.M.H. Sachtler, *Thin Solid Films* 21 (1974) 55.
- 4) H. Chon, R.A. Fisher, R.D. McCammon and J.G. Aston, *J. Chem. Phys.* 36 (1962) 1378.
- 5) R. Bouwman, H.P. van Keulen and W.M.H. Sachtler, *Ber. Bunsenges. physik. Chem.* 74 (1970) 198.
- 6) P.W. Palmberg, *Surface Sci.* 25 (1971) 598.
- 7) J.H. de Boer and J.H. Kaspersma, *Proc. Kon. Ned. Acad. Wetensch.* B72 (1969) 289.
- 8) P.G. Hall, *Chem. Commun.* 1966, 877.
- 9) J. Müller, *Chem Commun.* 1970, 1173.
- 10) D.F. Klemperer and J.C. Snaith, *Surface Sci.* 28 (1971) 209.
- 11) M.A. Chesters, M. Hussain and J. Pritchard, *Surface Sci.* 35 (1973) 161.
- 12) B.E. Nieuwenhuys and W.M.H. Sachtler, submitted to *Surface Sci.*
- 13) B.E. Nieuwenhuys, D.Th. Meijer and W.M.H. Sachtler, submitted to *Phys. Stat. Sol.*
- 14) J. Mulliken, *J. Am. Chem. Soc.* 74 (1952) 811.
- 15) P.M. Gundry and F.C. Tompkins, *Trans. Faraday Soc.* 56 (1960) 846.
- 16) T.B. Grimley, in "Molecular Processes on Solid Surfaces" (E. Drauglis, R.D. Gretz and R.J. Jaffee, eds.) p. 299, McGraw-Hill, New York, 1969.
- 17) R.A. van Santen, private communication.
- 18) P. Hohenberg and W. Kohn, *Phys. Rev.* 136 (1964) B 864.
- 19) W. Kohn and L.J. Sham, *Phys. Rev.* 140 (1965) A 1133.
- 20) N.D. Lang and W. Kohn, *Phys. Rev. B* 1 (1970) 4555.
- 21) N.D. Lang and W. Kohn, *Phys. Rev. B* 3 (1971) 1215.
- 22) N.D. Lang, *Phys. Rev. B* 4 (1971) 4234.
- 23) J.E. Lennard-Jones, *Trans. Faraday Soc.* 28 (1932) 334.
- 24) H. Margenau and W.G. Pollard, *Phys. Rev.* 60 (1941) 128.
- 25) J. Bardeen, *Phys. Rev.* 58 (1940) 727.
- 26) E.J.R. Prosen and R.G. Sachs, *Phys. Rev.* 61 (1942) 65.
- 27) C. Mavroyannis, *Mol. Phys.* 6 (1963) 593.
- 28) M.J. Lynch and J.B. Swan, *Aust. J. Phys.* 21 (1968) 811.

- 29) O. Klemperer and J.P.G. Shepherd, Adv. Phys. 12 (1963) 355.
- 30) J. Topping, Proc. Roy. Soc. (London) A114 (1927) 67.
- 31) A.R. Miller, Proc. Cambridge, Phil. Soc. 42 (1946) 292.

Chapter IX

SOME GENERAL REMARKS ON THE BOND OF ADSORBED NITROGEN AND XENON

The main objective of this study is to identify the nature of the bond between weakly adsorbed gases and surfaces of transition metals. The adsorption systems studied are N_2 and Xe on a number of metals belonging to Groups VIII b, c and I b of the periodic system.

N_2 is strongly adsorbed on many transition metals. On a W(100) plane, for instance, the adsorption is dissociative with a reported heat of adsorption of 73 kcal/mole¹. On the other hand, the interaction between N_2 and metals of Group VIII b and c is weak². Adsorption on these metals can only be detected at a relatively low temperature, the adsorption being non-dissociative. Some authors, therefore, explain the bonding of N_2 on these metals in terms of physical adsorption³.

The present study has revealed a marked difference in adsorption behaviour of N_2 on the different metals of Group VIII b and c. On Pt and Ir this difference is not only manifested in the initial heat of adsorption, which amounts to 13 - 14 kcal/mole on Ir and 9 kcal/mole on Pt, but also in a completely different crystal face specificity of both heat of adsorption and change in work function. From our results we have argued that the interaction between N_2 and Group VIII b and c metals is of chemical nature. Of relevance in this respect is, in our opinion, also the similarity of nitrogen adsorption complexes³⁻¹⁰ to transition metal complexes with di-nitrogen as a ligand¹¹⁻¹³, as manifested for instance in the infrared absorption frequencies. Extrapolating this parallelism to the bonding, it appears plausible to describe the bonding of N_2 on Group VIII b and c metal surfaces as a donation of electrons from the $3\sigma_g$ orbitals of the N_2 molecules to the metal stabilized by back donation of electrons from the metal d-band into the vacant degenerate $1\pi_g$ antibonding orbitals of nitrogen. If this view is correct the metal-N-N complex is linear or nearly so. The available experimental results do not rule out yet the possible presence of

a different type of adsorption, in addition to the form bonded perpendicular to the surface. For instance, the existence of adsorbed N_2 bonded with the N-N bond parallel to the surface cannot be excluded.

The second system described in this work is Xe adsorbed on transition metals.

It has long been realized by a number of authors¹⁴ that the adsorption of inert gases on metals cannot be understood by assuming an interaction merely due to dispersion forces. Especially the large surface potential of inert gases adsorbed on transition metals, first observed by Mignolet in 1950¹⁵, is incompatible with the general view of interaction by dispersion forces.

Yet, up to now, the different theories dealing with the dispersion force interaction of a gas with a metal were tested with the experimentally found heats of adsorption of inert gases on transition metals^{16,17}.

The present study demonstrates in a convincing way the inaccuracy of this procedure; the following results are incompatible with an interaction entirely due to dispersion forces:

1. The crystal face dependence of the initial heat of adsorption of Xe on Pt and on Ir. The initial heat of adsorption on the (111) and (100) regions is larger than on (110) tip regions.
2. The large surface potential of adsorbed Xe.
3. The experimentally found relatively large heats of adsorption, especially on Group VIII metals.

A model frequently used for explaining the large surface potential of inert gases^{15,18} assumes a dispersion force interaction to which an interaction term is added which is due to a classical polarization of the adsorbate in a hypothetical surface field. Also this model is rejected since it fails to explain the following results:

- a. The sign of the adsorption dipole.
- b. The observed relationship between the heat of adsorption and the surface potential of Xe.
- c. The absolute values of the experimentally found heats of adsorption on Group VIII metals.

Our results appear completely consistent with a charge-transfer no-bond interaction between adsorbate and metal¹⁹. The agreement between experiment and this model appears from the sign of the adsorption dipole, the observed linear proportionality between the surface potential and the

heat of adsorption on different metals, the relatively strong binding of Xe on crystal faces with a high work function and the magnitudes of the heats of adsorption on various transition metals. Hence, it appears that the interaction between Xe and transition metals may be considered as a weak chemisorption since electron transfer between adsorbate and metal takes place.

The final conclusions emerging from this work are largely due to the strategy followed in this study: the separation of the chemical and geometric effects in adsorption by working with different crystal faces of a given metal single crystal and by measuring the adsorption of the same gas on different metals, in particular the corresponding crystal faces or on films of comparable face distribution in their surface.

References

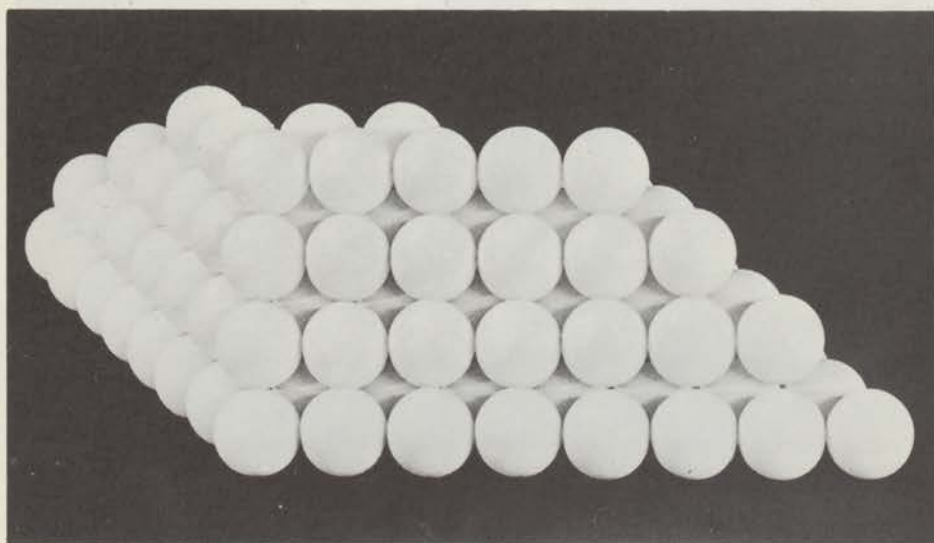
- 1) L.R. Clavenna and L.D. Schmidt, *Surface Sci.* 22 (1970) 365.
- 2) B.M.W. Trapnell, *Proc. Roy. Soc. (London)* A218 (1953) 566.
- 3) R. van Hardeveld and A. van Montfoort, *Surface Sci.* 4 (1966) 396.
- 4) References 22, 23, 25, 26 of chapter II.
- 5) R. van Hardeveld and F. Hartog, *Advan. Catalysis* 22 (1972) 75.
- 6) L.M. Røev, S.V. Batyckho and M.T. Rusov, *Kin. Cat.* 12 (1971) 956.
- 7) J.K. Burdett and J.J. Turner, *Chem. Commun.* (1971) 885.
- 8) J.K. Burdett, M.A. Graham and J.J. Turner, *J. Chem. Soc., Dalton Trans.* 15 (1972) 1620.
- 9) M. Moskovits and G.A. Ozin, *J. Chem. Phys.* 58 (1973) 1251.
- 10) D.W. Green, J. Thomas and D.M. Gruen, *J. Chem. Phys.* 58 (1973) 5453.
- 11) J.E. Ferguson and J.L. Love, *Rev. Pure and Appl. Chem.* 20 (1970) 33.
- 12) B. Folkesson, *Acta Chem. Scand.* 27 (1973) 276.
- 13) A.D. Allen, R.O. Harris, B.R. Loescher, J.R. Stevens and R.N. Whiteley, *Chem. Rev.* 73 (1973) 11.
- 14) References 2, 9, 14, 19 and 23 of chapter VI.
- 15) J.C.P. Mignolet, *Disc. Faraday Soc.* 8 (1950) 105.
- 16) H. Chon, R.A. Fisher, R.D. McCammon and J.G. Aston, *J. Chem. Phys.* 36 (1962) 1378.
- 17) C. Mavroyannis, *Mol. Phys.* 6 (1963) 593.
- 18) References 7 - 10 of chapter VIII.
- 19) References 2 and 15 of chapter VIII.

APPENDIX

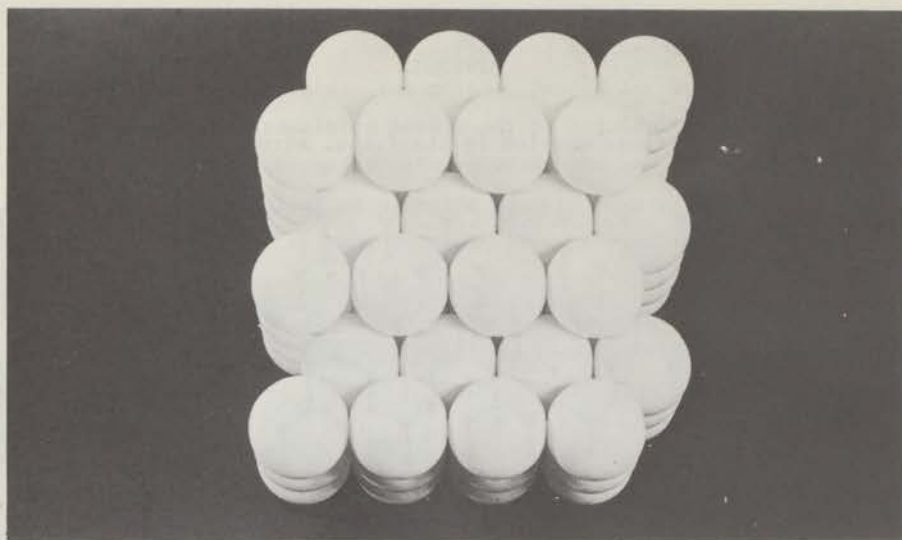
Surfaces modeled in the f.c.c. structure.



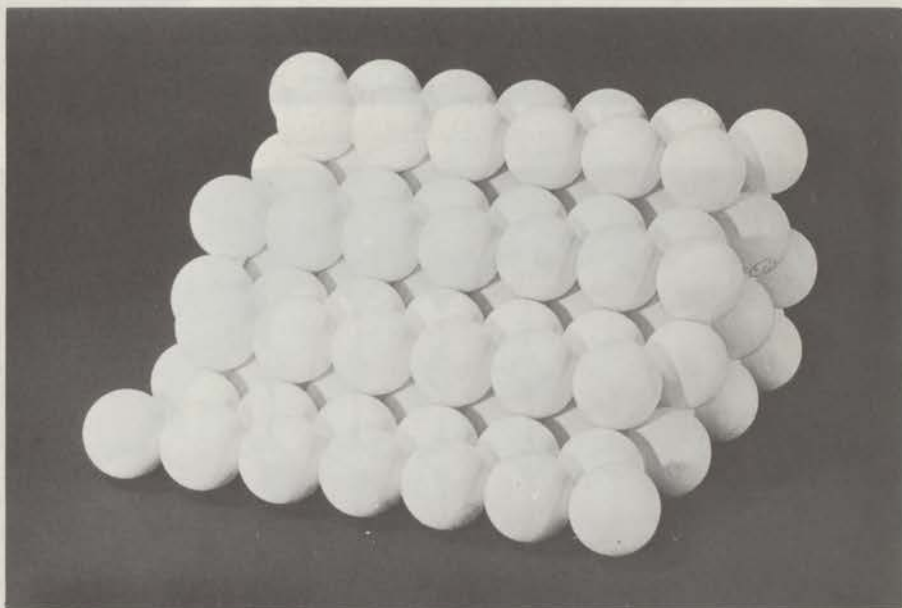
(111) face



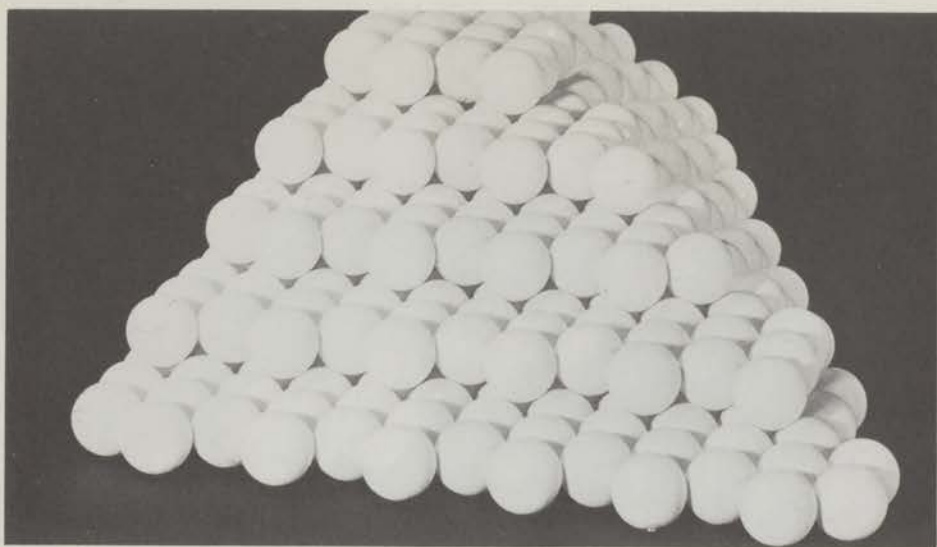
(100) face



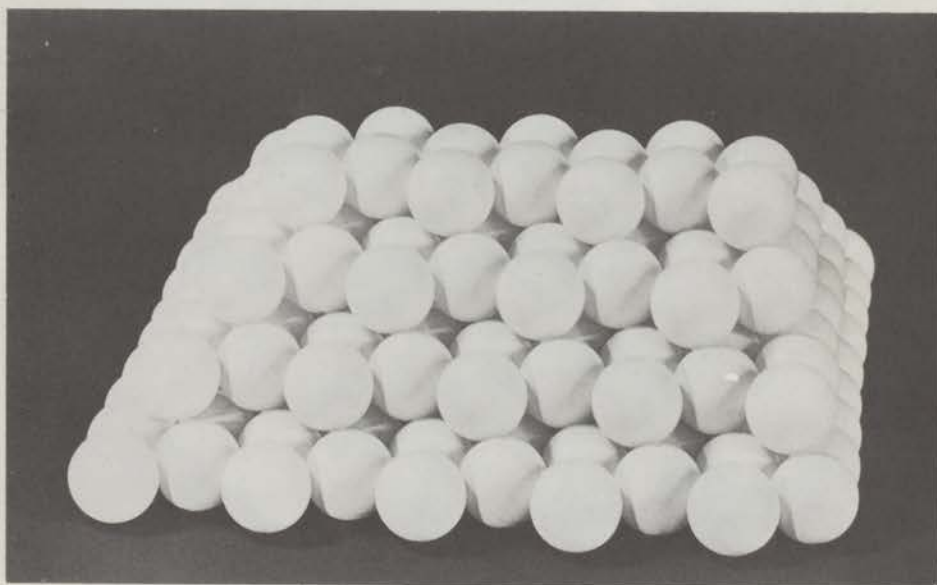
(110) face



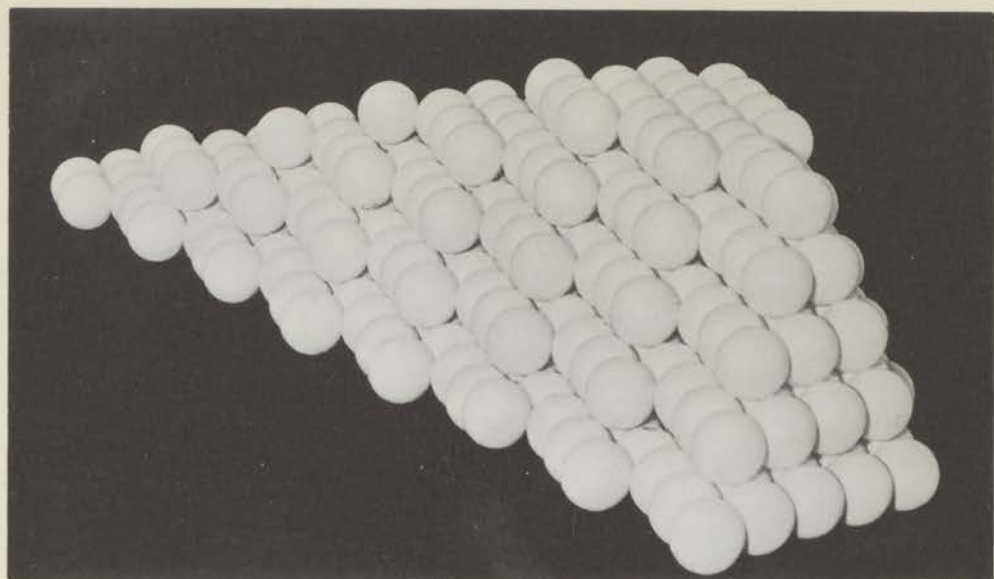
(311) face



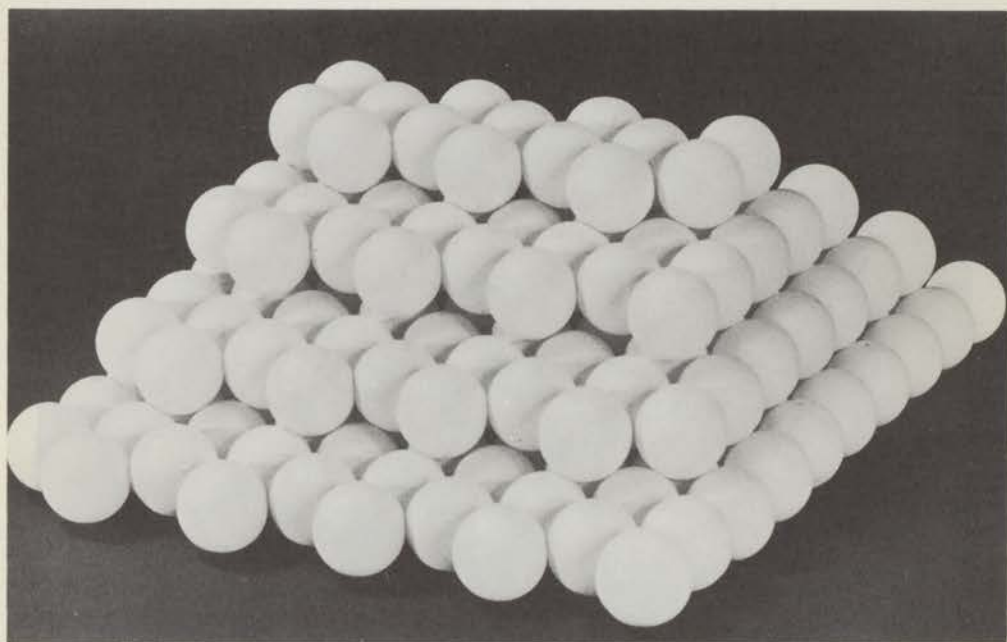
(321) face



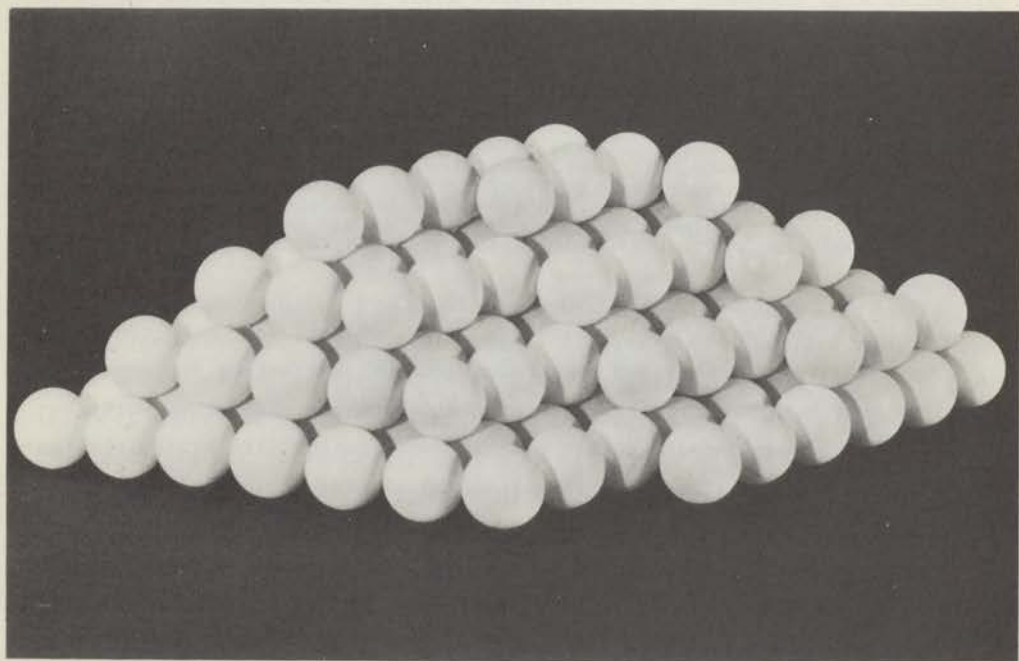
(210) face



(310) face



(531) face



(320) face

S A M E N V A T T I N G

In dit proefschrift wordt een studie beschreven over de adsorptie van N_2 en Xe op diverse metalen. De gebruikte technieken zijn veldelektronenmikroskopie en foto-elektronenemissie. De dissertatie bestaat uit drie delen.

In het eerste deel (hoofdstuk I) worden enige algemene opmerkingen over adsorptie van gassen op metalen gemaakt. Het belang van adsorptiestudies voor heterogene katalyse en andere takken van wetenschap wordt besproken. Aangetoond wordt dat het gebruik van afzonderlijke kristalvlakken voor adsorptiestudies vaak van essentieel belang is. Een aantal experimentele technieken voor adsorptiestudies op metalen wordt vermeld en de werking van de in dit proefschrift gebruikte technieken wordt beschreven. Veldelektronenmikroskopie is een nagenoeg ideale techniek om de afhankelijkheid bij gasadsorptie van de rangschikking der metaalatomen in het oppervlak te bestuderen. Dit geldt vooral voor de door ons gebruikte moderne variant van de veldelektronenmikroskoop: de probe-hole techniek. Deze verschaft ons de unieke mogelijkheid om de diverse vlakken van een éénkristal te onderzoeken bij geheel identieke experimentele omstandigheden. De mogelijkheden en beperkingen van deze techniek worden besproken. Tenslotte wordt in dit hoofdstuk de doelstelling van het onderzoek kort aangegeven.

Het tweede deel (hoofdstukken II t/m IV) behandelt de adsorptie van N_2 op enige overgangsmetalen.

Hoofdstukken II en III gaan over N_2 adsorptie op diverse kristalvlakken van respectievelijk Pt en Ir. In hoofdstuk II wordt ook de gebruikte apparatuur beschreven. Hoofdstuk IV geeft aan hoe de elektronenuittreearbeidverandering van Ni, Rh en Pt films door N_2 adsorptie afhangt van de temperatuur bij welke de films voor het toelaten van N_2 verhit werden.

Deze temperatuur is karakteristiek voor de mate van evenwichtsinstelling van de betrokken film.

Op al de genoemde metalen wordt N_2 slechts zwak gebonden. Op Pt bedraagt de initiële adsorptiewarmte 9 kcal/mole op alle onderzochte kristalvlakken dus zowel op de dichtgestapelde als op de atomair ruwere vlakken. Op Ir daarentegen, wordt N_2 sterk vlakken specifiek gebonden. Drie duidelijk onderscheidbare toestanden zijn aangetoond; een γ_1 toestand met een adsorptiewarmte van maximaal 7 - 8 kcal/mole, deze toestand komt voor op (100) vlakken; een γ_2 toestand met een adsorptiewarmte van maximaal 10 - 11 kcal/mole op de vlakken rond (110) en een sterker gebonden γ_3 toestand die voorkomt op de atomair ruwe vlakken (210), (320) en (531) - (731). De initiële adsorptiewarmte van N_2 in de laatstgenoemde toestand bedraagt 13 - 14 kcal/mole.

De verandering in de uittree-arbeid is bij beide metalen duidelijk vlakken specifiek. Zo blijkt dat op Pt de uittree-arbeid sterk verlaagd wordt op de ruwe vlakken terwijl de verlaging op de gladde vlakken veel geringer is. Heel anders is het gedrag van N_2 op Ir. Daar wordt juist een grote verlaging van de uittree-arbeid gevonden op het dichtgestapelde (100) vlak. Op de ruwe vlakken rond (731) en (210) wordt de uittree-arbeid slechts weinig verlaagd. Ondanks deze kleine afname in de uittree-arbeid op de ruwe vlakken neemt de emissiestroom van deze vlakken bij constante veldsterkte gedurende N_2 adsorptie sterk af.

Bij Pt films wordt de verlaging van de uittree-arbeid door N_2 adsorptie kleiner als de films door verwarming tot evenwicht gebracht worden. Bij Rh en Ni films neemt daarentegen de uittree-arbeidverlaging door dit proces toe.

Al deze resultaten worden besproken aan de hand van literatuurgegevens. Onze resultaten bevestigen de hypothese van Van Hardeveld c.s. dat N_2 adsorptie afhangt van de oppervlaktestructuur van het metaal. Deze kristalvlak-afhankelijkheid is echter veel ingewikkelder dan door deze auteurs voorgesteld was. Bovendien is er een opvallend groot verschil in adsorptiegedrag van N_2 op de besproken metalen. De binding tussen N_2 en deze metalen kan niet als fysische adsorptie beschouwd worden, maar blijkt een echte chemische oorsprong te hebben.

Het derde deel van dit proefschrift (hoofdstukken V t/m VIII) behandelt de adsorptie van Xe op overgangsmetalen.

In hoofdstuk V zien we hoe de oppervlaktepotentiaal van Xe verandert als de films tot evenwicht worden gebracht. Enige tegenstrijdige meningen in de literatuur hierover worden besproken aan de hand van deze resultaten.

Hoofdstukken VI en VII hebben betrekking op Xe adsorptie op diverse kristalvlakken van Ir en Pt. De initiële adsorptiewarmte neemt op beide metalen af in de reeks (321) > (111) ~ (100) > (210) > (110). De oppervlaktepotentiaal van Xe op Ir is groter op de dichtgestapelde vlakken (111) en (100) dan op de ruwe vlakken. Op alle vlakken neemt de adsorptiewarmte af bij toenemende bedekkingsgraad. Deze afname is op de gladde vlakken veel groter dan op de ruwe vlakken.

In hoofdstuk VIII zien we dat de oppervlaktepotentiaal en de adsorptiewarmte van Xe nauw met elkaar verbonden zijn. Er blijkt tussen deze grootheden een relatie te bestaan die binnen de meetfout als lineair beschouwd mag worden.

Aan de hand van de door ons verkregen resultaten kon over een aantal fundamentele kwesties over adsorptie van edelgassen op metalen een uitspraak worden gedaan. Eerst wordt de onenigheid in de literatuur over de aard van de adsorptieplaatsen en over de pakking van de geadsorbeerde Xe atomen op het oppervlak behandeld (hoofdstukken VI en VII). Uit onze resultaten mag geconcludeerd worden dat Xe bij lage overall-bedekking op de tip geadsorbeerd wordt in die adsorptieplaatsen waar de geadsorbeerde Xe atomen maximaal door de metaal-atomen omringd worden. Bij hoge bedekkingsgraad blijft op de ruwe vlakken dit "site karakter" van de adsorptie gehandhaafd. Op de dichtgestapelde vlakken daarentegen wordt bij hoge bedekkingsgraad een dichtgestapelde Xe laag gevormd waarbij niet noodzakelijk een directe relatie met de atomaire oppervlaktestructuur van het kristalvlak aanwezig behoeft te zijn. Deze resultaten zijn uiteraard van belang voor de bepaling van de grootte van metaaloppervlakken d.m.v. "fysische" adsorptie.

In hoofdstuk VIII wordt de aard van de wisselwerking tussen Xe en het metaal behandeld. Het blijkt dat de binding niet uitsluitend door dispersiekrachten beschreven kan worden. Een veelvuldig gebruikte verklaring voor de grote oppervlaktepotentiaal en de hoge adsorptiewarmte van Xe op overgangsmetalen is een model waarbij de interactie beschouwd wordt als een combinatie van dispersiekrachten en een interactie door een klassieke polarisatie van Xe atomen in een hypothetisch oppervlakteveld. Dit model wordt verworpen op grond van de volgende feiten:

- (1) De door ons gevonden hoge adsorptiewarmte van Xe op groep VIII metalen kan volgens dit model niet verklaard worden.
 - (2) De gevonden lineaire relatie tussen de adsorptiewarmte en de oppervlaktepotentiaal is strijdig met dit model.
 - (3) Het model voorspelt het verkeerde teken voor de adsorptiedipool.
- Daarentegen zijn de experimentele resultaten in goede overeenstemming met een model dat de binding tussen Xe en het metaal beschrijft als een "charge-transfer no-bond" interactie.

Het blijkt dus dat de adsorptie van edelgassen op metalen, een adsorptiesysteem dat herhaaldelijk gebruikt wordt om de juistheid van bepaalde theorieën over interactie tussen metalen en gassen door dispersiekrachten te testen, volgens de in de inleiding gegeven definitie feitelijk geen fysische adsorptie is, maar een chemisch karakter heeft aangezien er tussen Xe en het metaal een elektronenoverdracht optreedt.

Aan het tot stand komen van dit proefschrift is medewerking verleend door verscheidene instanties en personen, die ik hiervoor graag wil bedanken.

In de eerste plaats gaat mijn erkentelijkheid uit naar de Nederlandse Organisatie voor Zuiver-Wetenschappelijk Onderzoek (Z.W.O.) en de Stichting Scheikundig Onderzoek Nederland (S.O.N.) voor de financiële steun, die ik gedurende de eerste drie jaren van dit onderzoek (juni 1968 - augustus 1971) van deze instanties heb mogen ontvangen.

Voorts dank ik de heren F.C. Kauffeld en W.C. Bauer voor de zeer knappe wijze, waarop zij de gecompliceerde veldemissiecellen ontwikkeld hebben. De heer B.J. Erades dank ik voor het vervaardigen van de vele en vaak lastige glasconstructies.

De heren O.G. van Aardenne en D.Th. Meijer ben ik erkentelijk voor de voortreffelijke wijze, waarop zij in het kader van hun doctoraalstudie meegewerkt hebben aan het onderzoek.

Mevrouw I.E. Muller-Hordijk ben ik dank verschuldigd voor het uitstekend verzorgen van de lay-out en het uittypen van de manuscripten.

De heren M. Pison en J.J. Pot hebben de figuren en foto's verzorgd.

Dr. V. Ponec en drs. P.E.C. Franken wil ik gaarne danken voor de leerzame en interessante discussies, die ik met hen gevoerd heb.

Tenslotte dank ik alle niet genoemde collega's en medewerkers van de Gorlaeus Laboratoria voor hun bijdrage aan de totstandkoming van dit proefschrift.

Verder ben ik de directies van de betreffende wetenschappelijke tijdschriften erkentelijk voor de verleende toestemming tot het herdrukken van de hun aangeboden manuscripten.

CURRICULUM VITAE

Na het behalen van het eindexamen HBS-B aan het Drachtster Lyceum te Drachten begon ik in oktober 1961 met een studie in de scheikunde aan de Rijksuniversiteit te Leiden. Het kandidaatsexamen, letter F, werd afgelegd in juni 1965. De studie werd voortgezet onder leiding van de hoogleraren Dr. W.M.H. Sachtler en Dr. L.J. Oosterhoff en de lector Dr. W.J.A. Maaskant. Het doctoraalexamen met als hoofdvak heterogene katalyse en als bijvakken theoretisch anorganische chemie en theoretisch organische chemie werd in juni 1968 cum laude afgelegd.

Van november 1963 tot juni 1968 vervulde ik een assistentschap op de afdeling anorganische chemie bij het propaedeutisch praktikum. Vanaf juni 1968 ben ik als wetenschappelijk medewerker, sinds juni 1972 als wetenschappelijk medewerker I aan de researchgroep heterogene katalyse verbonden. Vanaf juni 1971 vervul ik in deze researchgroep de taak van conservator.

The following is a list of the names of the persons who were present at the meeting held on the 20th day of May, 1900.

1. Mr. J. W. Smith
2. Mr. J. W. Smith
3. Mr. J. W. Smith
4. Mr. J. W. Smith
5. Mr. J. W. Smith
6. Mr. J. W. Smith
7. Mr. J. W. Smith
8. Mr. J. W. Smith
9. Mr. J. W. Smith
10. Mr. J. W. Smith
11. Mr. J. W. Smith
12. Mr. J. W. Smith
13. Mr. J. W. Smith
14. Mr. J. W. Smith
15. Mr. J. W. Smith
16. Mr. J. W. Smith
17. Mr. J. W. Smith
18. Mr. J. W. Smith
19. Mr. J. W. Smith
20. Mr. J. W. Smith

